Effects of Vegetation Processes on Water Resources at Global and Continental Scales

Anna M. Ukkola

Supervisors:
I. Colin Prentice
Trevor Keenan
Ian Wright
Albert van Dijk

A THESIS SUBMITTED TO MACQUARIE UNIVERSITY
for the degree of Doctor of Philosophy

Faculty of Science and Engineering
Department of Biological Sciences

September 2015

MACQUARIE University
SYDNEY·AUSTRALIA

Author statement

I certify that the work in this thesis entitled “Effects of vegetation processes on water resources at global and continental scales” has not previously been submitted for a degree nor has it been submitted as part of requirements for a degree to any other university or institution other than Macquarie University. I also certify that the thesis is an original piece of research and it has been written by me. Any help and assistance that I have received in my research work and the preparation of the thesis itself have been appropriately acknowledged. In addition, I certify that all information sources and literature used are indicated in the thesis.

_____

Anna Ukkola

Table of Contents

List of Figures

List of Tables

List of Publications

Chapter 2 Ukkola A.M. and Prentice I.C., A worldwide analysis of trends in water-balance evapotranspiration, *Hydrology and Earth System Sciences*, 17, 4177-4187, 2013.

Chapter 3 Ukkola A.M., Prentice I.C., Keenan T.F., van Dijk A.I.J.M, Viney N.R., Myneni R.B. and Bi J., Reduced streamflow in water-stressed climates consistent with CO_2 effects on vegetation, *Nature Climate Change* (accepted).

Chapter 4 Ukkola A.M., Keenan T.F., Kelley D.I. and Prentice I.C., Vegetation buffers the water-resource impacts of environmental change, *Proceedings of the National Academy of Sciences* (in prep.).

Other publications obtained during candidature:

Ukkola A.M. and Murray S.J., Hydrological evaluation of the LPX dynamic global vegetation model for small river catchments in the UK, *Hydrological Processes*, 28, 1939-1950, 2014.

Abstract

Global environmental change is expected to alter the spatial and temporal distribution of water resources but quantifying its effects on the terrestrial water balance remains a challenge. Evapotranspiration (ET) is a key ecosystem variable linking water, energy and carbon cycles, but although global aggregate ET is expected to increase in a warming climate, regional changes in ET have remained particularly poorly constrained due in part to the difficulty in measuring ET. The effects of vegetation and increasing atmospheric CO_2 represent a further complication. Experiments have shown that elevated atmospheric CO_2 affects vegetation productivity and water use, but it remains uncertain whether these processes have led to detectable changes in ET or runoff at ecosystem scales. This thesis aims to quantify large-scale variations in ET, and, in particular, to better constrain the effects of elevated CO_2 on catchment-scale hydrology. The approach relies on observations to the greatest extent possible, and the water-balance method (the difference of precipitation and streamflow at the river catchment scale) is used to quantify ET throughout, as it remains the most firmly observationally based measure of ET.

The first data chapter of the thesis attributes causes of water-balance ET trends globally by considering all key drivers, including climate, land use and vegetation effects. The study statistically accounts for ET trends in energy-limited “wet” and water-limited “dry” river catchments and finds ET is primarily controlled by precipitation in both environments (with precipitation explaining 45-55% and 80-95% of interannual variability and trends in ET in wet and dry catchments, respectively). There is some evidence for vegetation effects based on model simulations, but the detection and attribution of ET trends is hindered by uncertainties in the data available for global analysis and the lack of direct observations of vegetation properties covering the study period 1960-1999.

Making use of high quality streamflow observations for Australia, the second chapter quantifies recent CO_2 effects on runoff, ET and vegetation cover across Australian river catchments in varying climates. The CO_2 effect was quantified by concurrently analysing vegetation cover (Normalised Difference Vegetation Index) and water-balance ET, relying solely on observations. Contrary to common expectation, the analysis shows that vegetation is not only greening, but also consuming more water in sub-humid and semi-arid climates, leading to significant (24-28%) reductions in runoff over the period 1982-2010. The analysis pointed to increased runoff in the wet and arid climates but the results were not statistically significant and it was thus not possible to detect a CO_2 effect in the wettest or driest climates based on the measurements.

Finally, future water resources in Australia are projected using bias-corrected, state-of-the-art climate model projections to drive the Land Surface Processes and eXchanges dynamic global vegetation model (LPX). LPX explicitly simulates vegetation CO_2 responses and is shown to capture observed CO_2 effects on ET. LPX results are contrasted with projections from the empirical Budyko framework, which accounts for only the climatic effects on ET. Future precipitation patterns remain highly uncertain across much of Australia, but predicted vegetation effects are robust. Vegetation is shown to buffer the effects of climate change, alleviating water stress in highly populated regions with robust declines in precipitation due to CO_2-induced water savings. In northern Australia, CO_2 fertilisation reduces runoff but is accompanied by increased vegetation productivity.

The findings of this thesis highlight the importance of considering vegetation in studies of water resources. Recent increases in atmospheric CO_2 are shown to have left a detectable imprint on Australian ecosystems, and the impacts are projected to continue to the end of the 21st century and beyond.

Acknowledgements

I would like to thank Macquarie University for giving me the opportunity to study such an interesting topic and for supporting me through the international Macquarie University Research Excellence scholarship during the past 3.5 years. I would also like to extend my gratitude to the CSIRO Water for a Healthy Country Flagship, who supported me through a top-up scholarship and a generous travel budget, which allowed me to attend international conferences and overseas lab visits to meet leading scientists in my field.

But first and foremost, I want to thank my supervisors, particularly my principal supervisor Colin Prentice. Colin is a leading scientist in the broad field of earth system science and over the years has shared his incredible insights into so many topics. Colin has been an extremely encouraging supervisor and has never judged me for asking plenty of silly questions. No doubt I've ended up learning more about plants than I ever intended but it has been a great adventure. My co-supervisor Trevor Keenan joined the team in late 2013 and has been enormous help in the final stages of my PhD. With an eye for detail, Trevor has helped me perfect my work and I've learnt lots about efficient scientific writing from him in the last few months. I am also grateful to my adjunct supervisor Albert van Dijk at Australian National University who has provided some very insightful comments about Australian hydrology. Finally, I would like to thank my associate supervisor Ian Wright, who has had to sign more forms for me than either of us can remember but has always been there for me at difficult times.

I've had the privilege to work with some great collaborators in Australia and overseas. In particular, I would like to thank Ranga Myneni and his students at Boston University for teaching me so much about remote sensing and their continuing encouragement and support. I would also like to thank everyone I've met at CSIRO Land and Water, particularly Neil Viney for providing pivotal datasets. Belinda Medlyn's group at Macquarie University have always looked after us PhDs and instilled a healthy dose of scepticism about vegetation models on us modellers.

My research group, Biosphere and Climate Dynamics, has been very supportive throughout and always looked after one another. I am eternally grateful to Doug Kelley and Rhys Whitley for their enormous patience and help with computer programming and everything else, I certainly would not have got through without them. I've spent some truly entertaining moments with Kevin Willis, Annika Herbert, Ines Hessler and others during, often very extended, lunch hours and in the pub over a drink or two.

My family in Finland might still not really know what I have spent the last three years studying but have nevertheless enthusiastically cheered me on the whole way through. My sister has kept me entertained on Skype after long days at work and cheered me up with the occasional treats from home that have unexpectedly arrived in the post. My “family-in-law” in London and Australia have been more generous and supportive than I’ll ever deserve and took me under their wing when I first arrived in Sydney alone, having never visited Australia before. Finally, I would like to thank my partner Ned and all the wonderful friends here in Australia and back home. Ned took the big decision to give up his job in London and relocate to Australia halfway through my studies (although being an Aussie it was about time he spent some time in the country), and has supported me through to the chequered flag.

Chapter 1

Introduction

1.1. Global environmental change and hydrology

1.1.1. Introduction

Global environmental change is expected to change the spatial and temporal distribution of water resources, with inevitable consequences for societies and ecosystems. Global warming should accelerate the global hydrological cycle (Huntington, 2006) via increased atmospheric water demand (Roderick et al., 2007; Sheffield et al., 2012), resulting in increases in global evapotranspiration (ET hereafter) and precipitation over land and oceans (Douville et al., 2013). Interactions between climate and land surface processes are expected to lead to changes in the partitioning of precipitation into ET and runoff and adding to this are dynamical vegetation responses to changing climate and CO_2, with consequences for hydrological processes.

There is already evidence that global land precipitation, ET and runoff have changed (reviewed in Collins et al., 2013) but large uncertainties prevail due to interactions of climatic, ecosystem and anthropogenic effects as well as inadequacies in global datasets (Alkama et al., 2011; New et al., 2001). Superimposed on these effects are growing water demand due to increasing global population (Vörösmarty, 2000) and spatially and temporally uneven distribution of water resources. Much effort has been invested in detecting and attributing recent changes in the global hydrological cycle but large uncertainties remain in quantifying the spatial and temporal changes in all hydrological components.

ET is a key ecosystem variable linking energy, water and carbon cycles and results from interactions among the atmosphere, soil and vegetation (Brutsaert, 1982). ET is the sum of plant transpiration, interception and soil evaporation. Up to 60% of precipitation is evaporated globally (Teuling et al., 2009), and 90% in Australia when averaged over the continent (Glenn et al., 2011). Transpiration is the largest contributor to terrestrial ET (Dirmeyer et al., 2006; Lawrence et al., 2007) and recent studies have estimated it accounts for up to 80-90% of global ET (Jasechko et al., 2013; Miralles et al., 2011), although there are large differences among estimates (Sutanto et al., 2014).

ET cannot be measured directly and global and regional ET trends have thus remained poorly constrained due to a lack of suitable long-term observations (Douville et al., 2013). Multiple methods have been employed to estimate actual and potential ET, including satellite retrieval schemes (Courault et al., 2005; Glenn et al., 2011), land surface models (Douville et al., 2013; Li and Mölders, 2008; Teuling et al., 2009), empirical formulations (Wang et al.,

2010; Zeng et al., 2012; Zhang et al., 2004), pan evaporation (Brutsaert, 2013; Liu et al., 2009; Roderick and Farquhar, 2002) and hydrometric (Nouri et al., 2013) and water balance (Zhang et al., 2012) methods. Satellite retrieval schemes include thermal and vegetation index based methods (reviewed in e.g. Glenn et al., 2011a) and, like land surface models (LSM), generally rely on well-known theoretical formulations, including the Penman-Monteith and Priestley-Taylor equations, to derive ET from land surface and meteorological variables (Wang and Dickinson, 2012). LSMs and satellite retrieval models provide continuous spatial fields of ET but there are large disagreements between different models due to specific formulations and parameterisations (Wang and Dickinson, 2012). Hydrometric methods include lysimeter, sapflow and eddy covariance measurements (amongst others reviewed in Nouri et al., 2013). They remain the most direct measurements of ET but are restricted to stand- to site-scales. *In situ* eddy covariance measurements of latent heat flux from flux towers (e.g. Baldocchi et al., 2001) have been widely used for calibrating remotely sensed ET products (Glenn et al., 2011) and to evaluate large-scale models and datasets (e.g. Jung et al., 2009). Empirical and statistical formulations include the Budyko framework (Budyko, 1974; Zhang et al., 2004), which relies on the concept of energy and water availability and can be applied to annual and longer time scales. Other statistical methods include e.g. regression-based models (Zeng et al., 2012). Pan evaporation measurements have been used to estimate potential ET (Roderick et al., 2009), but these only very indirectly relate to actual ET, and are restricted to site scales.

At the ecosystem scale, the water balance method (the difference between observed precipitation and runoff integrated over a river basin) remains the most firmly observationally based estimator of ET. The method assumes no net changes in soil moisture and is thus only applicable at annual or longer time scales when these changes can be assumed to be relatively small. Soil moisture can in principle drive interannual variability in ET (as much as it is a consequence of it) (Seneviratne et al., 2010) but studies have shown that soil moisture is mainly controlled by precipitation (Sheffield and Wood, 2008), explicitly included in the water balance method. Attempts to account for soil water changes have emerged to apply the method to sub-annual time scales, notably the use of gravity field measurements from the Gravity Recovery and Climate Experiment (GRACE) satellite mission to obtain monthly changes in terrestrial soil water storage (e.g. Seoane et al., 2013; Zeng et al., 2012). However, GRACE temporal coverage remains short (~13 years) and the spatial resolution relatively coarse (1º × 1º; http://grace.jpl.nasa.gov) rendering it unsuitable for many long-term catchment-scale studies (Werth and Günther, 2010). Despite good availability of global precipitation and runoff datasets, the water-balance method has not been widely employed to explore historical trends in actual ET globally.

1.1.2. Australian hydrology and ecosystems

Australia is the driest inhabited continent as measured by runoff per unit area (McMahon et al., 1992). The majority of the country is arid or semi-arid with potential ET (PET) exceeding precipitation, but in some coastal locations annual precipitation exceeds 3000 mm (Figure 1.1.). Precipitation over the continent is extremely variable year-to-year and interannual runoff variability over the continent is twice that typical for the Northern Hemisphere (Chiew and McMahon, 1993). Interannual variations in climate are strongly driven by coupled ocean-atmosphere modes, particularly the El Niño Southern Oscillation (ENSO; Risbey et al., 2009). The continent is prone to climate extremes, including flooding and droughts (Alexander and Arblaster, 2009); the "Millennium drought" over eastern Australia during 2001-2009 (van Dijk et al., 2013) and extensive flooding in Queensland during the strong 2010/2011 La Niña (Bureau of Meteorology, 2012) are recent examples. Water resources in Australia have been identified as particularly vulnerable to climate change effects (Preston and Jones, 2008b), arising from the aridity of the continent, extreme climate variability and increasing water demand by the growing population (Jones et al., 2008; Preston and Jones, 2008a), and the country has been identified as a likely hot spot for future water scarcity (Prudhomme et al., 2014). The population is largely concentrated on coastal and inland eastern and southwestern Australia, as are agricultural activities that typically rely on irrigation and represent 65-70% of Australia's water consumption (http://www.irrigators.org.au/?page=facts).

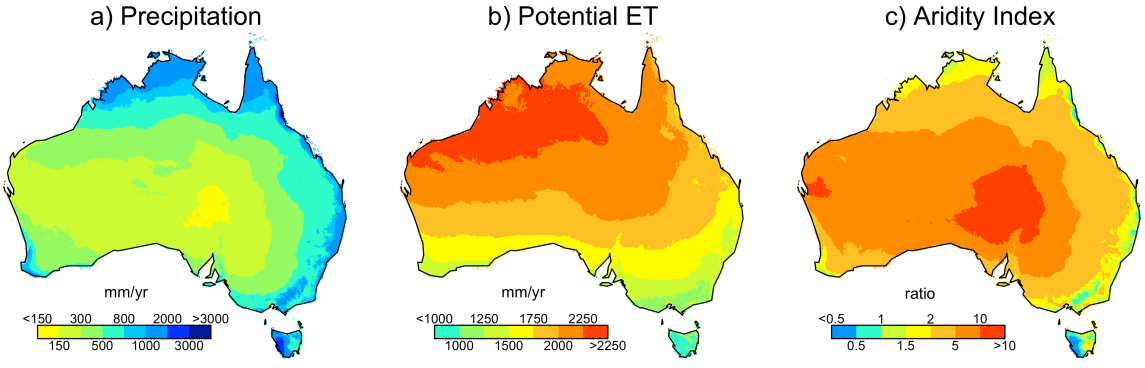

Figure 1.1. a) Mean annual precipitation (P), b) Priestley-Taylor potential ET and c) climatological aridity index (PET/P) across Australia. The data show the 1982-2010 mean derived from the ANUCLIM climate archive (Xu and Hutchinson, 2013).

Australia is characterised by a large variety of climate regimes and ecosystems. Central and western Australia is arid and supports only sparse shrub- and grassland vegetation (Figure 1.2.). Precipitation arrives mainly in the form of infrequent storms (Risbey et al., 2009). Northern Australia has a highly seasonal monsoonal climate with a distinct winter dry season and summer wet season and is dominated by savanna ecosystems (Whitley et al., 2011). Southwestern Australia has a Mediterranean climate with dominant winter rainfall and interannual variations in climate are strongly influenced by the Southern Annular Mode (Risbey et al., 2009, 2013). East coast Australia receives seasonally uniform rainfall and vegetation varies from tropical evergreen forests in the north to temperate evergreen forests in the south (Figure 1.2.). The effects of ENSO are particularly pronounced in eastern Australia. Australian ecosystems are also characterised by frequent fire with *ca.* 6.4% of the continent burning annually and around 91% of the area experiencing fire periodically (Bradstock et al., 2012), with consequences for vegetation composition and hydrology.

High quality long-term records of runoff and climate are available the continent and, together with a large variety of climatic and vegetation regimes represented in Australia, make it an ideal study case for climate change effects on hydrology and vegetation. Previous studies have also indicated the continent may play a regional to global role in controlling carbon (Poulter et al., 2014) and water cycling (Jung et al., 2010) and changes to Australian ecosystems and hydrology might thus have wider consequences.

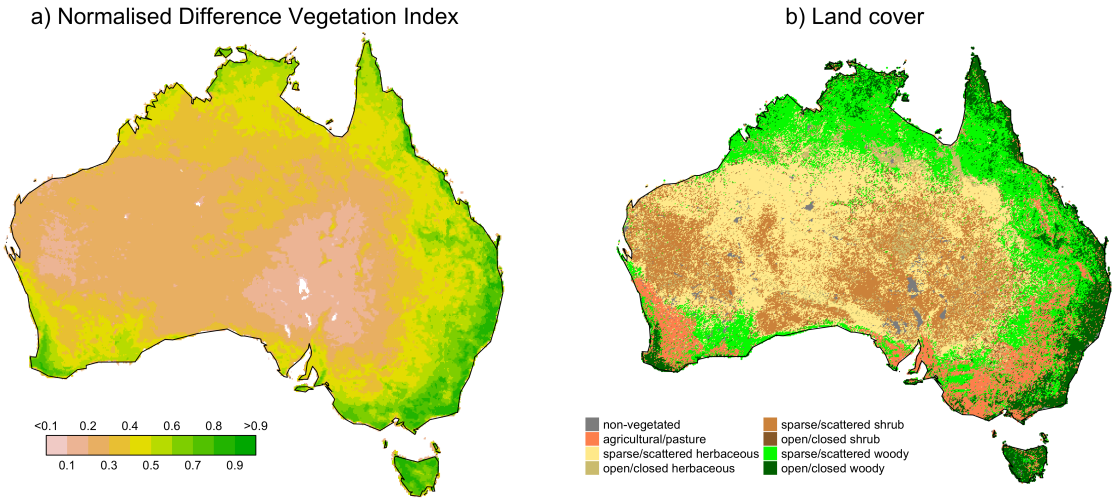

Figure 1.2. a) Mean annual Normalised Difference Vegetation Index. The data show the 1982-2010 mean derived from the GIMMS NDVI3g dataset (Pinzon and Tucker, 2014). b) Major land cover types derived from the Dynamic Land Cover Dataset of Australia (Lymburner et al., 2011).

1.2. Controls on evapotranspiration and runoff

1.2.1 Climate

Climate, above all precipitation, is the dominant driver of terrestrial ET and runoff globally (e.g. Dai et al., 2009; Gerten et al., 2008; Milliman et al., 2008) and in Australia (van Dijk et al., 2013; Glenn et al., 2011; Petrone et al., 2010). Energy and water availability are considered the first-order drivers of ET and runoff (Robock and Li, 2006; Teuling et al., 2009) and the relationship over annual to multi-annual time scales has widely been described using the empirical Budyko framework (Budyko, 1974; Zhang et al., 2004). Many formulations of the framework exist (e.g. Choudhury, 1999; Fu, 1981; Pike, 1964). The Fu-Zhang equation (Zhang et al., 2004) predicts actual ET (E_a) from precipitation (P) and PET using the climatic aridity index (AI; PET/P) (Figure 1.3):

$$Ea = P\left[1 + AI - (1 + AI^{\omega})^{1/\omega}\right] \quad (1)$$

where ω is the framework parameter representing catchment properties such as soil, topography and vegetation (Yang et al., 2007; Zhang et al., 2004). PET represents atmospheric water demand and the capacity for ET when water is not limiting, and (depending on the formulation) accounts for the effects of net radiation, air temperature and wind speed. It is a useful indicator of ecosystem conditions together with P and determines the upper limit for actual ET, which by definition never exceeds PET. In regions where precipitation is greater than PET, actual ET is assumed to be limited by the amount of available energy. Conversely, when PET exceeds precipitation, actual ET is limited by water supply and regions become progressively more water-limited with increasing aridity. Several studies have used the concept of demand and supply limitation to investigate the effects of climate on ET and/or runoff (Donohue et al., 2011; Hickel and Zhang, 2006; Teuling et al., 2009) and found a strong empirical fit between observed water-balance ET and the framework, particularly in arid regions.

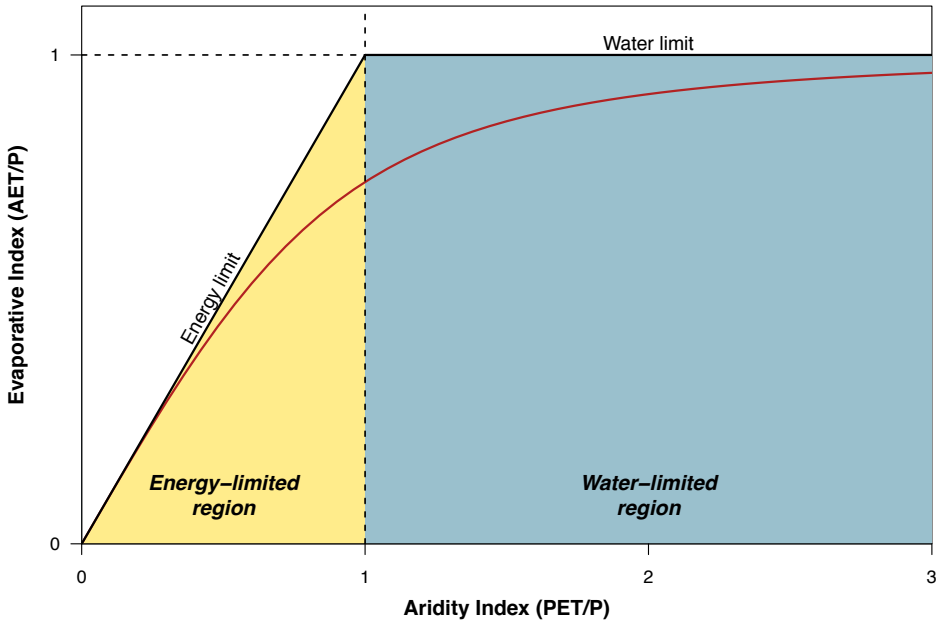

Figure 1.3. Illustration of the Budyko framework. The red line represents the fitted Budyko relationship using the Fu-Zhang formulation (Zhang et al., 2004) and a parameter value of 3.0.

In common with actual ET, many methods have been developed for estimating PET. Widely used formulations include the Priestley-Taylor equation (Priestley and Taylor, 1972) and the 'combination' Penman (Penman, 1948) and Penman-Monteith (Monteith, 1965) equations. The Priestley-Taylor equation determines PET as a function of net radiation (R_n) and air temperature (T_a) (all equations as given in Fisher et al., 2011):

$$PET = \alpha \frac{\Delta}{\Delta + \gamma} R_n \tag{2}$$

where α is an empirical constant, usually taken to be 1.26, Δ is the slope of the saturation vapour pressure curve (a function of T_a), and γ the psychrometric constant (0.066 kPa K^{-1} at sea level). Equilibrium evaporation (E_q) denotes evaporation from a well-watered surface in the absence of advection (Eichinger et al., 1996; Fisher et al., 2011), and depends only on net radiation and temperature; the Priestley-Taylor PET is 1.26 E_q. The Penman equation extends Equation (2) to include atmospheric components D (vapour pressure deficit) and u (wind speed):

$$PET = \frac{\Delta}{\Delta + \gamma} R_n + 2.6 \frac{\gamma}{\Delta + \gamma} D\gamma\lambda\rho(1 + 0.54u) \tag{3}$$

where λ is the latent heat of vaporisation (2.448 MJ kg^{-1}) and ρ is air density (1.234 kg m^{-3}). Monteith provided a variation on this equation with a stronger theoretical basis, including resistance terms – this is the Penman-Monteith (P-M) equation

$$AET = \frac{\Delta R_n + c_p \rho D / r_a}{\Delta + \gamma + \gamma(r_s / r_a)} \quad (4)$$

where r_a is aerodynamic resistance, r_s stomatal resistance and c_p the specific heat of air. The P-M equation has a clear physical basis (Allen, 2005) and considers a comprehensive set of drivers. However, the equation requires the estimation of stomatal and aerodynamic resistance terms, which are difficult to measure, cannot be calculated from standard meteorological data, and render the formulation strongly dependent on vegetation properties. Furthermore, the equation is only applicable for estimation of PET when r_s can be assumed to be negligible, either over well-watered vegetation or open water (Fisher et al., 2011). The so-called FAO P-M formulation (Allen et al., 1998) is a widely used derivation of the original P-M equation used to estimate crop 'reference ET', but whilst it removes the need to estimate resistance terms, it was specifically designed for low grass vegetation, and lacks the physical basis of the original P-M equation.

There is no general agreement about the 'correct' formulation of PET. This thesis employs the Priestley-Taylor formulation throughout, as it has been shown to be appropriate for estimation of large-scale PET, and has minimal data requirements. Although Priestley-Taylor began as an empirical approximation, Raupach (2000, 2001) provided a theoretical basis for it. He demonstrated the suitability of Priestley-Taylor for large-scale PET whereby mean D over a large area is a function of ET itself modified by convective boundary layer growth; whereas P-M is appropriate for estimation of ET at a point, when D can be considered as an external variable. The parameter α was obtained empirically (Priestley and Taylor, 1972) but the value of 1.26 has been shown to agree with theoretical derivations (Eichinger et al., 1996; Raupach, 2000, 2001) and is consistent with the observation that the E_q term of Equation (3) is generally larger than the second atmospheric term (commonly four to five times; Penman, 1948; Shuttleworth, 1991). Furthermore, α accounts for advective processes not considered in the Penman formulation, which is prone to underestimating PET in areas of strong advection (Chang, 1968). Many other studies (e.g. van Dijk et al., 2012; Guerschman et al., 2009; Potter and Zhang, 2009; Potter et al., 2005; Shao et al., 2012; Zhang et al., 2004) have also adopted the Priestley-Taylor method for catchment-scale analysis.

1.2.2. Vegetation and land use

1.2.2.1. CO_2- and climate-induced vegetation processes

CO_2 effects on vegetation productivity and water use at the leaf-scale are relatively understood well from experiments (Ainsworth and Long, 2004; Field et al., 1995; De Kauwe et al., 2013; Leakey et al., 2009; Nowak et al., 2004; Wong et al., 1979). Elevated CO_2 allows plants to close their stomata partially, whilst maintaining a similar influx of CO_2 for photosynthesis. This increases water use efficiency, the amount of water required to produce a unit of biomass, and reduces the transpiration flux. On the other hand, CO_2 is the substrate for photosynthesis and elevated concentrations should stimulate carbon assimilation, in principle leading to increased biomass and leaf cover ('greening'). This CO_2 fertilisation effect increases water use at the canopy scale, counteracting leaf-level water savings from partial stomatal closure. Possible secondary effects of CO_2-induced vegetation structural changes include changes to interception evaporation due to increased canopy cover whereas shading by increased foliage cover may decrease the amount of radiation reaching the soil surface, reducing soil evaporation. The CO_2 effects are expected to vary with aridity and vegetation type. They should manifest most strongly in water-limited environments, where moisture is the main limitation on vegetation growth (Donohue et al., 2013). Furthermore, both experiments and theory show that C_3 plants, typical in wetter, colder climates, should show more pronounced responses to elevated CO_2 than C_4 plants, common in hot, arid climates (Leakey et al., 2009).

Despite clear experimental evidence about the underlying processes, the magnitude of CO_2-induced greening and water savings at catchment to global scales, and the net effect on ET and runoff, remain poorly constrained. Multiple attempts have appeared (Betts et al., 2007; Gedney et al., 2006; Gerten et al., 2008; Piao et al., 2007) but have generally relied on models, which have tended to disagree on the direction and magnitude of the CO_2 effect (Alkama et al., 2011).

Furthermore, climate change may also have wider implications for vegetation composition and function, with consequences for hydrology. Vegetation is very sensitive to changes in climate, including precipitation and temperature, and changes in climatic conditions may alter vegetation biomass, productivity and composition (Diffenbaugh and Field, 2013; Friend et al., 2014). Higher temperatures may enhance plant growth in colder regions, but decrease productivity in warmer regions through increased aridity. Increased CO_2 is likely to favour C_3 plants, increasing the distribution of woody vegetation in regions currently dominated by

mainly herbaceous C_4 plants. Moreover, changes in fire, an important landscape process in Australia, may change vegetation composition and functioning (Kelley and Harrison, 2014). The impact of these processes on, and their interactions with, hydrology remain poorly understood.

1.2.2.2. Land use and land cover change

Humans have altered at least 40% of the Earth's land surface (Sterling and Ducharne, 2008) and greatly reduced the world's natural vegetation cover through clearing of woody vegetation for the expansion of croplands and pasture (Sterling et al., 2012). Cleared lands have actual ET rates a third lower than forests in a range of climates (Zhang et al., 2001) due to decreased transpiration and interception losses as a result of deforestation (Bradshaw et al., 2007; Gordon et al., 2005). Gordon et al. (2005) estimated deforestation has reduced global terrestrial vapour flows by 4%, with the largest reductions in the tropics, central Europe, eastern USA and China. This is in agreement with an estimate of 5% later proposed by Sterling et al. (2012), with largest contributions from non-irrigated croplands (–3.5%) and grazing land (–2.8%). The decreased ET should in principle increase runoff (Bosch and Hewlett, 1982) if precipitation remains unchanged but deforestation may also lead to reduced rainfall (D'Almeida et al., 2007). On the other hand, widespread irrigation in dry regions has led to water withdrawals from rivers and increased water availability for ET, and whilst this should decrease runoff, irrigation may also increase regional precipitation (Lo and Famiglietti, 2013). These interactions are further complicated by potential changes to albedo and surface temperature, roughness and convective processes, and adding to the complexity of land use/land cover change feedbacks with the hydrological cycle (Strengers et al., 2010). Land cover processes may also contribute to climate extremes. Teuling et al. (2010) reported higher initial evaporation over grasslands compared to forest ecosystems during the 2003 European heat wave and drought. This led to accelerated soil moisture depletion in grasslands, and a subsequent shift from suppression of temperatures due to evaporative cooling to increased heating, likely contributing to the extreme temperatures observed.

1.3. Historical and future water resources

1.3.1. Historical changes

1.3.1.1. Precipitation

Precipitation is a key climatic variable and recent trends in global and regional land precipitation have received much attention in the literature. It is generally agreed that rising temperatures should increase global aggregate precipitation following the Clausius-Clapyeron relationship on temperature and water vapour scaling. The latest IPCC assessment report (AR5; Hartmann et al., 2013) compared four precipitation datasets for the period 1901-2008 with three out of four datasets showing significant global upward trends varying between 1.01 and 2.77 mm yr^{-1} per decade. This is in contrast to the fourth assessment report (Trenberth et al., 2007), which found few significant global trends across six land precipitation products during 1950-2005 (Trenberth et al., 2007). Whilst different precipitation products generally agree on broad large-scale trends and spatial patterns, they often show significant differences regionally (Fekete et al., 2004). The AR5 shows robust increases in much of conterminal USA, southern South America and western Europe throughout the 20^{th} century, and decreases in eastern Australia and the Mediterranean region since the 1950s. More generally, decreases have occurred in subtropical and non-monsoonal tropical regions and increases in high northern latitudes (Trenberth, 2011). Furthermore, regional changes in precipitation intensity and frequency have been observed. The AR5 concludes likely increases in precipitation intensity and frequency in Europe, North and South America but trends remain unclear elsewhere (Collins et al., 2013). Changes to seasonal distribution have also been observed with a tendency towards wetter wet seasons in humid regions and drier dry seasons in more arid regions (Chou et al., 2013).

In Australia, precipitation changes have been mainly seasonal and vary regionally. A number of recent studies have reported declines in autumn and winter precipitation over southern and southwestern Australia since the 1950s (Hendon et al., 2007; Nicholls, 2006, 2010), due to a reduction in extratropical storms consistent with the upward trend in the Southern Annular Mode (Delworth and Zeng, 2014). These reductions have also translated to annual scales due to the region's dominant winter precipitation regime. Annual rainfall has increased in the north due to increased wet season (summer) rainfall and decreased along the east coast between 1950 and 2005, although the east coast trends are less robust and sensitive to the choice of time period (Nicholls, 2006).

The uncertainties in global and regional precipitation estimates arise from incomplete observations and methodologies and have been extensively discussed in the literature (New et al., 2001; Trenberth, 2011). Many global land precipitation products have been developed. The most widely used gridded precipitation products (e.g. Harris et al., 2014; Schneider et al., 2008) rely on interpolation of *in situ* rain gauge measurements, which measure precipitation quantities directly but have variable spatial and temporal coverage and do not necessarily capture spatial variability well particularly in areas of complex topography (Adam et al., 2006). Precipitation gauges also suffer from systematic biases due to gauge undercatch leading to underestimation of precipitation typically by 10% (Legates and Willmott, 1990) and greater for snowfall (up to 100% for some events; Bogdanova et al., 2002). Some precipitation products correct for these biases (e.g. Weedon et al., 2011) but it is likely to remain a source of uncertainty particularly in snow-prone regions. Satellite products have been developed to provide complete spatial coverage but do not offer temporal coverage beyond 1974 (New et al., 2001). Furthermore, they only measure instantaneous rates of precipitation and algorithms used to convert radiometric measurements to precipitation at the surface remain uncertain (Krajewski et al., 2010; Trenberth, 2011). Merged satellite-gauge products (e.g. the Global Precipitation Climatology Project; Adler et al., 2003) have been developed to overcome limitations of each method but discrepancies between different precipitation datasets persist, particularly in data-poor regions including arid and tropical regions, hindering efforts to detect large-scale precipitation trends (New et al., 2001).

1.3.1.2. Evapotranspiration

As ET cannot be measured directly, the detection of long-term ET trends has largely relied on models or indirect evidence such as pan evaporation. Several studies have reported decreasing pan evaporation in many parts of the world (Brutsaert, 2006; Roderick and Farquhar, 2002); this has been attributed to reductions in solar radiation due to increased aerosol loads and assumed to indicate decreased actual ET (Roderick and Farquhar, 2002). The significance of pan evaporation as an indicator of actual ET has, however, remained debated and Brutsaert (2006) showed decreasing pan evaporation was in fact consistent with increasing actual ET and reported a global trend of 0.44 mm yr^{-2} during 1950-2000 based on pan evaporation and meteorological data. Elsewhere Zhang et al. (2012) reported a significant global increasing trend of 1.09 mm yr^{-2} over land during 1983-2006 using the Penman-Monteith (P-M) equation (Leuning et al., 2008) and 0.53 mm yr^{-2} using a model-tree ensemble (Jung et al., 2009). They also illustrate the uncertainties in radiation products used

to determine ET and using the P-M formulation and three alternative radiation datasets calculate a global trend varying between 0.28 and 1.65 mm yr^{-2}. Jung et al. (2010) showed a positive trend in global land ET of 0.7 mm yr^{-2} between 1982 and 1997 but no trend 1998 onwards. The recent halt was attributed to decreased moisture availability in the Southern Hemisphere (Jung et al., 2010) and a shift to El Niño conditions (Miralles et al., 2013). Many studies report global trends for the post-1982 satellite era and ET changes earlier in the 20th century remain uncertain.

Whilst global estimates point to increasing ET, regional patterns remain poorly constrained (Wang et al., 2010). Teuling et al. (2009) analysed water-balance ET trends in Europe and North America. They report a decrease in Europe during 1958-1982 and subsequent increases and attribute this to changing aerosol loads (the so-called "dimming and brightening" phenomenon; Wild et al., 2005). They attribute mid-century increases and subsequent decreases in North America mainly to precipitation. Zeng et al. (2012, 2014) produced global ET datasets using a statistical and a model-tree ensemble method, respectively, and report significant increases in much of sub-Saharan Africa, northern Canada and Siberia, and eastern Europe. Contrary to Teuling et al. (2009), they do not report significant trends in most of North America or Europe. In Australia, Roderick and Farquhar (2004) reported decreasing pan evaporation trend of –4 mm yr^{-2} during 1970-2002 and argue it is due to decreased atmospheric demand resulting from reduced net radiation, vapour pressure deficit and/or wind speed indicating the continent has become less arid. However, they do not relate their findings to actual ET.

The discrepancies between different ET methods at catchment to global scales (Fisher et al., 2011; Zhang et al., 2012) have resulted in large uncertainties in the recent evolution of terrestrial ET. This has also hindered the attribution of ET changes to specific processes (Douville et al., 2013). Historical ET trends thus remain a topic of further research.

1.3.1.3. Runoff

Several studies have reported global runoff trends based on observations and models. Based on 221 river basins, Labat et al. (2004) reported a 4% increase in runoff per 1ºC rise in temperature globally, amounting to a 0.18 mm yr^{-2} increase during the 20th century (Alkama et al., 2010). Their finding is in agreement with Piao et al. (2007) and Alkama et al. (2010) who report a global trend of 0.17 mm yr^{-2} and 0.19 mm yr^{-2}, respectively, for the same period using the ORCHIDEE land surface model (Krinner et al., 2005). However, the findings

of Labat et al. (2004) have been brought into question due to the wavelet method used to reconstruct runoff time series from limited observational records, and failure to account for anthropogenic effects (Legates et al., 2005; Peel and McMahon, 2006). Their results have not been reproduced in later studies. Dai et al. (2009) considered trends in the world's largest 925 river basins corresponding to 80% of global ocean-draining area and find statistically significant trends in only a third of the 200 largest basins during 1948-2004, with 70% of those downward trends. Earlier studies support the lack of persistent trends in large river basins (Cluis and Laberge, 2001; Lammers et al., 2001; Pekarova et al., 2003), but robust regional increases have been reported over parts of the Americas (Dai et al., 2009; Groisman et al., 2001; Lins and Slack, 1999; Milliman et al., 2008) including Mississippi and Parana, and reductions in Southern Europe (Milliman et al., 2008). Other studies have reported increased streamflow in arctic rivers (Peterson et al., 2002), possibly due to increased snowmelt (Dai et al., 2009).

Most studies have shown the trends are primarily climate-driven (Dai et al., 2009; Gerten et al., 2008; Milliman et al., 2008). Piao et al. (2007) attributed 53% of runoff variations simulated using the ORCHIDEE model during the 20th century to climate and Gerten et al. (2008) reported a value of 70% based on the LPJmL vegetation model (Rost et al., 2008). More recently, Gedney et al. (2014) showed based on the JULES land surface model (Best et al., 2011) that reduced shortwave radiation due to atmospheric aerosol loading decreased runoff in the Northern Hemisphere up to 25% until the 1980s. Previously, based on the Labat et al. (2004) streamflow dataset and the MOSES II Land Surface Model (Essery et al., 2003), Gedney et al. (2006) attributed the global increase to CO_2-induced vegetation physiological effect with a minimal contribution from climate; however, their study has been criticised for the streamflow dataset used (Peel and McMahon, 2006) and for not considering potential CO_2-induced increases in foliage cover which can counteract water savings from decreased stomatal conductance (Piao et al., 2007). On the other hand, Piao et al. (2007) showed land use change can explain 50% of historical runoff increases and is of comparable magnitude with climate (see above). Their findings are supported by Sterling et al. (2012) who project a 6.8% increase in runoff during 1950-2000 due to land surface changes also using the ORCHIDEE model.

In Australia, Chiew and McMahon (1993) investigated trends across 30 unimpaired Australian basins during varying periods of at least 25 years and found significant trends in only two basins. Later studies agree on significant reductions in runoff (*ca.* 10-20%) in southwestern parts of the country since the 1970s (McFarlane et al., 2012; Petrone et al., 2010). Runoff began declining in the 1970s in response to a step reduction in precipitation

and despite no significant changes in precipitation since the early 1990s, runoff has continued to decline to the 21st century. Petrone et al. (2010) suggest this may be due to falling water tables and a shift from perennial to ephemeral streams, reducing runoff generation.

Alkama et al. (2011) discuss reasons for the discrepancies in runoff trends and identify observational and methodological uncertainties hindering the detection and attribution of recent runoff trends. River discharge observations remain spatially scarce and the length and quality of records is variable. Gaps in the data are typically filled using statistical methods or simulated values (Dai et al., 2009; Labat et al., 2004), rendering time series uncertain when large number of gaps are filled. Furthermore, streamflow is calculated from an empirical relationship between measured river stage and discharge, and is prone to errors, particularly in rivers with varying channel conditions (Alkama et al., 2011) and due to gauge bypass during high flows (Wilby, 2006). Observational uncertainties are compounded by discrepancies in hydrological models, which have been widely employed to attribute observed trends and to create continuous fields of runoff where observations are not available (Alkama et al., 2013; Dai et al., 2009; Gedney et al., 2006; Piao et al., 2007). Furthermore, these models do not generally simulate human influences such as damming and irrigation water withdrawals, but they may account for a large proportion of streamflow and these effects must thus be carefully evaluated and removed from observations (Peel and McMahon, 2006). Different studies have investigated trends over varying time periods hindering comparison between studies and due to the relatively short observational period in many river basins, the results are sensitive to the choice of time period (Dai et al., 2009).

1.3.1.4. Vegetation

Many studies have reported vegetation trends for the post-1981 satellite era relying on remotely sensed vegetation indices, such as the Normalised Difference Vegetation Index (NDVI). Global Advanced Very High Resolution Radiometer (AVHRR) NDVI records extend to early 1980s and have been widely to investigate long-term changes in vegetation properties, including foliage cover, productivity, biomass and structure (Beck et al., 2011 and references therein). Other vegetation indices have since been developed, such as the Enhanced Vegetation Index (EVI), to overcome some of the problems associated with NDVI, including saturation at high foliage cover (Glenn et al., 2008), and are available at a much finer spatial resolution than AVHRR NDVI. However, EVI records do not extend beyond 2000

and AVHRR NDVI datasets thus remain the longest continual global record of vegetation for investigating long-term climate change effects on vegetation.

Using AVHRR NDVI, Myneni et al. (1997) reported increased vegetation growth in high northern latitudes between 1981 and 1991 in response to a lengthening of the growing season. This was supported by an increased amplitude of seasonal atmospheric CO_2 variations and earlier drawdown of CO_2 during spring. Lucht et al. (2002) attributed the high-latitude greening to increasing temperatures using the LPJ dynamic global vegetation model, with a temporary decline in the trend in the years following the Pinatubo eruption. In the tropical regions, Zhou et al. (2014) reported a widespread decline in forest greenness in the Congo basin since 2000 due to reduced water availability based on MODIS (MODerate resolution Imaging Spectroradiometer) EVI and NDVI data. Earlier studies have shown extensive, persistent declines in Amazonian forest greenness during the 2005 and 2010 droughts, demonstrating the vulnerability of tropical forests to climate disturbances (Saatchi et al., 2013; Xu et al., 2011; Zhou et al., 2014). Elsewhere, Beck et al. (2011) compared four global NDVI datasets during 1982-1999 and reported consistent decreases in vegetation cover in eastern Australia and increases in western Australia and the northern tundra belt. The datasets only moderately agreed on increases in North America and decreases over southeast Asia but were inconsistent over Europe and Africa. Los (2013) showed generally increasing NDVI globally since 1982 and attributed this to a CO_2 fertilisation effect. Recently, Donohue et al. (2013) reported an increase of 11% in foliage cover due to increased CO_2 across world's warm, arid regions where vegetation is predominantly water-limited. In Australia, Donohue et al. (2009) showed a continent-wide increase in vegetation cover of 8% over 1981-2006, most of which resulted from increased non-deciduous perennial vegetation. They attributed the increase mainly to precipitation, which rose by 7% over the same time period.

1.3.2. Projected future changes

1.3.2.1. Precipitation

Global climate models (GCM) project robust increases in air temperature and it is expected global aggregate precipitation over land and oceans will also increase by 1-3% per 1ºC temperature rise (Collins et al., 2013; Li et al., 2013; Roderick et al., 2014). Models from the latest CMIP5 model intercomparison project show precipitation sensitivity to temperature is lower over land than oceans, and tropical land than extratropical land (Li et al., 2013).

Precipitation changes will, however, vary regionally, with the contrast between wet and dry regions and seasons projected to increase (Collins et al., 2013). Likely increases are projected in high and moist mid-latitudes of the Northern Hemisphere, resulting from increases particularly during autumn and winter and decreases in many dry mid-latitude regions, leading to a general tendency of wet areas getting wetter and dry drier in the mid- to high latitudes (Collins et al., 2013; Trenberth et al., 2007). Precipitation in subtropical arid and semi-arid regions is projected to decline, strongly in southwestern Australia, South Africa and the Mediterranean but less so over Asia (Trenberth, 2011), largely due to seasonal reductions during winter and spring. Tropical precipitation increases are greatest in regions that are already wet, with summer rainfall projected to increase more than winter (dry) season rainfall (Li et al., 2013). However, despite recent advances in modelling techniques, specific regional patterns remain poorly constrained, partly due to differences between models but equally due to model internal variability. This is particularly true in regions where small changes are projected (Deser et al., 2010, 2012). In Australia, reductions are projected in southern and particularly southwestern Australia and arise from reductions in winter and spring precipitation. Elsewhere, changes are uncertain or within the limits of current interannual variability (Knutti and Sedláček, 2012).

1.3.2.2. Evapotranspiration and runoff

GCMs predict robust increases in ET over oceans and similar patterns to precipitation over land (Collins et al., 2013) with increases particularly in mid- and high northern latitudes. However, GCMs suffer from systematic biases in their simulation of runoff and ET (Hagemann et al., 2013) and cannot reproduce the fine-scale processes regulating terrestrial hydrology (Hempel et al., 2013; Prudhomme et al., 2014) and it has thus been common practice to project future water resources using hydrological models forced with GCM-produced climatology. Using a set of hydrological and biome models from the Inter-sectoral Impact Model Intercomparison Project (ISI-MIP), Davie et al. (2013) projected decreases in runoff in central America, southern Australia and the Mediterranean and increases in northern high latitudes and India from the model ensemble. However, they report a large inter-model spread leading to significant uncertainties particularly in the tropics and parts of northern mid-latitudes. The biome models, capable of simulating dynamic CO_2 effects and vegetation functioning, tended to produced larger increases and smaller decreases in regional runoff but the magnitude of the CO_2 effect was not consistent across all models. The findings of Davie et al. (2013) are in general agreement with Hagemann et al. (2013) who projected reductions in northern and southern subtropical zones, particularly southern Africa,

Australia and China as well as the Mediterranean region based on eight hydrological models. Hagemann et al. (2013) and Haddeland et al. (2013) also show the uncertainty resulting from the choice of hydrological model is comparable to or larger than uncertainties arising from GCMs in some regions.

Several studies have also investigated vegetation and hydrological responses in doubled CO_2 experiments. All but the lowest emissions scenarios predict a doubling (or more) of atmospheric CO_2 by the end of the 21st century (van Vuuren et al., 2011) and whilst doubled-CO_2 experiments should not be considered as projections *per se*, they offer a useful method for isolating future ecosystem responses to rising CO_2 from climate impacts (Leipprand and Gerten, 2006). Such studies have generally pointed to decreased ET and increased runoff globally (Betts et al., 2007; Kergoat et al., 2002; Leipprand and Gerten, 2006; Li and Mölders, 2008), but pronounced regional differences exist. In colder temperature-limited regions, the tendency is towards decreased ET but in semi-arid regions simulated CO_2 fertilisation tends to increase ET, though the responses are also seasonal in nature (Leipprand and Gerten, 2006).

1.3.2.3. Vegetation

Future vegetation responses to changing climate and CO_2 remain highly uncertain in part due to poorly quantified feedbacks between the biosphere and climate system (Friend et al., 2014). Cramer et al. (2001) simulated future vegetation types and productivity based on six global dynamic vegetation models (DGVM) and projected increased net ecosystem productivity in mid- to high northern latitudes and decreases in the tropical regions, partly due to expansion of grassland and savanna biomes. Sitch et al. (2008) compared five DGVMs, which were shown to agree on increased global productivity during the 21st century mainly in response to increased CO_2 but regional patterns in vegetation cover remained highly uncertain between different models. The study also showed the models produce larger discrepancies in their response to changing climate than CO_2. Friend et al. (2014) similarly reported CO_2-induced increases in vegetation carbon globally but regional decreases including southwestern Australia, southern Mediterranean regions and southwestern Africa and large model discrepancies in areas including the Amazon and much of USA and Australia. By contrast, Kelley and Harrison (2014) reported increased net primary productivity in Australia mainly due to CO_2 fertilisation, accompanied by an increase of 10% in carbon storage despite increased wildfire by the end of the 21st century.

Several studies have also investigated vegetation dynamics under doubled or quadrupled CO_2. Kergoat et al. (2002) simulated modest increases in global leaf area index under doubling CO_2, driven by significant increases in mid- and high northern latitudes mainly due to increased temperature. This is in agreement with Notaro et al. (2007) who projected increased grass and tree cover in the Northern Hemisphere (6.1% and 0.5%, respectively) and increased tree cover in Southern Hemisphere (0.9%) over a 144 year simulation period reaching quadrupled CO_2 concentration compared to the 1975 level of 335 ppm. In Australia as well as Amazonia and South Africa, the study simulated decreased forest cover due to soil drying. By contrast, O'Ishi et al. (2009) simulated increased vegetation cover in semi-arid subtropical zones and expansion of woody vegetation into sparsely vegetated regions under quadrupled CO_2, leading to a 13% increase in global temperature due to reduced surface albedo.

1.4. Thesis approach

This thesis aims to improve our understanding of water-vegetation interactions at regional scales. In particular, it attempts to better constrain the effects of elevated CO_2 on catchment-scale hydrology, which has remained poorly constrained due to model uncertainties. To overcome this, the thesis relies on observations to the maximum extent possible, reflected in the use of water-balance ET throughout. The thesis mainly concentrates on ET as studies of ET trends have been far fewer than runoff and ET directly interacts with, and results from, vegetation and climate processes. The thesis first investigates ET trends globally, before concentrating on Australia to make use of high quality hydrological data available for the continent. Each thesis chapter is written as a journal article, either published, in review or submitted.

The first chapter statistically accounts for historical water-balance ET trends globally during 1961-1999. A comprehensive analysis of global water-balance ET trends has been lacking, despite good availability of global runoff and precipitation datasets. Moreover, many studies have investigated the controls on large-scale ET but often concentrating on a limited set of potential drivers. This chapter simultaneously considers all key drivers of ET proposed in the literature, derived from observations with the exception of vegetation information simulated with the widely-used Land surface Processes and eXchanges (LPX) dynamic global vegetation model.

The second chapter quantifies the effects of rising CO_2 on vegetation and hydrology across 190 river catchments in Australia. To the authors' knowledge the study represents the first attempt to account for catchment-scale hydrological effects of elevated CO_2 based on observations alone. It makes use of principles derived from a novel ecological framework and simultaneously considers responses in vegetation and ET based on clear hypotheses about underlying processes.

The third chapter presents projections of future water resources in Australia. The LPX model was successfully evaluated against observed CO_2 effects from Chapter 2 and employed to simulate future ET and runoff and evolution of CO_2 effects. LPX was contrasted with the empirical Budyko framework, which captures climate effects on ET, to separate vegetation and climatic impacts on hydrology.

The final chapter concludes the key findings arising from the thesis and discusses scope for future work and caveats.

1.5. Candidate's role

Chapter 2 *Ukkola A.M. and Prentice I.C., A worldwide analysis of trends in water-balance evapotranspiration, Hydrology and Earth System Sciences, 17, 4177-4187, 2013.*
The work originated from discussions between A.U. and I.C.P. A.U. performed LPX model runs, processed and acquired all datasets and performed statistical and graphical analyses. A.U. and I.C.P. interpreted the data together. A.U. wrote the first draft and modified the paper after comments from I.C.P. and anonymous reviewers.

Chapter 3 *Ukkola A.M., Prentice I.C., Keenan T.F., van Dijk A.I.J.M, Viney N.R., Myneni R.B. and Bi J., Reduced streamflow in water-stressed climates consistent with CO_2 effects on vegetation, Nature Climate Change (accepted).*
The work originated from discussions between A.U., T.K. and I.C.P. I.C.P. developed the underlying theory and main methods, with contributions from A.U. and T.K. A.U. performed all statistical and graphical analyses and processed and acquired all datasets. R.M. and J.B. provided the vegetation cover data and N.V. the runoff data used in this study. A.U., I.C.P. and T.K. interpreted the data, with assistance from all co-authors. A.U. wrote the first draft and accommodated comments from all co-authors.

Chapter 4 *Ukkola A.M., Keenan T.F., Kelley D.I. and Prentice I.C., Vegetation buffers the water-resource impacts of environmental change, Environmental Research Letters (in prep.).* The work arose from discussions between A.U., T.K. and I.C.P. A.U. performed all statistical and graphical analyses and data processing, with programming assistance from D.K. A.U. coded and performed Budyko model simulations and D.K. the LPX runs. A.U. wrote the first draft and edited the manuscript based on comments from co-authors.

1.6. References

Adam, J. C., Clark, E. A. and Lettenmaier, D. P.: Correction of Global Precipitation Products for Orographic Effects, J. Clim., 19, 15–38, 2006.

Adler, R. F., Huffman, G. J., Chang, A., Ferraro, R., Xie, P.-P., Janowiak, J., Rudolf, B., Schneider, U., Curtis, S., Bolvin, D. T., Gruber, A., Susskind, J., Arkin, P. and Nelkin, E.: The Version-2 Global Precipitation Climatology Project (GPCP) Monthly Precipitation Analysis (1979–Present), J. Hydrometeorol., 4, 1147–1167, 2003.

Ainsworth, E. A. and Long, S. P.: What have we learned from 15 years of free-air CO_2 enrichment (FACE)? A meta-analytic review of the responses of photosynthesis , canopy properties and plant production to rising CO_2, New Phytol., 165, 351–372, 2004.

Alexander, L. V and Arblaster, J. M.: Assessing trends in observed and modelled climate extremes over Australia in relation to future projections, Int. J. Climatol., 29, 417–435, doi:10.1002/joc, 2009.

Alkama, R., Decharme, B., Douville, H. and Ribes, A.: Trends in Global and Basin-Scale Runoff over the Late Twentieth Century: Methodological Issues and Sources of Uncertainty, J. Clim., 24, 3000–3014, doi:10.1175/2010JCLI3921.1, 2011.

Alkama, R., Kageyama, M. and Ramstein, G.: Relative contributions of climate change, stomatal closure, and leaf area index changes to 20th and 21st century runoff change: A modelling approach using the Organizing Carbon and Hydrology in Dynamic Ecosystems (ORCHIDEE) land surface model, J. Geophys. Res., 115, D17112, doi:10.1029/2009jd013408, 2010.

Alkama, R., Marchand, L., Ribes, A. and Decharme, B.: Detection of global runoff changes: results from observations and CMIP5 experiments, Hydrol. Earth Syst. Sci., 17, 2967–2979, doi:10.5194/hess-17-2967-2013, 2013.

Allen, R.: Penman-Monteith equation, in Encyclopedia of Soils in the Environment, edited by D. Hillel, pp. 180–188, Academic Press., 2005.

Allen, R. G., Pereira, L. S., Raes, D. and Smith, M.: Crop evapotranspiration -guidelines for computing crop water requirements - FAO irrigation and drainage paper 56, Rome, Italy., 1998.

Baldocchi, D., Falge, E., Gu, L., Olson, R., Hollinger, D., Running, S., Anthoni, P., Bernhofer, C., Davis, K., Evans, R., Fuentes, J., Goldstein, A., Katul, G., Law, B., Lee, X., Malhi, Y., Meyers, T., Munger, W., Oechel, W., Paw, K. T. U., Pilegaard, K., Schmid, H. P. and Valentini, R.: FLUXNET : A new tool to study the temporal and spatial variability of ecosystem-scale carbon dioxide, water vapor, and energy flux densities, Bull. Am. Meteorol. Soc., 82, 2415–2434, 2001.

Beck, H. E., McVicar, T. R., van Dijk, A. I. J. M., Schellekens, J., de Jeu, R. a. M. and Bruijnzeel, L. A.: Global evaluation of four AVHRR–NDVI data sets: Intercomparison and assessment against Landsat imagery, Remote Sens. Environ., 115, 2547–2563, doi:10.1016/j.rse.2011.05.012, 2011.

Best, M. J., Pryor, M., Clark, D. B., Rooner, G. G., Essery, R. L. H., Menard, C. B., Edwards, J. M., Hendry, M. A., Porson, A., Gedney, N., Mercado, L. M., Sitch, S., Blyth, E., Boucher, O., Cox, P. M., Grimmond, C. S. B. and Harding, R. J.: The Joint UK Land Environment Simulator (JULES), model description-Part 1: energy and water fluxes, Geosci. Model Dev., 4, 677–699, 2011.

Betts, R. A., Boucher, O., Collins, M., Cox, P. M., Falloon, P. D., Gedney, N., Hemming, D. L., Huntingford, C., Jones, C. D., Sexton, D. M. H. and Webb, M. J.: Projected increase in continental runoff due to plant responses to increasing carbon dioxide, Nature, 448, 1037–1041, doi:10.1038/nature06045, 2007.

Bogdanova, E. G., Golubev, V. S., Ilyin, B. M. and Dragomilova, I. V: A new model for bias correction of precipitation measurements, and its application to polar regions of Russia, Russ. Meteorol. Hydrol., 10, 68–94, 2002.

Bosch, J. M. and Hewlett, J. D.: A review of catchment experiments to determine the effect of vegetation changes on water yield and evapotranspiration, J. Hydrol., 55, 3–23, 1982.

Bradshaw, C. J. A., Sodhi, N. S., Peh, K. S. H. and Brook, B. W.: Global evidence that deforestation amplifies flood risk and severity in the developing world, Glob. Chang. Biol., 13, 2379–2395, doi:10.1111/j.1365-2486.2007.01446.x, 2007.

Bradstock, R. A., Williams, R. J. and Gill, A.: Flammable Australia: fire regimes, biodiversity and ecosystems in a changing world., 2012.

Brutsaert, W.: Evaporation into the atmosphere, D. Reidel Publishing Company, Dordrecht, Holland., 1982.

Brutsaert, W.: Indications of increasing land surface evaporation during the second half of the 20th century, Geophys. Res. Lett., 33, L20403, doi:10.1029/2006GL027532, 2006.

Brutsaert, W.: Use of pan evaporation to estimate terrestrial evaporation trends: The case of the Tibetan Plateau, Water Resour. Res., 49, 3054–3058, doi:10.1002/wrcr.20247, 2013.

Budyko, M. I.: Climate and Life, Academic, New York., 1974.

Bureau of Meteorology: Annual Australian Climate Statement 2011, [online] Available from: http://www.bom.gov.au/announcements/media_releases/climate/change/20120104.shtml (Accessed 23 December 2014), 2012.

Chang, J.-H.: Climate and Agriculture. An Ecological Survey, Aldine, Chicago., 1968.

Chiew, F. H. S. and McMahon, T. A.: Detection of trend or change in annual flow of Australian rivers, Int. J. Climatol., 13, 643–653, 1993.

Chou, C., Chiang, J. C. H., Lan, C.-W., Chung, C.-H., Liao, Y.-C. and Lee, C.-J.: Increase in the range between wet and dry season precipitation, Nat. Geosci., 6, 263–267, doi:10.1038/ngeo1744, 2013.

Choudhury, B. J.: Evaluation of an empirical equation for annual evaporation using field observations and results from a biophysical model, J. Hydrol., 216, 99–110, 1999.

Cluis, D. and Laberge, C.: Climate change and trend detection in selected rivers within the Asia-Pacific region, Water Int., 26, 411–424, 2001.

Collins, M., Knutti, R., Arblaster, J., Dufresne, J. L., Fichefet, T., Friedlingstein, P., Gao, X., Gutowski, W. J., Johns, T., Krinner, G., Shongwe, M., Tebaldi, C., Weaver, A. J. and Wehner, M.: Long-term Climate Change: Projections, Commitments and Irreversibility, in Climate Change 2013: The Physical Science Basis. Contribution of Working Group I to the Fifth Assessment Report of the Intergovernmental Panel on Climate Change, edited by T. F. Stocker, D. Qin, G.-K. Plattner, M. Tignor, S. K. Allen, J. Boschung, A. Nauels, Y. Xia, V. Bex, and P. M. Midgley, pp. 1029–1136, Cambridge University Press, Cambridge, United Kingdom and New York, NY, USA., 2013.

Courault, D., Seguin, B. and Olioso, A.: Review on estimation of evapotranspiration from remote sensing data: From empirical to numerical modeling approaches, Irrig. Drain. Syst., 19, 223–249, doi:10.1007/s10795-005-5186-0, 2005.

Cramer, W., Bondeau, A., Woodward, F. I., Prentice, I. C., Betts, R. a., Brovkin, V., Cox, P. M., Fisher, V., Foley, J. a., Friend, A. D., Kucharik, C., Lomas, M. R., Ramankutty, N., Sitch, S., Smith, B., White, A. and Young-Molling, C.: Global response of terrestrial ecosystem structure and function to CO_2 and climate change: results from six dynamic global vegetation models, Glob. Chang. Biol., 7, 357–373, doi:10.1046/j.1365-2486.2001.00383.x, 2001.

D'Almeida, C., Vörösmarty, C. J., Hurtt, G. C., Marengo, J. A., Dingman, S. L. and Keim, B. D.: The effects of deforestation on the hydrological cycle in Amazonia: a review on scale and resolution, Int. J. Climatol., 27, 633–647, doi:10.1002/joc.1475, 2007.

Dai, A., Qian, T., Trenberth, K. E. and Milliman, J. D.: Changes in Continental Freshwater Discharge from 1948 to 2004, J. Clim., 22, 2773–2792, doi:10.1175/2008JCLI2592.1, 2009.

Davie, J. C. S., Falloon, P. D., Kahana, R., Dankers, R., Betts, R., Portmann, F. T., Wisser, D., Clark, D. B., Ito, a., Masaki, Y., Nishina, K., Fekete, B., Tessler, Z., Wada, Y., Liu, X., Tang, Q., Hagemann, S., Stacke, T., Pavlick, R., Schaphoff, S., Gosling, S. N., Franssen, W. and Arnell, N.: Comparing projections of future changes in runoff from hydrological and biome models in ISI-MIP, Earth Syst. Dyn., 4, 359–374, doi:10.5194/esd-4-359-2013, 2013.

Delworth, T. L. and Zeng, F.: Regional rainfall decline in Australia attributed to anthropogenic greenhouse gases and ozone levels, Nat. Geosci., 7, 583–588, doi:10.1038/NGEO2201, 2014.

Deser, C., Knutti, R., Solomon, S. and Phillips, A. S.: Communication of the role of natural variability in future North American climate, Nat. Clim. Chang., 2, 775–779, 2012.

Deser, C., Phillips, A., Bourdette, V. and Teng, H.: Uncertainty in climate change projections: the role of internal variability, Clim. Dyn., 38, 527–546, doi:10.1007/s00382-010-0977-x, 2010.

Diffenbaugh, N. S. and Field, C. B.: Changes in ecologically critical terrestrial climate conditions., Science, 341, 486–92, doi:10.1126/science.1237123, 2013.

Van Dijk, a. I. J. M., Peña-Arancibia, J. L. and Bruijnzeel, L. a.: Land cover and water yield: inference problems when comparing catchments with mixed land cover, Hydrol. Earth Syst. Sci., 16, 3461–3473, doi:10.5194/hess-16-3461-2012, 2012.

Van Dijk, A. I. J. M., Beck, H. E., Crosbie, R. S., de Jeu, R. a. M., Liu, Y. Y., Podger, G. M., Timbal, B. and Viney, N. R.: The Millennium Drought in southeast Australia (2001-2009): Natural and human causes and implications for water resources, ecosystems, economy, and society, Water Resour. Res., 49, 1–18, doi:10.1002/wrcr.20123, 2013.

Dirmeyer, P. A., Gao, X., Zhao, M., Guo, Z., Oki, T. and Hanasaki, N.: GSWP-2: Multimodel analysis and implications for our perception of the land surface, Bull. Am. Meteorol. Soc., 87, 1381–1397, 2006.

Donohue, R. J., Roderick, M. L. and McVicar, T. R.: Assessing the differences in sensitivities of runoff to changes in climatic conditions across a large basin, J. Hydrol., 406, 234–244, doi:10.1016/j.jhydrol.2011.07.003, 2011.

Donohue, R. J., Roderick, M. L., McVicar, T. R. and Farquhar, G. D.: Impact of CO_2 fertilization on maximum foliage cover across the globe's warm, arid environments, Geophys. Res. Lett., 40, 1–5, doi:10.1002/grl.50563, 2013.

Donohue, R., McVicar, T. R. and Roderick, M.: Climate-related trends in Australian vegetation cover as inferred from satellite observations, 1981-2006, Glob. Chang. Biol., 15, 1025–1039, 2009.

Douville, H., Ribes, A., Decharme, B., Alkama, R. and Sheffield, J.: Anthropogenic influence on multidecadal changes in reconstructed global evapotranspiration, Nat. Clim. Chang., 3, 59–62, doi:10.1038/nclimate1632, 2013.

Eichinger, W. E., Parlange, M. B. and Stricker, H.: On the concept of equilibrium evaporation and the value of the Priestley-Taylor coefficient, Water Resour. Res., 32, 161–164, 1996.

Essery, R. L. H., Best, M. J., Betts, R. A., Cox, P. M. and Taylor, C. M.: Explicit representation of sub-grid heterogeneity in a GCM land surface scheme, J. Hydrometeorol., 4, 530–543, 2003.

Fekete, B. M., Vörösmarty, C. J., Roads, J. O. and Willmott, C. J.: Uncertainties in precipitation and their impacts on runoff estimates, J. Clim., 17, 294–304, 2004.

Field, C. B., Jackson, R. B. and Mooney, H. A.: Stomatal response to increased CO_2: Implication from the leaf to the global scale, Plant. Cell Environ., 18, 1214–1225, 1995.

Fisher, J. B., Whittaker, R. J. and Malhi, Y.: ET come home: potential evapotranspiration in geographical ecology, Glob. Ecol. Biogeogr., 20, 1–18, doi:10.1111/j.1466-8238.2010.00578.x, 2011.

Friend, A. D., Lucht, W., Rademacher, T. T., Keribin, R., Betts, R., Cadule, P., Ciais, P., Clark, D. B., Dankers, R., Falloon, P. D., Ito, A., Kahana, R., Kleidon, A., Lomas, M. R., Nishina, K., Ostberg, S., Pavlick, R., Peylin, P., Schaphoff, S., Vuichard, N., Warszawski, L., Wiltshire, A. and Woodward, F. I.: Carbon residence time dominates uncertainty in terrestrial vegetation responses to future climate and atmospheric CO2, Proc. Natl. Acad. Sci. U. S. A., 111, 3280–3285, doi:10.1073/pnas.1222477110, 2014.

Fu, B. P.: On the calculation of the evaporation from land surface, Sci. Atmos. Sin., 5, 23–31 (in Chinese), 1981.

Gedney, N., Cox, P. M., Betts, R. A., Boucher, O., Huntingford, C. and Stott, P. A.: Detection of a direct carbon dioxide effect in continental river runoff records, Nature, 439, 835–838, doi:10.1038/nature04504, 2006.

Gedney, N., Huntingford, C., Weedon, G. P., Bellouin, N., Boucher, O. and Cox, P. M.: Detection of solar dimming and brightening effects on Northern Hemisphere river flow, Nat. Geosci., 7, 796–800, doi:10.1038/ngeo2263, 2014.

Gerten, D., Rost, S., von Bloh, W. and Lucht, W.: Causes of change in 20th century global river discharge, Geophys. Res. Lett., 35, L20405, doi:10.1029/2008gl035258, 2008.

Glenn, E. P., Doody, T. M., Guerschman, J. P., Huete, A. R., King, E. a., McVicar, T. R., Van Dijk, A. I. J. M., Van Niel, T. G., Yebra, M. and Zhang, Y.: Actual evapotranspiration estimation by ground and remote sensing methods: the Australian experience, Hydrol. Process., 25, 4103–4116, doi:10.1002/hyp.8391, 2011.

Glenn, E. P., Huete, A. R., Nagler, P. L. and Nelson, S. G.: Relationship between remotely-sensed vegetation indices, canopy attributes, and plant physiological processes: what vegetation indices can and cannot tell us about the landscape, Sensors, 8, 2136–2160, 2008.

Gordon, L. J., Steffen, W., Jönsson, B. F., Folke, C., Falkenmark, M. and Johannessen, Å.: Human modification of global water vapor flows from the land surface, Proc. Natl. Acad. Sci., 102, 7612–7617, doi:10.1073/pnas.0500208102, 2005.

Groisman, P. Y., Knight, R. W. and Karl, T. R.: Heavy precipitation and high streamflow in the contiguous United States: trends in the twentieth century, Bull. Am. Meteorol. Soc., 82, 219–225, 2001.

Guerschman, J. P., Van Dijk, A. I. J. M., Mattersdorf, G., Beringer, J., Hutley, L. B., Leuning, R., Pipunic, R. C. and Sherman, B. S.: Scaling of potential evapotranspiration with MODIS data reproduces flux observations and catchment water balance observations across Australia, J. Hydrol., 369, 107–119, doi:10.1016/j.jhydrol.2009.02.013, 2009.

Haddeland, I., Heinke, J., Biemans, H., Eisner, S., Flörke, M., Hanasaki, N., Konzmann, M., Ludwig, F., Masaki, Y., Schewe, J., Stacke, T., Tessler, Z. D., Wada, Y. and Wisser, D.: Global water resources affected by human interventions and climate change., Proc. Natl. Acad. Sci. U. S. A., 111, 3151–3256, doi:10.1073/pnas.1222475110, 2013.

Hagemann, S., Chen, C., Clark, D. B., Folwell, S., Gosling, S. N., Haddeland, I., Hanasaki, N., Heinke, J., Ludwig, F., Voss, F. and Wiltshire, a. J.: Climate change impact on available water resources obtained using multiple global climate and hydrology models, Earth Syst. Dyn., 4, 129–144, doi:10.5194/esd-4-129-2013, 2013.

Harris, I., Jones, P. D., Osborn, T. J. and Lister, D. H.: Updated high-resolution grids of monthly climatic observations - the CRU TS3.10 Dataset, Int. J. Climatol., 34, 623–642, doi:10.1002/joc.3711, 2014.

Hartmann, D. L., Klein Tank, A. M. G., Rusticucci, M., Alexander, L. V, Brönnimann, S., Charabi, Y., Dentener, F. J., Dlugokencky, E. J., Easterling, D. R., Kaplan, A., Soden, B. J., Thorne, P. W., Wild, M. and Zhai, P. M.: Observations: Atmosphere and Surface, in Climate Change 2013: The Physical Science Basis. Contribution of Working Group I to the Fifth Assessment Report of the

Intergovernmental Panel on Climate Change, edited by T. F. Stocker, D. Qin, G.-K. Plattner, M. Tignor, S. K. Allen, J. Boschung, A. Nauels, Y. Xia, V. Bex, and P. M. Midgley, pp. 159–254, Cambridge University Press, Cambridge, United Kingdom and New York, NY, USA., 2013.

Hempel, S., Frieler, K., Warszawski, L., Schewe, J. and Piontek, F.: A trend-preserving bias correction – the ISI-MIP approach, Earth Syst. Dyn., 4, 219–236, doi:10.5194/esd-4-219-2013, 2013.

Hendon, H. H., Thompson, D. W. J. and Wheeler, M. C.: Australian rainfall and surface temperature variations associated with the Southern Hemisphere Annular Mode, J. Clim., 20, 2452–2467, 2007.

Hickel, K. and Zhang, L.: Estimating the impact of rainfall seasonality on mean annual water balance using a top-down approach, J. Hydrol., 331, 409–424, doi:10.1016/j.jhydrol.2006.05.028, 2006.

Huntington, T. G.: Evidence for intensification of the global water cycle: Review and synthesis, J. Hydrol., 319, 83–95, doi:10.1016/j.jhydrol.2005.07.003, 2006.

Jasechko, S., Sharp, Z. D., Gibson, J. J., Birks, S. J., Yi, Y. and Fawcett, P. J.: Terrestrial water fluxes dominated by transpiration, Nature, 1–5, doi:10.1038/nature11983, 2013.

Jones, R. N., Preston, B., Brooke, C., Aryal, S., Benyon, R. and Blackmore, J.: Climate change and Australian water resources: first risk assessment and gap analysis, Canberra, Australia., 2008.

Jung, M., Reichstein, M. and Bondeau, a.: Towards global empirical upscaling of FLUXNET eddy covariance observations: validation of a model tree ensemble approach using a biosphere model, Biogeosciences, 6, 2001–2013, doi:10.5194/bg-6-2001-2009, 2009.

Jung, M., Reichstein, M., Ciais, P., Seneviratne, S. I., Sheffield, J., Goulden, M. L., Bonan, G., Cescatti, A., Chen, J., de Jeu, R., Dolman, A. J., Eugster, W., Gerten, D., Gianelle, D., Gobron, N., Heinke, J., Kimball, J., Law, B. E., Montagnani, L., Mu, Q., Mueller, B., Oleson, K., Papale, D., Richardson, A. D., Roupsard, O., Running, S., Tomelleri, E., Viovy, N., Weber, U., Williams, C., Wood, E., Zaehle, S. and Zhang, K.: Recent decline in the global land evapotranspiration trend due to limited moisture supply, Nature, 467, 951–954, doi:10.1038/nature09396, 2010.

De Kauwe, M. G., Medlyn, B. E., Zaehle, S., Walker, A. P., Dietze, M. C., Hickler, T., Jain, A. K., Luo, Y., Parton, W. J., Prentice, I. C., Smith, B., Thornton, P. E., Wang, S., Wang, Y.-P., Wårlind, D., Weng, E., Crous, K. Y., Ellsworth, D. S., Hanson, P. J., Seok Kim, H.-, Warren, J. M., Oren, R. and Norby, R. J.: Forest water use and water use efficiency at elevated CO_2: a model-data intercomparison at two contrasting temperate forest FACE sites, Glob. Chang. Biol., 19, 1759–1779, doi:10.1111/gcb.12164, 2013.

Kelley, D. I. and Harrison, S. P.: Enhanced Australian carbon sink despite increased wildfire during the 21st century, Environ. Res. Lett., 9, 104015, doi:10.1088/1748-9326/9/10/104015, 2014.

Kergoat, L., Lafont, S., Douville, H., Berthelot, B., Dedieu, G., Planton, S. and Royer, J.-F.: Impact of doubled CO_2 on global-scale leaf area index and evapotranspiration: Conflicting stomatal conductance and LAI responses, J. Geophys. Res., 107, 4808, doi:10.1029/2001jd001245, 2002.

Knutti, R. and Sedláček, J.: Robustness and uncertainties in the new CMIP5 climate model projections, Nat. Clim. Chang., 3, 369–373, doi:10.1038/nclimate1716, 2012.

Krajewski, W. F., Villarini, G. and Smith, J. A.: Radar-rainfall uncertainties, Bull. Am. Meteorol. Soc., 91, 87–94, 2010.

Krinner, G., Viovy, N., de Noblet-Ducoudré, N., Ogée, J., Polcher, J., Friedlingstein, P., Ciais, P., Sitch, S. and Prentice, I. C.: A dynamic global vegetation model for studies of the coupled atmosphere-biosphere system, Global Biogeochem. Cycles, 19, GB1015, doi:10.1029/2003GB002199, 2005.

Labat, D., Goddéris, Y., Probst, J. L. and Guyot, J. L.: Evidence for global runoff increase related to climate warming, Adv. Water Resour., 27, 631–642, doi:10.1016/j.advwatres.2004.02.020, 2004.

Lammers, R. B., Shiklomanov, I., Vörösmarty, C. J., Fekete, B. M. and Peterson, B. J.: Assessment of contemporary Arctic river runoff based on observational discharge records, J. Geophys. Res., 106, 3321–3334, 2001.

Lawrence, D. M., Thornton, P. E., Oleson, K. W. and Bonan, G. B.: The partitioning of evapotranspiration into transpiration, soil evaporation and canopy evaporation in a GCM: impacts on land-atmosphere interaction, J. Hydrometeorol., 8, 862–880, doi:10.1175/JHM596.1., 2007.

Leakey, A. D. B., Ainsworth, E. a, Bernacchi, C. J., Rogers, A., Long, S. P. and Ort, D. R.: Elevated CO_2 effects on plant carbon, nitrogen, and water relations: six important lessons from FACE, J. Exp. Bot., 60, 2859–2876, doi:10.1093/jxb/erp096, 2009.

Legates, D. R., Lins, H. F. and McCabe, G. J.: Comments on “Evidence for global runoff increase related to climate warming” by Labat et al, Adv. Water Resour., 28, 1310–1315, doi:10.1016/j.advwatres.2005.04.006, 2005.

Legates, D. R. and Willmott, C. J.: Mean seasonal and spatial variability in gauge-corrected, global precipitation, Int. J. Climatol., 10, 111–127, 1990.

Leipprand, A. and Gerten, D.: Global effects of doubled atmospheric CO_2 content on evapotranspiration , soil moisture and runoff under potential natural vegetation Global effects of doubled atmospheric CO_2 content on evapotranspiration , soil moisture and runoff under potential natu, Hydrol. Sci. J., 51, 171–185, 2006.

Leuning, R., Zhang, Y. Q., Rajaud, A., Cleugh, H. and Tu, K.: A simple surface conductance model to estimate regional evaporation using MODIS leaf area index and the Penman-Monteith equation, Water Resour. Res., 44, W10419, 2008.

Li, G., Harrison, S. P., Bartlein, P. J., Izumi, K. and Prentice, I. C.: Precipitation scaling with temperature in warm and cold climates: an analysis of CMIP5 simulations, Geophys. Res. Lett., 40, 4018–4024, doi:10.1002/grl.50730, 2013.

Li, Z. and Mölders, N.: Interaction of impacts of doubling CO_2 and changing regional land-cover on evaporation, precipitation, and runoff at global and regional scales, Int. J. Climatol., 28, 1653–1679, doi:10.1002/joc.1666, 2008.

Lins, H. F. and Slack, J. R.: Streamflow trends in the United States, Geophys. Res. Lett., 26, 227–230, 1999.

Liu, B., Ma, Z., Xu, J. and Xiao, Z.: Comparison of pan evaporation and actual evaporation estimated by land surface model in Xinjiang from 1960 to 2005, J. Geogr. Sci., 19, 502–512, doi:10.1007/s11442-009-0502-5, 2009.

Lo, M.-H. and Famiglietti, J. S.: Irrigation in California's Central Valley strengthens the southwestern U.S. water cycle, Geophys. Res. Lett., 40, 301–306, doi:10.1002/grl.50108, 2013.

Los, S. O.: Analysis of trends in fused AVHRR and MODIS NDVI data for 1982-2006: Indication for a CO_2 fertilization effect in global vegetation, Global Biogeochem. Cycles, 27, 1–13, doi:10.1002/gbc.20027, 2013.

Lucht, W., Prentice, I. C., Myneni, R. B., Sitch, S., Friedlingstein, P., Cramer, W., Bousquet, P., Buermann, W. and Smith, B.: Climatic Control of the High-Latitude Vegetation Greening Trend and Pinatubo Effect, Scien, 296, 1687–1689, 2002.

Lymburner, L., Tan, P., Mueller, N., Thackway, R., Lewis, A., Thankappan, M., Randall, L., Islam, A. and Senarath, U.: The National Dynamic Land Cover Dataset, Symonston, Australia., 2011.

McFarlane, D., Stone, R., Martens, S., Thomas, J., Silberstein, R., Ali, R. and Hodgson, G.: Climate change impacts on water yields and demands in south-western Australia, J. Hydrol., 475, 488–498, doi:10.1016/j.jhydrol.2012.05.038, 2012.

McMahon, T., Gan, K. and Finlayson, B. L.: Anthropogenic changes to the hydrological cycle in Australia, in Australia's renewable resources: sustainability and global change, edited by R. M. Gifford and M. Barson, pp. 35–66, Bureau of Rural Resources proceedings no. 14 and CSIRO, Parkes, NSW., 1992.

Milliman, J. D., Farnsworth, K. L., Jones, P. D., Xu, K. H. and Smith, L. C.: Climatic and anthropogenic factors affecting river discharge to the global ocean, 1951–2000, Glob. Planet. Change, 62, 187–194, doi:10.1016/j.gloplacha.2008.03.001, 2008.

Miralles, D. G., van den Berg, M. J., Gash, J. H., Parinussa, R. M., de Jeu, R. a. M., Beck, H. E., Holmes, T. R. H., Jiménez, C., Verhoest, N. E. C., Dorigo, W. a., Teuling, A. J. and Johannes Dolman, A.: El Niño–La Niña cycle and recent trends in continental evaporation, Nat. Clim. Chang., 4, 122–126, doi:10.1038/nclimate2068, 2013.

Miralles, D. G., De Jeu, R. A. M., Gash, J. H., Holmes, T. R. H. and Dolman, A. J.: Magnitude and variability of land evaporation and its components at the global scale, Hydrol. Earth Syst. Sci., 15, 967–981, doi:10.5194/hess-15-967-2011, 2011.

Monteith, J. L.: Evaporation and the environment, Symp. Soc. Explor. Biol., 19, 205–234, 1965.

Myneni, R. B., Keeling, C. D., Tucker, C. J., Asrar, G. and Nemani, R. R.: Increased plant growth in the northern high latitudes from 1981 to 1991, Nature, 386, 698–702, 1997.

New, M., Todd, M., Hulme, M. and Jones, P.: Precipitation measurements and trends in the twentieth century, Int. J. Climatol., 21, 1889–1922, doi:10.1002/joc.680, 2001.

Nicholls, N.: Detecting and attributing Australian climate change: a review, Aust. Meteorol. Mag., 55, 199–211, 2006.

Nicholls, N.: Local and remote causes of the southern Australian autumn-winter rainfall decline, 1958-2007, Clim. Dyn., 34, 835–845, 2010.

Notaro, M., Vavrus, S. and Liu, Z.: Global Vegetation and Climate Change due to Future Increases in CO_2 as Projected by a Fully Coupled Model with Dynamic Vegetation, J. Clim., 20, 70–90, doi:10.1175/JCLI3989.1, 2007.

Nouri, H., Beecham, S., Kazemi, F. and Hassanli, A. M.: A review of ET measurement techniques for estimating the water requirements of urban landscape vegetation, Urban Water J., 10, 247–259, 2013.

Nowak, R. S., Ellsworth, D. S. and Smith, S. D.: Functional responses of plants to elevated atmospheric CO_2 -do photosynthetic and productivity data from FACE experiments support early predictions?, New Phytol., 162, 253–280, doi:10.1111/j.1469-8137.2004.01033.x, 2004.

O'ishi, R., Abe-Ouchi, A., Prentice, I. C. and Sitch, S.: Vegetation dynamics and plant CO_2 responses as positive feedbacks in a greenhouse world, Geophys. Res. Lett., 36, L11706, doi:10.1029/2009gl038217, 2009.

Peel, M. C. and McMahon, T. A.: Continental Runoff: A quality-controlled global runoff data set, Nature, 444, E14, doi:10.1038/nature05480, 2006.

Pekarova, P., Miklanek, P. and Pekar, J.: Spatial and temporal runoff oscillation analysis of the main rivers of the world during the 19th-20th centuries, J. Hydrol., 274, 62–79, 2003.

Penman, H. L.: Natural evaporation from open water, bare soil and grass, Proc. R. Soc. London Ser. A Math. Phys. Eng. Sci., 193, 120–146, 1948.

Peterson, B. J., Holmes, R. M., McClelland, J. W., Vörösmarty, C. J., Lammers, R. B., Shiklomanov, A. I., Shiklomanov, I. and Rahmstorf, S.: Increasing river discharge to the Arctic Ocean, Science, 298, 2171–2173, 2002.

Petrone, K. C., Hughes, J. D., Van Niel, T. G. and Silberstein, R. P.: Streamflow decline in southwestern Australia, 1950–2008, Geophys. Res. Lett., 37, L11401, doi:10.1029/2010gl043102, 2010.

Piao, S., Friedlingstein, P., Ciais, P., de Noblet-Ducoudre, N., Labat, D. and Zaehle, S.: Changes in climate and land use have a larger direct impact than rising CO_2 on global river runoff trends, Proc. Natl. Acad. Sci., 104, 15242–15247, doi:10.1073/pnas.0707213104, 2007.

Pike, J. G.: The estimation of annual runoff from meteorological data in a tropical climate, J. Hydrol., 2, 116–123, 1964.

Pinzon, J. E. and Tucker, C. J.: A non-stationary 1981-2012 AVHRR NDVI3g time series, Remote Sens., 6, 6929–6960, doi:10.3390/rs6086929, 2014.

Potter, N. J. and Zhang, L.: Interannual variability of catchment water balance in Australia, J. Hydrol., 369, 120–129, doi:10.1016/j.jhydrol.2009.02.005, 2009.

Potter, N. J., Zhang, L., Milly, P. C. D., McMahon, T. a. and Jakeman, a. J.: Effects of rainfall seasonality and soil moisture capacity on mean annual water balance for Australian catchments, Water Resour. Res., 41, W06007, doi:10.1029/2004WR003697, 2005.

Poulter, B., Frank, D., Ciais, P., Myneni, R. B., Andela, N., Bi, J., Broquet, G., Canadell, J. G., Chevallier, F., Liu, Y. Y., Running, S. W., Sitch, S. and van der Werf, G. R.: Contribution of semi-arid ecosystems to interannual variability of the global carbon cycle., Nature, 509, 600–603, doi:10.1038/nature13376, 2014.

Preston, B. and Jones, R. N.: Screening climatic and non-climatic risks to Australian catchments, Geogr. Res., 46, 258–274, 2008a.

Preston, B. L. and Jones, R. N.: Evaluating sources of uncertainty in Australian runoff projections, Adv. Water Resour., 31, 758–775, doi:10.1016/j.advwatres.2008.01.006, 2008b.

Priestley, C. H. B. and Taylor, R. J.: On the Assessment of Surface Heat Flux and Evaporation Using Large-Scale Parameters, Mon. Weather Rev., 100, 81–92, 1972.

Prudhomme, C., Giuntoli, I., Robinson, E. L., Clark, D. B., Arnell, N. W., Dankers, R., Fekete, B. M., Franssen, W., Gerten, D., Gosling, S. N., Hagemann, S., Hannah, D. M., Kim, H., Masaki, Y., Satoh, Y., Stacke, T., Wada, Y. and Wisser, D.: Hydrological droughts in the 21st century, hotspots and uncertainties from a global multimodel ensemble experiment., Proc. Natl. Acad. Sci. U. S. A., 111, 3262–7, doi:10.1073/pnas.1222473110, 2014.

Raupach, M. R.: Equilibrium evaporation and the convective boundary layer, Boundary-Layer Meteorol., 96, 107–141, 2000.

Raupach, M. R.: Combination theory and equilibrium evaporation, Q. J. R. Meteorol. Soc., 127, 1149–1181, 2001.

Risbey, J. S., Pook, M. J. and McIntosh, P. C.: Spatial trends in synoptic rainfall in Southern Australia, Geophys. Res. Lett., 40, 3781–3785, doi:10.1002/grl.50739, 2013.

Risbey, J. S., Pook, M. J., McIntosh, P. C., Wheeler, M. C. and Hendon, H. H.: On the Remote Drivers of Rainfall Variability in Australia, Mon. Weather Rev., 137, 3233–3253, doi:10.1175/2009mwr2861.1, 2009.

Robock, A. and Li, H.: Solar dimming and CO_2 effects on soil moisture trends, Geophys. Res. Lett., 33, L20708, doi:10.1029/2006GL027585, 2006.

Roderick, M. L. and Farquhar, G. D.: The cause of decreased pan evaporation over the past 50 years, Science, 298, 1410–1411, doi:10.1126/science.1075390, 2002.

Roderick, M. L. and Farquhar, G. D.: Changes in Australian pan evaporation from 1970 to 2002, Int. J. Climatol., 24, 1077–1090, doi:10.1002/joc.1061, 2004.

Roderick, M. L., Hobbins, M. T. and Farquhar, G. D.: Pan Evaporation Trends and the Terrestrial Water Balance. I. Principles and Observations, Geogr. Compass, 3, 746–760, doi:10.1111/j.1749-8198.2008.00213.x, 2009.

Roderick, M. L., Rotstayn, L. D., Farquhar, G. D. and Hobbins, M. T.: On the attribution of changing pan evaporation, Geophys. Res. Lett., 34, L17403, doi:10.1029/2007GL031166, 2007.

Roderick, M. L., Sun, F., Lim, W. H. and Farquhar, G. D.: A general framework for understanding the response of the water cycle to global warming over land and ocean, Hydrol. Earth Syst. Sci., 18, 1575–1589, doi:10.5194/hess-18-1575-2014, 2014.

Rost, S., Gerten, D., Bondeau, A., Lucht, W., Rohwer, J. and Schaphoff, S.: Agricultural green and blue water consumption and its influence on the global water system, Water Resour. Res., 44, W09405, doi:10.1029/2007wr006331, 2008.

Saatchi, S., Asefi-Najafabady, S., Malhi, Y., Aragão, L. E. O. C., Anderson, L. O., Myneni, R. B. and Nemani, R.: Persistent effects of a severe drought on Amazonian forest canopy., Proc. Natl. Acad. Sci. U. S. A., 110, 565–70, doi:10.1073/pnas.1204651110, 2013.

Schneider, U., Fuchs, T., Meyer-Christoffer, A. and Rudolf, B.: Global Precipitation Analysis Products of the GPCC, Offenbach am Main, Germany., 2008.

Seneviratne, S. I., Corti, T., Davin, E. L., Hirschi, M., Jaeger, E. B., Lehner, I., Orlowsky, B. and Teuling, A. J.: Investigating soil moisture–climate interactions in a changing climate: A review, Earth-Science Rev., 99, 125–161, doi:10.1016/j.earscirev.2010.02.004, 2010.

Seoane, L., Ramillien, G., Frappart, F. and Leblanc, M.: Regional GRACE-based estimates of water mass variations over Australia: validation and interpretation, Hydrol. Earth Syst. Sci., 17, 4925–4939, doi:10.5194/hess-17-4925-2013, 2013.

Shao, Q., Traylen, A. and Zhang, L.: Nonparametric method for estimating the effects of climatic and catchment characteristics on mean annual evapotranspiration, Water Resour. Res., 48, W03517, doi:10.1029/2010WR009610, 2012.

Sheffield, J. and Wood, E. F.: Global Trends and Variability in Soil Moisture and Drought Characteristics, 1950–2000, from Observation-Driven Simulations of the Terrestrial Hydrologic Cycle, J. Clim., 21, 432–458, doi:10.1175/2007JCLI1822.1, 2008.

Sheffield, J., Wood, E. F. and Roderick, M. L.: Little change in global drought over the past 60 years., Nature, 491, 435–438, doi:10.1038/nature11575, 2012.

Shuttleworth, W. J.: Evaporation models in hydrology, in Land surface evaporation: measurement and parameterisation, edited by T. J. Schmugge and J.-C. André, pp. 93–120, Springer-Verlag, New York., 1991.

Sitch, S., Huntingford, C., Gedney, N., Levy, P. E., Lomas, M., Piao, S. L., Betts, R., Ciais, P., Cox, P., Friedlingstein, P., Jones, C. D., Prentice, I. C. and Woodward, F. I.: Evaluation of the terrestrial carbon cycle, future plant geography and climate-carbon cycle feedbacks using five Dynamic Global Vegetation Models (DGVMs), Glob. Chang. Biol., 14, 2015–2039, doi:10.1111/j.1365-2486.2008.01626.x, 2008.

Sterling, S. M. and Ducharne, A.: Comprehensive data set of global land cover change for land surface model applications, Global Biogeochem. Cycles, 22, GB3017, 2008.

Sterling, S. M., Ducharne, A. and Polcher, J.: The impact of global land-cover change on the terrestrial water cycle, Nat. Clim. Chang., 2, 1–6, doi:10.1038/nclimate1690, 2012.

Strengers, B. J., Müller, C., Schaeffer, M., Haarsma, R. J., Severijns, C., Gerten, D., Schaphoff, S., van den Houdt, R. and Oostenrijk, R.: Assessing 20th century climate-vegetation feedbacks of land-use change and natural vegetation dynamics in a fully coupled vegetation-climate model, Int. J. Climatol., 30, 2055–2065, doi:10.1002/joc.2132, 2010.

Sutanto, S. J., van den Hurk, B., Hoffmann, G., Wenninger, J., Dirmeyer, P. a., Seneviratne, S. I., Röckmann, T., Trenberth, K. E. and Blyth, E. M.: HESS Opinions: A perspective on different approaches to determine the contribution of transpiration to the surface moisture fluxes, Hydrol. Earth Syst. Sci. Discuss., 11, 2583–2612, doi:10.5194/hessd-11-2583-2014, 2014.

Teuling, a. J., Hirschi, M., Ohmura, A., Wild, M., Reichstein, M., Ciais, P., Buchmann, N., Ammann, C., Montagnani, L., Richardson, a. D., Wohlfahrt, G. and Seneviratne, S. I.: A regional perspective on trends in continental evaporation, Geophys. Res. Lett., 36, L02404, doi:10.1029/2008GL036584, 2009.

Teuling, A. J., Seneviratne, S. I., Stöckli, R., Reichstein, M., Moors, E., Ciais, P., Luyssaert, S., van den Hurk, B., Ammann, C., Bernhofer, C., Dellwik, E., Gianelle, D., Gielen, B., Grünwald, T., Klumpp, K., Montagnani, L., Moureaux, C., Sottocornola, M. and Wohlfahrt, G.: Contrasting response of European forest and grassland energy exchange to heatwaves, Nat. Geosci., 3, 722–727, doi:10.1038/ngeo950, 2010.

Trenberth, K.: Changes in precipitation with climate change, Clim. Res., 47, 123–138, doi:10.3354/cr00953, 2011.

Trenberth, K. E., Jones, P. D., Ambenje, P., Bojariu, R., Easterling, D. R., Klein Tank, A. M. G., Parker, D., Rahimzadeh, F., Renwick, J. A., Rusticucci, M., Soden, B. and Zhai, P.: Observations: surface and atmospheric climate change, in Climate Change 2007: The Physical Science Basis. Contribution of Working Group I to the Fourth Assessment Report of the Intergovernmental Panel on Climate Change, edited by S. Solomon, D. Qin, M. Manning, Z. Chen, M. Marquis, K. B. Averyt, M. Tignor, and H. L. Miller, Cambridge University Press, Cambridge, United Kingdom and New York, NY, USA., 2007.

Vörösmarty, C. J.: Global Water Resources: Vulnerability from Climate Change and Population Growth, Science, 289, 284–288, doi:10.1126/science.289.5477.284, 2000.

Van Vuuren, D. P., Edmonds, J., Kainuma, M., Riahi, K., Thomson, A., Hibbard, K., Hurtt, G. C., Kram, T., Krey, V., Lamarque, J.-F., Masui, T., Meinshausen, M., Nakicenovic, N., Smith, S. J. and Rose, S.

K.: The representative concentration pathways: an overview, Clim. Change, 109, 5–31, doi:10.1007/s10584-011-0148-z, 2011.

Wang, K. and Dickinson, R. E.: A review of global terrestrial evapotranspiration: observation, modeling, climatology and climatic variability, Rev. Geophys., 50, RG2005, doi:10.1029/2011RG000373, 2012.

Wang, K., Dickinson, R. E., Wild, M. and Liang, S.: Evidence for decadal variation in global terrestrial evapotranspiration between 1982 and 2002: 2. Results, J. Geophys. Res., 115, D20113, doi:10.1029/2010JD013847, 2010.

Weedon, G. P., Gomes, S., Viterbo, P., Shuttleworth, W. J., Blyth, E., Österle, H., Adam, J. C., Bellouin, N., Boucher, O. and Best, M.: Creation of the WATCH Forcing Data and Its Use to Assess Global and Regional Reference Crop Evaporation over Land during the Twentieth Century, J. Hydrometeorol., 12, 823–848, doi:10.1175/2011JHM1369.1, 2011.

Werth, S. and Günther, A.: Calibration analysis for water storage variability of the global hydrological model WGHM, Hydrol. Earth Syst. Sci., 14, 59–78, 2010.

Whitley, R. J., Macinnis-Ng, C. M. O., Hutley, L. B., Beringer, J., Zeppel, M., Williams, M., Taylor, D. and Eamus, D.: Is productivity of mesic savannas light limited or water limited? Results of a simulation study, Glob. Chang. Biol., 17, 3130–3149, doi:10.1111/j.1365-2486.2011.02425.x, 2011.

Wilby, R. L.: When and where might climate change be detectable in UK river flows?, Geophys. Res. Lett., 33, L19407, doi:10.1029/2006gl027552, 2006.

Wild, M., Gilgen, H., Roesch, A., Ohmura, A., Long, C. N., Dutton, E. G., Forgan, B., Kallis, A., Russak, V. and Tsvetkov, A.: From dimming to brightening: decadal changes in solar radiation at Earth's surface, Science, 308, 847–850, doi:10.1126/science.1103215, 2005.

Wong, S. C., Cowan, I. R. and Farquhar, G. D.: Stomatal conductance correlates with photosynthetic capacity, Nature, 282, 424–426, 1979.

Xu, L., Samanta, A., Costa, M. H., Ganguly, S., Nemani, R. R. and Myneni, R. B.: Widespread decline in greenness of Amazonian vegetation due to the 2010 drought, Geophys. Res. Lett., 38, L07402, doi:10.1029/2011GL046824, 2011.

Xu, T. and Hutchinson, M. F.: New developments and applications in the ANUCLIM spatial climatic and bioclimatic modelling package, Environ. Model. Softw., 40, 267–279, doi:10.1016/j.envsoft.2012.10.003, 2013.

Yang, D., Sun, F., Liu, Z., Cong, Z., Ni, G. and Lei, Z.: Analyzing spatial and temporal variability of annual water-energy balance in nonhumid regions of China using the Budyko hypothesis, Water Resour. Res., 43, W04426, doi:10.1029/2006WR005224, 2007.

Zeng, Z., Piao, S., Lin, X., Yin, G., Peng, S., Ciais, P. and Myneni, R. B.: Global evapotranspiration over the past three decades: estimation based on the water balance equation combined with empirical models, Environ. Res. Lett., 7, 014026, doi:10.1088/1748-9326/7/1/014026, 2012.

Zeng, Z., Wang, T., Zhou, F., Ciais, P., Mao, J., Shi, X. and Piao, S.: A worldwide analysis of spatiotemporal changes in water balance-based evapotranspiration from 1982 to 2009, J. Geophys. Res. Atmos., 119, 1–17, 2014.

Zhang, L., Dawes, W. R. and Walker, G. R.: Response of mean annual evapotranspiration to vegetation changes at catchment scale, Water Resour. Res., 37, 701–708, 2001.

Zhang, L., Hickel, K., Dawes, W. R., Chiew, F. H. S., Western, A. W. and Briggs, P. R.: A rational function approach for estimating mean annual evapotranspiration, Water Resour. Res., 40, W02502, doi:10.1029/2003wr002710, 2004.

Zhang, Y., Leuning, R., Chiew, F. H. S., Wang, E., Zhang, L., Liu, C., Sun, F., Peel, M. C., Shen, Y. and Jung, M.: Decadal Trends in Evaporation from Global Energy and Water Balances, J. Hydrometeorol., 13, 379–391, doi:10.1175/JHM-D-11-012.1, 2012.

Zhou, L., Tian, Y., Myneni, R. B., Ciais, P., Saatchi, S., Liu, Y. Y., Piao, S., Chen, H., Vermote, E. F., Song, C. and Hwang, T.: Widespread decline of Congo rainforest greenness in the past decade., Nature, 509, 86–90, doi:10.1038/nature13265, 2014.

Chapter 2

A worldwide analysis of trends in water-balance evapotranspiration

A.M. Ukkola[1,2] and I.C. Prentice[1,3]

[1]Department of Biological Sciences, Macquarie University,
North Ryde, NSW 2109, Australia
[2] CSIRO Water for a Healthy Country Flagship,
Black Mountain, ACT 2601, Australia
[3]AXA Chair of Biosphere and Climate Impacts, Department of
Life Sciences and Grantham Institute for Climate Change,
Imperial College, Silwood Park, Ascot SL5 7PY, United Kingdom

This chapter is presented as the published journal article (with a subsequent update to a reference):

Ukkola A.M. and Prentice I.C., A worldwide analysis of trends in water-balance evapotranspiration, *Hydrology and Earth System Sciences*, 17, 4177-4187, 2013.

Hydrol. Earth Syst. Sci., 17, 4177–4187, 2013
www.hydrol-earth-syst-sci.net/17/4177/2013/
doi:10.5194/hess-17-4177-2013

Hydrology and Earth System Sciences
Open Access

A worldwide analysis of trends in water-balance evapotranspiration

A. M. Ukkola[1,2] **and I. C. Prentice**[1,3]

[1]Department of Biological Sciences, Macquarie University, North Ryde, NSW 2109, Australia
[2]CSIRO Water for a Healthy Country Flagship, Black Mountain, ACT 2601, Australia
[3]AXA Chair of Biosphere and Climate Impacts, Department of Life Sciences and Grantham Institute for Climate Change, Imperial College, Silwood Park, Ascot SL5 7PY, UK

Correspondence to: A. M. Ukkola (anna.ukkola@students.mq.edu.au)

Received: 23 April 2013 – Published in Hydrol. Earth Syst. Sci. Discuss.: 3 May 2013
Revised: 9 September 2013 – Accepted: 17 September 2013 – Published: 25 October 2013

Abstract. Climate change is expected to alter the global hydrological cycle, with inevitable consequences for freshwater availability to people and ecosystems. But the attribution of recent trends in the terrestrial water balance remains disputed. This study attempts to account statistically for both trends and interannual variability in water-balance evapotranspiration (ET), estimated from the annual observed streamflow in 109 river basins during "water years" 1961–1999 and two gridded precipitation data sets. The basins were chosen based on the availability of streamflow time-series data in the Dai et al. (2009) synthesis. They were divided into water-limited "dry" and energy-limited "wet" basins following the Budyko framework. We investigated the potential roles of precipitation, aerosol-corrected solar radiation, land use change, wind speed, air temperature, and atmospheric CO_2. Both trends and variability in ET show strong control by precipitation. There is some additional control of ET trends by vegetation processes, but little evidence for control by other factors. Interannual variability in ET was overwhelmingly dominated by precipitation, which accounted on average for 54–55 % of the variation in wet basins (ranging from 0 to 100 %) and 94–95 % in dry basins (ranging from 69 to 100 %). Precipitation accounted for 45–46 % of ET trends in wet basins and 80–84 % in dry basins. Net atmospheric CO_2 effects on transpiration, estimated using the Land-surface Processes and eXchanges (LPX) model, did not contribute to observed trends in ET because declining stomatal conductance was counteracted by slightly but significantly increasing foliage cover.

1 Introduction

Climate change is expected to alter the global hydrological cycle (Huntington, 2006), shifting the timing and distribution of freshwater resources (Kundzewicz et al., 2008) and changing the balance between precipitation, runoff and evapotranspiration (Zhang et al., 2012). Climatic effects may be compounded by changes in vegetation, whether due to land use/land cover change or vegetation physiological, compositional and structural responses caused by climate change or increasing atmospheric CO_2. Together these effects have the potential to change the amount of water available to the biosphere and for human use. Such changes have particular significance in regions already suffering from water deficits.

Evapotranspiration (ET) is the sum of evaporation from soil and open water, interception loss and plant transpiration. It is a key ecosystem variable linking hydrological, energy and carbon cycles and amounts to up to 60 % of global land precipitation (Oki and Kanae, 2006; Teuling et al., 2009). Because ET cannot be measured directly, multiple methods for estimating actual and potential ET have been employed, including satellite retrieval methods based on air temperature, net radiation and/or vegetation indices (Wang and Dickinson, 2012), eddy covariance measurements of latent heat flux (e.g. Baldocchi et al., 2001), radiation-based calculations (Xu and Singh, 2000), and pan evaporation measurements (Brutsaert, 2006; Roderick and Farquhar, 2002). There are few long-term, large-scale observational data sets that can be used to analyse variations in ET, and the situation is exacerbated by disagreements among estimates of ET obtained by different methods (Zhang et al., 2012). Many studies have attempted to account for recent historical trends in the hydrological cycle,

Published by Copernicus Publications on behalf of the European Geosciences Union.

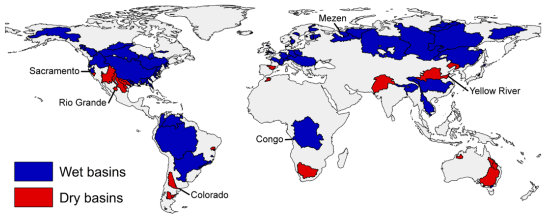

Fig. 1. Map of the study basins, classified into wet and dry according to aridity index (Sect. 2.1). The basins indicated are those used as examples in Fig. 4.

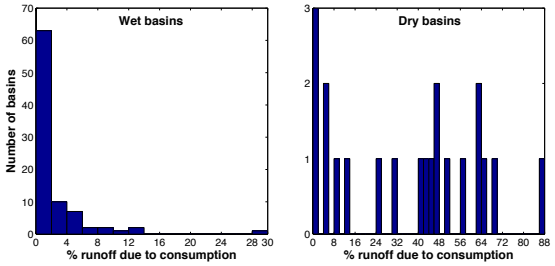

Fig. 2. The mean proportion of annual runoff (in %) due to consumption in wet and dry basins.

usually with runoff as the principal variable of interest (e.g. Dai et al., 2009; Gedney et al., 2006; Gerten et al., 2008; Labat et al., 2004; Piao et al., 2007), but no consensus on causation has emerged (Alkama et al., 2011). The direction of historical trends in runoff has also remained unclear, with Dai et al. (2009) and Milliman et al. (2008) finding a predominantly negative or non-existent trend across a large number of river basins, in contrast to an increase in global runoff reported by Labat et al. (2004). However, the data set of Labat et al. (2004) has been criticised, particularly for the wavelet method used to reconstruct the runoff time series (Legates et al., 2005; Peel and McMahon, 2006).

Many studies have recognised the importance of climate variability and trends, particularly in precipitation (e.g. Alkama et al., 2010; Dai et al., 2009; Gerten et al., 2008; Milliman et al., 2008), as drivers of changes in ET and/or runoff. Gerten et al. (2008) attributed 70 % of a simulated runoff increase over the 20th century to climate (precipitation and air temperature) based on the LPJmL vegetation model (Bondeau et al., 2007; Rost et al., 2008; Sitch et al., 2003). Piao et al. (2007) reported a value of 53 % using the ORCHIDEE biosphere model (Krinner et al., 2005). Other postulated climatic drivers of ET include solar shortwave radiation (particularly global "dimming" and "brightening" due to changes in aerosol loading; Roderick and Farquhar, 2002; Wild et al., 2008) and wind speed (McVicar et al., 2012), both of which influence evaporative demand and therefore ET. Changes to land-surface properties have also been invoked to account for historical runoff trends (Gedney et al., 2006; Piao et al., 2007). Deforestation decreases transpiration and interception losses (Bradshaw et al., 2007; Gordon et al., 2005) and consequently increases runoff (Bosch and Hewlett, 1982), if precipitation is unchanged. In dry areas, on the other hand, the expansion of croplands has been made possible by widespread irrigation, which increases water availability for ET and therefore tends to reduce runoff (Gordon et al., 2005), if precipitation is unchanged (the qualifications are important because deforestation can also lead to reduced rainfall while irrigation can increase it; D'Almeida et al., 2007; Lo and Famiglietti, 2013). Piao et al. (2007) concluded that land use change can account for about 50 % of global reconstructed runoff trends, but this has been contested (e.g. by Alkama et al., 2011). Rising atmospheric CO_2 concentration also can indirectly change ET and runoff via two opposing processes: partial stomatal closure which tends to reduce transpiration (Gedney et al., 2006; Sellers et al., 1996) and compensating increases in foliage cover, which tend to increase it (Betts et al., 1997). The net effect of rising atmospheric CO_2 on runoff trends is disputed (e.g. Alkama et al., 2011; Gedney et al., 2006; Gerten et al., 2008; Piao et al., 2007). It remains unclear, based on published analyses, whether or not changes in vegetation structure and function have left a detectable imprint on runoff. Studies focusing on ET have variously relied on trends in pan evaporation (Brutsaert, 2006; McVicar et al., 2012; Roderick and Farquhar, 2002, 2004), empirical equations (Wang et al., 2010; Zeng et al., 2012; Zhang et al., 2012) or land surface models (Douville et al., 2012; Li and Mölders, 2008; Teuling et al., 2009). But pan measurements are only very indirectly related to actual ET, while model simulations and empirical calculations are uncertain and produce a large range of estimates (Mueller et al., 2011; Zhang et al., 2012).

This study aims to account for trends and interannual variability in ET during the period 1961–1999. Despite uncertainties afflicting both precipitation and streamflow data, the difference between these two variables (the "water balance ET") integrated over a catchment remains the most firmly observationally based estimator of ET. We use the Dai et al. (2009) synthesis for streamflow data, and two alternative gridded precipitation data sets in order to take some account of precipitation uncertainties. We consider all the proposed drivers of annual ET, relying on observational data sets where possible, but with transient foliage cover and stomatal conductance simulated by the Land Processes and eXchanges Dynamic Global Vegetation Model (LPX DGVM) (Prentice et al., 2011; Murray et al., 2011). In Sect. 2, we first describe the data sets, the LPX DGVM and analysis methods. Section 3 investigates (i) the interannual variability and (ii) trends in water balance ET and relates those to variability in potential drivers of ET. Finally, conclusions are presented in Sect. 4.

Table 1. The proportion of interannual variability explained by all predictor variables and precipitation only (expressed as R^2), and the unique effect of meteorological and land surface variables as inferred from variance partitioning (expressed as adj. R^2) across wet and dry basins using CRU- and GPCC-based ET and precipitation, respectively.

	Wet		Dry	
Predictor	CRU	GPCC	CRU	GPCC
All variables	66 %	68 %	96 %	96 %
Precipitation	54 %	55 %	95 %	94 %
Unique effect:				
Meteorological	35 %	40 %	51 %	56 %
Land surface	2 %	3 %	1 %	1 %

2 Methods

2.1 Study basins

The study basins were chosen based on the availability of monthly river discharge data from Dai et al. (2009) so that spatial and temporal coverage could be maximised. Altogether 109 basins were chosen, covering approximately 33 % of the unglaciated land surface (Fig. 1). Only basins with ≤ 10 missing months during 1961–1999 were included in the analysis; gaps in the data were filled by linear interpolation between the values for the same month in the year before and the year after the gap. Basin boundaries were acquired from the Global Runoff Data Centre (GRDC; http://grdc.bafg.de/), Geoscience Australia National Catchment Boundaries v.1.1.3. (http://www.ga.gov.au/), the US Geological Survey HYDRO1k project (Peel et al., 2010) and the European Environment Agency (http://www.eea.europa.eu/data-and-maps/data/european-river-catchments-1).

The basins were divided into "energy-limited" (wet) and "water-limited" (dry) basins according to the Budyko framework (Budyko, 1974; Donohue et al., 2007; Li et al., 2013) (Fig. 1). This separation was achieved using the climatological aridity index A ($A = E_p/P$, where E_p = annual mean potential ET and P = annual mean precipitation), averaged over the basin area. Basins with $A \leq 1.5$ were classified as "wet" and those with $A > 1.5$ as "dry" (Zhang et al., 2012). A value of A was calculated for each basin based on 1961–1999 mean values of precipitation in the Climatic Research Unit (CRU) TS 3.1 archive at 0.5° resolution (Harris et al., 2013). E_p for each basin was calculated using the Priestley–Taylor method as in Gallego-Sala et al. (2010), using 1961–1999 mean values of cloud cover and air temperature from CRU TS 3.1. The Priestley–Taylor method has been shown to be appropriate for large-scale potential ET estimates (Raupach, 2000, 2001) and has been employed in other catchment-scale studies (e.g. Guerschman et al., 2009; Zhang et al., 2004).

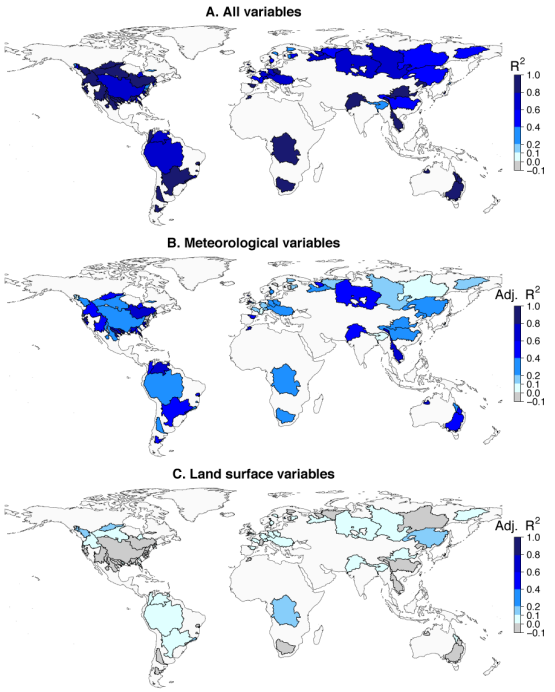

Fig. 3. The proportion of interannual variability in water balance ET explained by all predictor variables in each basin **(A)**; and the unique effect of meteorological **(B)** and land surface **(C)** variables in controlling ET variability, determined by variance partitioning. All values shown are based on CRU precipitation.

2.2 Data

Observed river discharge data (converted to runoff units) were acquired from the Dai et al. (2009) data set, which includes monthly streamflow at the farthest downstream gauging stations for the world's 925 largest river basins during the period 1900–2006. The data were compiled by Dai et al. (2009) mainly from Global Runoff Data Centre (GRDC), University of New Hampshire (UNH) and National Center for Atmospheric Research (NCAR) records. As the observed streamflow records are likely to include changes due to human disturbances (dams and water withdrawals), monthly water consumption estimates from the Global Water Use (GWU) model nested in the WaterGAP-2 model (Alcamo et al., 2003) were added to the observed runoff values. GWU estimates consumption based on three submodels for agricultural, industrial and domestic water use sectors at 0.5° spatial resolution. The correction is minimal in the majority of wet basins, with consumption accounting for 2 % of runoff on average (ranging from 0 to 29 %; Fig. 2). This leads to an average reduction of 2 % in annual water balance ET estimates. In dry basins, the correction amounts to 37 % of annual runoff

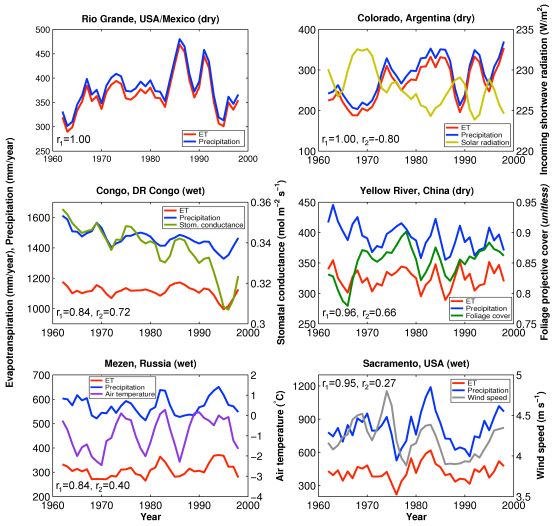

Fig. 4. Examples of interannual variability in water balance ET and its relationship with precipitation, solar radiation, stomatal conductance, foliage cover, air temperature and wind speed. Three-year block averages were used to smooth time series. Correlation coefficients for ET against precipitation (r_1) and the second plot variable (r_2) are shown. The location of each basin is indicated in Fig. 1.

on average (varying from 0 to 87 %; Fig. 2), but since runoff generally only forms a small component of the water balance in dry basins, a large relative change in runoff translates to a much smaller change in ET estimates. As such, the correction leads to an average reduction of 12 % in ET.

Water balance ET was calculated as the difference between observed annual precipitation and runoff. Water year (October–September) totals were used to account for the effects of water storage in snowpacks during Northern Hemisphere winter. The water balance method has the advantage of being based on observations but assumes negligible changes in soil water storage. Two ET values were calculated for each basin using two alternative precipitation data sets from the CRU TS 3.1 archive (Harris et al., 2013) and Global Precipitation Climatology Centre (GPCC) Full Data Reanalysis Product v.4 (Rudolf et al., 1994; Schneider et al., 2008; http://www.esrl.noaa.gov/psd/data/gridded/data.gpcc.html). Both precipitation data sets are gridded at 0.5° spatial resolution and were produced by three-dimensional interpolation of station data from multiple sources. Neither data set has been corrected for the possible effects of gauge undercatch.

Gridded monthly air temperature data at 0.5° spatial resolution were obtained from the CRU TS 3.1 archive. Monthly near-surface (10 m) wind speed data were acquired from National Centres for Environmental Prediction (NCEP) reanalysis product (NOAA-CIRES Climate Diagnostics Center, Boulder, Colorado, http://www.cdc.noaa.gov/) regridded to 0.5° from the original NCEP spatial resolution of 1.875° using bilinear interpolation (Prentice et al., 2011).

Downwelling shortwave radiation data were obtained from the EU WATCH Forcing Data archive (Weedon et al., 2011). These data are based on European Centre for Medium-Range Weather Forecasts reanalysis (ERA-40) data (Uppala et al., 2005). They provide daily values for the period 1901–2009, adjusted for observed cloud cover and modelled aerosol optical depths (based on representations of sulfate, black carbon, mineral dust, sea salt, biomass burning and secondary organic aerosols (Bellouin et al., 2007)).

Land use data were acquired from the HYDE v3.1 database of Klein Goldewijk (2001), which describes "pasture" (including rangeland) and cropland extent at 0.5° spatial resolution for the period 1700–2000 expressed as a fraction of each grid cell. Pasture and cropland extent were determined from historical data on agricultural activities using population density as a proxy for location (Klein Goldewijk and Ramankutty, 2004). The data were linearly interpolated to annual timescale from the original decadal time step (Prentice et al., 2011).

All daily or monthly data were converted to water year totals. Basin-specific values were extracted from each gridded variable using a point-based method, whereby cells with their centres within the catchment boundaries were selected.

2.3 LPX model

Dynamic global vegetation models (DGVMs) can represent time-dependent variations in ecosystem composition (in terms of plant functional types), structure (including height, biomass, leaf area index and foliage projective cover) and function (including gross and net primary production, ET and runoff) (Murray et al., 2013; Prentice and Cowling, 2013). The LPX DGVM (Prentice et al., 2011) is a development of the Lund-Potsdam-Jena (LPJ) model (Sitch et al., 2003; Gerten et al., 2004) with improved fire dynamics (Prentice et al., 2011). The model makes use of a photosynthesis–water balance scheme that explicitly couples CO_2 assimilation with transpiration (Gerten et al., 2004) but does not include nutrient constraints on assimilation. LPX has been evaluated against global and local hydrological data (Gerten et al., 2004; Murray et al., 2011; Ukkola and Murray, 2013) as well as a comprehensive set of vegetational, atmospheric and hydrological benchmarks (Kelley et al., 2012). The hydrological component is detailed in Gerten et al. (2004). A full description of the vegetation and carbon dynamics can be found in Sitch et al. (2003). Here we provide a brief discussion on the processes directly influencing ET in the model.

Stomatal conductance (g_c) is determined based on daytime assimilation rate (A_{dt}), ambient CO_2 concentration (c_a) and a plant functional type (PFT) specific minimum canopy

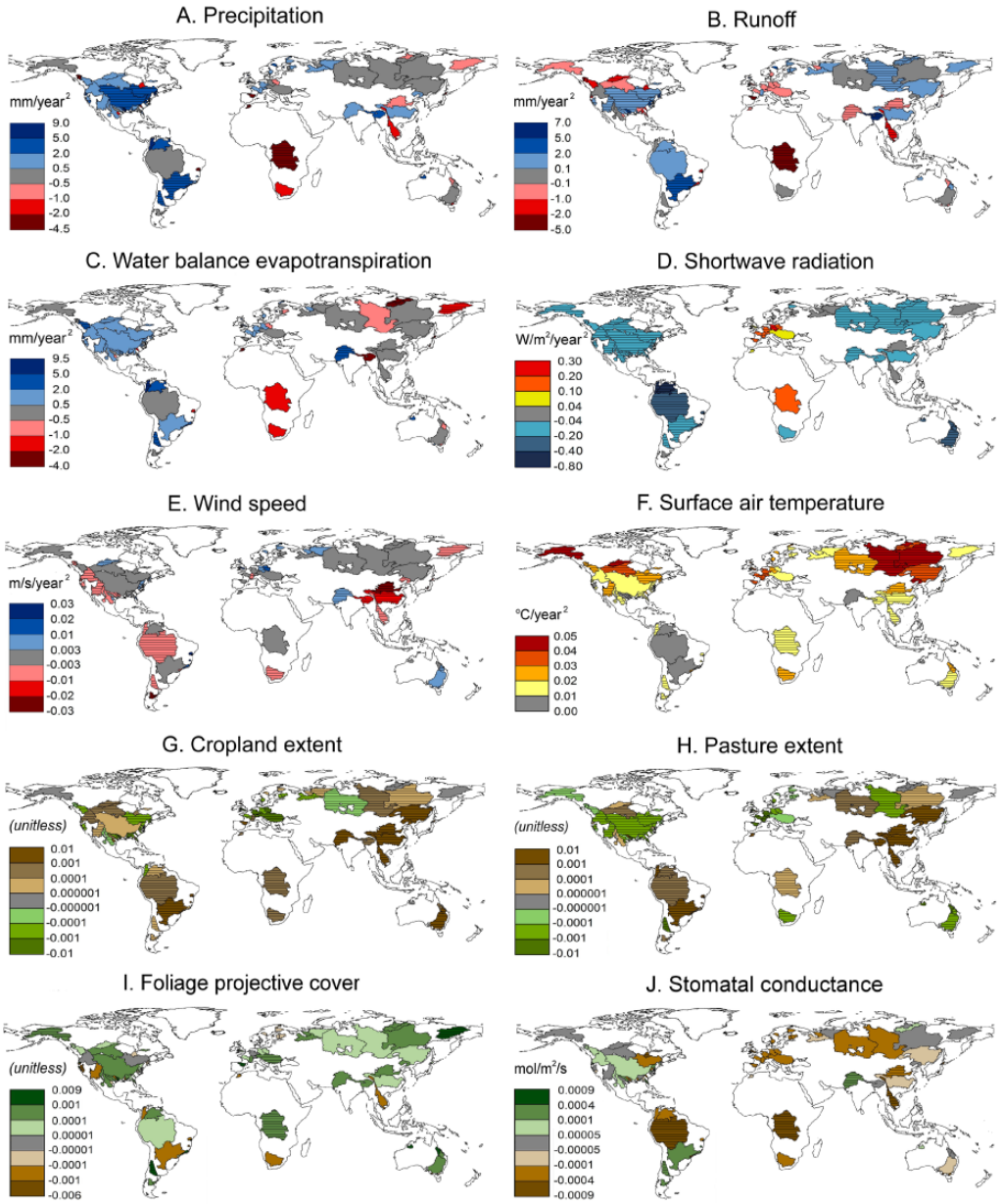

Fig. 5. Trends in observed CRU TS 3.1 precipitation, runoff, CRU-based water balance ET, solar radiation, wind speed, air temperature and land cover, and modelled stomatal conductance and foliage cover. Basins with significant trends are shown shaded.

conductance (g_{min}):

$$g_c = g_{min} + \frac{1.6A_{dt}}{c_a(1-\lambda)}, \quad (1)$$

where λ takes a maximum value of 0.8 for C_3 and 0.4 for C_4 plants. When soil water supply is limiting, g_c is reduced in such a way as to be consistent with Monteith's (1995) empirical formulation of the relationship between ET and g_c. The fractional foliage projective cover (FPC) for PFT is calculated annually as a function of total crown area (CA), plant population density (P) and the average individual FPC (Sitch

Table 2. Attribution of water balance ET trends (in mm yr^{-2}) in wet basins based on coefficients and p values from a multiple regression analysis, using CRU- and GPCC-based ET and precipitation, respectively. Significant p values (≤ 0.05) and coefficients are in italics.

	CRU	GPCC	CRU	GPCC
Predictor	Coefficient		p value	
Precipitation (mm yr^{-2})	*0.49*	*0.51*	*0.000*	*0.000*
Shortwave radiation (W m^{-2} yr^{-2})	−0.97	0.02	0.489	0.991
Wind speed (m s^{-1} yr^{-2})	7.98	−5.53	0.671	0.764
Air temperature (°C yr^{-2})	1.62	3.40	0.930	0.851
Pasture	62.59	38.49	0.516	0.688
Cropland	93.87	−20.30	0.413	0.859
LPX-simulated foliage cover	*340.85*	125.48	*0.040*	0.428
LPX-simulated stomatal conductance (mol m^{-2} s^{-1} yr^{-2})	−288.47	−232.18	0.658	0.718

Table 3. The proportion of ET trends explained by all predictor variables and precipitation only (expressed as R^2) across wet and dry basins, using CRU- and GPCC-based ET and precipitation, respectively.

	Wet		Dry	
	CRU	GPCC	CRU	GPCC
All variables	49 %	46 %	94 %	95 %
Precipitation	45 %	46 %	80 %	84 %

et al., 2003):

$$\mathrm{FPC} = \mathrm{CA} \cdot P \cdot \mathrm{FPC}_{\mathrm{ind}}. \quad (2)$$

Total FPC, the measure used in this study, varies between 0 (bare ground) and 1. Annual average FPC has been found to compare favourably against remotely sensed observations of the fraction of absorbed photosynthetically active radiation (fAPAR) (Kelley et al., 2012).

Both g_c and FPC influence simulated actual ET. FPC determines the amount of transpiring foliage, and controls interception loss by altering canopy storage capacity. g_c controls plant transpiration rates by linking CO_2 and water availabilities, so that transpiration is reduced at higher CO_2 concentrations and/or limited water supply and vice versa.

2.4 Model set-up

The model was spun up for 7000 yr using a repeating time series of detrended climate variables and stable CO_2 at 280 ppm, until the 50 yr means of the slow carbon pools varied by < 2 % (as detailed in Prentice et al., 2011). The model was subsequently run in transient mode for the period 1850–2006, forced with monthly gridded fields of mean, maximum and minimum air temperature, precipitation and cloud cover from the CRU TS 3.1 archive, wet day frequency from the CRU TS 3.0 archive and NCEP wind speed, together with global annually varying CO_2 concentrations (Etheridge et al., 1996; IPCC, 2001). Soil properties are prescribed based on Zobler (1986).

2.5 Analysis

We investigated what controls interannual variability in ET by comparing it to variability in precipitation, solar radiation, air temperature, wind speed, land use and vegetation processes by means of multiple regression. Seven river basins (Anabar, Lagarfljot, Olenek, Santa Mariada, Skjern, Teno and Yukon), mainly situated in high northern latitudes, were excluded from this analysis as they have invariant (zero) pasture and/or cropland extent, rendering the regression analysis invalid. Coefficients of determination (R^2) derived from the multiple regression analysis were used to indicate the proportion of variability in ET explained by the predictor variables.

Variance partitioning (Legendre, 2008) was used to further attribute variability. Predictor variables were assigned to one of two categories: meteorological variables (precipitation, solar radiation, air temperature and wind speed) and land-surface variables (pasture and cropland extent, stomatal conductance and foliage cover). The method makes it possible to estimate the *unique* effect of the two sets of predictors. It partitions variance into four components: the unique contributions of the two sets of predictors, the common contribution of the two sets (the results of correlations among predictors) and residual (random) variation not accounted for by the predictors. The unique effect of meteorological predictors was estimated as the difference between adjusted R^2 values derived from a multiple regression analysis using (i) both sets of predictors and (ii) land surface variables only, and vice versa.

Trends were calculated using ordinary least-squares linear regression based on annual values for water years (precipitation, runoff, ET, solar radiation, wind speed, air temperature and stomatal conductance) or calendar years (cropland,

Table 4. Attribution of water balance ET trends (in mm yr^{-2}) in dry basins based on coefficients and p values from a multiple regression analysis, using CRU- and GPCC-based ET and precipitation, respectively. Significant p values (≤ 0.05) and coefficients are in italics.

	CRU	GPCC	CRU	GPCC
Predictor	Coefficient		p value	
Precipitation (mm yr^{-2})	*0.87*	*0.88*	*0.000*	*0.000*
Shortwave radiation (W m^{-2} yr^{-2})	1.45	1.66	0.435	0.361
Wind speed (m s^{-1} yr^{-2})	15.15	20.87	0.398	0.211
Air temperature (°C yr^{-2})	−1.22	3.43	0.931	0.809
Pasture	0.59	−5.57	0.991	0.923
Cropland	131.05	125.61	0.255	0.276
LPX-simulated foliage cover	*356.38*	*331.35*	*0.010*	*0.016*
LPX-simulated stomatal conductance (mol m^{-2} s^{-1} yr^{-2})	−2210.41	−2007.65	0.082	0.121

pasture and foliage cover) for the period 1961–1999. To attribute trends in ET, a multiple regression of ET trends against those in predictor variables was performed, and coefficients and p values derived from the analysis were used to indicate the sign and significance of the relationship between ET and predictor trends, respectively.

3 Results and discussion

3.1 Interannual variability in water balance ET

Interannual variability in ET in both wet and dry basins was found to be strongly controlled by variability in precipitation. On average, we were able to explain 66–68 % of ET variability in wet basins (ranging from 13 to 100 %), and 96 % in dry basins (ranging from 79 to 100 %) (Fig. 3a; Table 1), with precipitation accounting for most of this (54–55 and 94–95 %, respectively). The relationship to precipitation was particularly evident in the dry basins (see e.g. the Rio Grande and Colorado basins in Fig. 4) and precipitation and ET magnitudes are very similar (i.e. almost all precipitation is evaporated and runoff is close to zero). In wet basins, precipitation plays a slightly weaker role in controlling ET variability, as hypothesised based on the Budyko framework. ET nevertheless tracks changes in precipitation in the majority of basins (see the Congo, Mezen and Sacramento basins in Fig. 4), with the exception of some northern high-latitude basins, which may be prone to larger than average precipitation uncertainties due to snow undercatch.

Solar radiation might be expected to exert a strong control on ET because it is the main determinant of the energy available for evaporation (Hobbins, 2004; Oliveira et al., 2011; Teuling et al., 2009), particularly in "energy-limited" wet basins. However, we found no strong positive correlations between ET and solar radiation variability and conversely, solar radiation was often found to correlate negatively with ET, likely as a result of increased cloud cover being associated with wet years. This was particularly evident in dry basins, where radiation was strongly reduced during years of increased precipitation and vice versa (see the Colorado Basin in Fig. 4).

Other climate variables showed significant correlations with interannual variation in ET only in a minority of basins. Air temperature variation was important in some cold northern basins (see the Mezen Basin in Fig. 4). Wind speed correlated with ET in some small coastal basins (see the Sacramento Basin in Fig. 4). Stomatal conductance tracked changes in ET in some mainly subtropical and tropical basins (see Congo in Fig. 4), whereas FPC correlated with ET in some (mainly dry) basins (see Yellow River in Fig. 4). Cropland and pasture extents change gradually and show no significant effects on interannual variability in ET. Changes in soil moisture could in principle drive interannual variability in ET (as much as they are a consequence of it) (Seneviratne et al., 2010) but were ignored in the water balance method. However, we found no significant lags between precipitation and ET on annual timescales (not shown), suggesting that time-varying retention of water in soils did not compromise the results.

Variance partitioning was used to further attribute interannual variability in ET to establish the unique contributions of meteorological and land-surface variables. Meteorological variables were found to exert a strong unique control, due to the overwhelming importance of precipitation variability (Fig. 3b). On average, meteorological variables explained 35–40 and 51–56 % of ET variability in wet and dry basins, respectively (Table 1). However, meteorological variables were less important in some temperate northern and boreal regions, possibly as a result of greater precipitation uncertainties. Land-surface variables were found to be important in some cold and tropical regions but generally show a much weaker control on ET than meteorological variables (Fig. 3c). On average, land-surface variables only account for 2–3 % of variability in wet and 1 % in dry basins (Table 1).

The basins where land-surface variables are significant tend to be forested, and some of them subject to wide-scale deforestation (e.g. Amazon and Congo) causing unusually large changes in the land surface.

3.2 Trends in water balance ET

Both positive and negative trends are observed in the water balance over the period 1961–1999 (Fig. 5). Precipitation, ET and runoff generally increased in the Americas, with some reductions in runoff in northern basins as a consequence of increased ET. Conversely, runoff and ET show reductions in Africa, likely as a result of a sharp decline in precipitation, particularly in the Congo Basin. Elsewhere, water balance trends are basin-dependent and where significant trends are present, ET and runoff have often changed in opposite directions, such as in parts of Siberia, Europe and India. Shortwave radiation decreased throughout the world, with the exception of Europe and parts of Africa (Fig. 5). No subsequent "brightening" was observed in North America, Australia or Asia during the period up to 1999. Wind speed decreased on the western coast of the Americas and Southeast Asia but changes elsewhere were slight. Air temperatures increased everywhere except in tropical South America. Land use changed almost throughout the world, with pasture expanding everywhere except North America and Europe and cropland expanding in most regions apart from Europe. Simulated FPC increased and stomatal conductance generally decreased, particularly in forested regions, as expected as a result of increasing atmospheric CO_2.

In wet basins, observed trends in water balance ET are generally explained by precipitation and to some extent increased foliage cover (when CRU TS 3.1 based ET is used; Table 2), pointing to a small but significant effect of increased atmospheric CO_2. Predictor variables can explain 46–49 % of the ET trend, with precipitation alone accounting for 45–46 % of the ET trend (Table 3). Other variables, including solar radiation, were not found to be significant predictors of the trend.

A previous study by Zhang et al. (2012) reported $R^2 = 9$ % for wet basins when water balance ET trends were compared to precipitation trends. Our analysis explains more of the ET trends than Zhang et al. (2012) but we are still only able to account for around half of the ET trends in wet basins. ET in wet basins may be inhibited by factors such as low vapour pressure deficit reducing evaporative demand. Soil moisture has been postulated as an important driver of ET (Jung et al., 2010) but was ignored in this study. However, other studies have shown soil moisture to be mainly driven by precipitation (Sheffield and Wood, 2008), which is explicitly included in our analysis. It is unlikely that not accounting for soil moisture trends results in major uncertainty. Data quality issues may also hinder attribution of trends, especially in sparsely populated tropical areas (Wohl et al., 2012). A stronger disagreement was found between CRU TS 3.1 and GPCC precipitation trends in the tropics compared to the rest of the world (not shown). Some wet basins also showed negative annual ET totals during some years as well as low actual/potential ET ratios and actual ET exceeding potential ET, pointing to likely biases in the observations (Kauffeldt et al., 2013). However, the results were found not to be sensitive to these physically implausible data. Other predictor variables also have inherent uncertainties, particularly land use data for the pre-satellite era.

In dry basins, ET trends are mainly explained by precipitation, which accounts for 80–84 % of the trend (Tables 3, 4). This agrees well with findings of Zhang et al. (2012), who reported $R^2 = 85$ % for dry basins. In addition, increasing foliage cover shows a significant positive effect on ET trends, implying a net increase in transpiration and interception as a result of increased atmospheric CO_2. This is in line with findings by Donohue et al. (2013) who reported a recent greening trend across the world's warm arid environments as a result of the CO_2 fertilisation effect. Together, all variables account for 94–95 % of the ET trend (Table 3).

4 Conclusions

Both trends and interannual variability in water balance ET are strongly controlled by precipitation. In the dry "water-limited" basins precipitation explains 80–95 % of ET changes, compared to 45–55 % in the wet basins. This conclusion was shown to be independent of the precipitation data set used, and it is consistent with the expectation of strong water limitation of ET in dry basins.

Vegetation processes were also found to influence ET. Foliage cover was found to be a significant control of ET trends in both wet and dry basins, and stomatal conductance variations correlated with the interannual variability of ET in some basins. Both stomatal conductance and foliage cover are expected to respond strongly to increasing atmospheric CO_2 concentrations (e.g. Betts et al., 1997, 2007; Gedney et al., 2006; Sellers et al., 1996), but in opposite directions. With large increases in CO_2 projected, it is likely that CO_2 effects will become increasingly apparent, but the sign and regional pattern of these effects over the longer term is not well constrained by the available evidence to date.

Solar shortwave radiation was generally not found to be a significant predictor of ET variability. This is despite the expectation that energy-limited basins, particularly, should respond to changes in the driving force for ET. However, persistent large differences among different, satellite-based radiation data products (Zhang et al., 2012) may hinder the attribution of ET to solar radiation changes. Land use change effects on ET were not found to be significant.

Acknowledgements. A. M. Ukkola is supported by an international Macquarie University Research Excellence scholarship and a CSIRO Water for a Healthy Country Flagship top-up scholarship. We thank Aiguo Dai for making the streamflow data publicly available. Lina Mercado drew our attention to the WATCH solar radiation data set, which is made available by the International Institute for Applied Systems Analysis, Austria.

Edited by: J. Liu

References

Alcamo, J., Döll, P., Henrichs, T., Kaspar, F., Lehner, B., Rösch, T., and Siebert, S.: Development and testing of the WaterGAP 2 global model of water use and availability, Hydrolog. Sci. J., 48, 317–337, 2003.

Alkama, R., Kageyama, M., and Ramstein, G.: Relative contributions of climate change, stomatal closure, and leaf area index changes to 20th and 21st century runoff change: A modelling approach using the Organizing Carbon and Hydrology in Dynamic Ecosystems (ORCHIDEE) land surface model, J. Geophys. Res., 115, D17112, doi:10.1029/2009jd013408, 2010.

Alkama, R., Decharme, B., Douville, H., and Ribes, A.: Trends in global and basin-scale runoff over the late twentieth century: methodological issues and sources of uncertainty, J. Climate, 24, 3000–3014, doi:10.1175/2010jcli3921.1, 2011.

Baldocchi, D., Falge, E., Gu, L., Olson, R., Hollinger, D., Running, S., Anthoni, P., Bernhofer, C., Davis, K., Evans, R., Fuentes, J., Goldstein A., Katul, G., Law, B., Lee, X., Malhi, Y., Meyers, T., Munger, W., Oechel, W., Paw U., K. T., Pilegaard K., Schmid, H. P., Valentini, R., Verma S., Vesala, T., Wilson, K., and Wofsy, S.: FLUXNET: A new tool to study the temporal and spatial variability of ecosystem-scale carbon dioxide, water vapor, and energy flux densities, B. Am. Meteorol. Soc., 82, 2415–2434, 2001.

Bellouin, N., Boucher, O., Haywood, J., Johnson, C., Jones, A., Rae, J., and Woodward, S.: Improved representation of aerosols for HadGEM2, Hadley Centre technical note 73, Exeter, United Kingdom, 42 pp., 2007.

Betts, R. A., Cox, P. M., Lee, S. E., and Woodward, F. I.: Contrasting physiological and structural vegetation feedbacks in climate change simulations, Nature, 387, 796–799, 1997.

Betts, R. A., Boucher, O., Collins, M., Cox, P. M., Falloon, P. D., Gedney, N., Hemming, D. L., Huntingford, C., Jones, C. D., Sexton, D. M. H., and Webb, M. J.: Projected increase in continental runoff due to plant responses to increasing carbon dioxide, Nature, 448, 1037–1041, doi:10.1038/nature06045, 2007.

Bondeau, A., Smith, P. C., Zaehle, S., Schaphoff, S., Lucht, W., Cramer, W., Gerten, D., Lotze-Campen, H., Müller, C., Reichstein, M., and Smith, B.: Modelling the role of agriculture for the 20th century global terrestrial carbon balance, Global Change Biol., 13, 679–706, doi:10.1111/j.1365-2486.2006.01305.x, 2007.

Bosch, J. M. and Hewlett, J. D.: A review of catchment experiments to determine the effect of vegetation changes on water yield and evapotranspiration, J. Hydrol., 55, 3–23, 1982.

Bradshaw, C. J. A., Sodhi, N. S., Peh, K. S. H., and Brook, B. W.: Global evidence that deforestation amplifies flood risk and severity in the developing world, Global Change Biol., 13, 2379–2395, doi:10.1111/j.1365-2486.2007.01446.x, 2007.

Brutsaert, W.: Indications of increasing land surface evaporation during the second half of the 20th century, Geophys. Res. Lett., 33, L20403, doi:10.1029/2006GL027532, 2006.

Budyko, M. I.: Climate and life, International Physics Series, Academic, New York, 1974.

Dai, A., Qian, T., Trenberth, K. E., and Milliman, J. D.: Changes in continental freshwater discharge from 1948 to 2004, J. Climate, 22, 2773–2792, doi:10.1175/2008JCLI2592.1, 2009.

D'Almeida, C., Vörösmarty, C. J., Hurtt, G. C., Marengo, J. A., Dingman, S. L., and Keim, B. D.: The effects of deforestation on the hydrological cycle in Amazonia: a review on scale and resolution, Int. J. Climatol., 27, 633–647, doi:10.1002/joc.1475, 2007.

Donohue, R. J., Roderick, M. L., and McVicar, T. R.: On the importance of including vegetation dynamics in Budyko's hydrological model, Hydrol. Earth Syst. Sci., 11, 983–995, doi:10.5194/hess-11-983-2007, 2007.

Donohue, R. J., Roderick, M. L., McVicar, T. R., and Farquhar, G. D.: Impact of CO_2 fertilisation on maximum foliage cover across the globe's warm, arid environments, Geophys. Res. Lett., 40, 3031–3035, doi:10.1002/grl.50563, 2013.

Douville, H., Ribes, A., Decharme, B., Alkama, R., and Sheffield, J.: Anthropogenic influence on multidecadal changes in reconstructed global evapotranspiration, Nat. Clim. Change, 3, 59–62, doi:10.1038/nclimate1632, 2012.

Etheridge, D., Steele, L., Langenfelds, R., Francey, R., Barnola, J.-M., and Morgan, V.: Natural and anthropogenic changes in atmospheric CO_2 over the last 1000 years from air in Antarctic ice and firn, J. Geophys. Res., 101, 4115–4128, 1996.

Gallego-Sala, A. V, Clark, J. M., House, J. I., Orr, H. G., Prentice, I. C., Smith, P., Farewell, T., and Chapman, S. J.: Bioclimatic envelope model of climate change impacts on blanket peatland distribution in Great Britain, Clim. Res, 45, 151–162, doi:10.3354/cr00911, 2010.

Gedney, N., Cox, P. M., Betts, R. A., Boucher, O., Huntingford, C., and Stott, P. A.: Detection of a direct carbon dioxide effect in continental river runoff records, Nature, 439, 835–838, doi:10.1038/nature04504, 2006.

Gerten, D., Schaphoff, S., Haberlandt, U., Lucht, W., and Sitch, S.: Terrestrial vegetation and water balance – hydrological evaluation of a dynamic global vegetation model, J. Hydrol., 286, 249–270, doi:10.1016/j.jhydrol.2003.09.029, 2004.

Gerten, D., Rost, S., von Bloh, W., and Lucht, W.: Causes of change in 20th century global river discharge, Geophys. Res. Lett., 35, L20405, doi:10.1029/2008gl035258, 2008.

Gordon, L. J., Steffen, W., Jönsson, B. F., Folke, C., Falkenmark, M., and Johannessen, Å.: Human modification of global water vapor flows from the land surface, P. Natl. Acad. Sci. USA, 102, 7612–7617, doi:10.1073/pnas.0500208102, 2005.

Guerschman, J. P., van Dijk, A. I. J. M., Mattersdorf, G., Beringer, J., Hutley, L. B., Leuning, R., Pipunic, R. C., and Sherman, B. S.: Scaling of potential evapotranspiration with MODIS data reproduces flux observations and catchment water balance observations across Australia, J. Hydrol., 369, 107–119, doi:10.1016/j.jhydrol.2009.02.013, 2009.

Harris, I., Jones, P. D., Osborn, T. J., and Lister, D. H.: Updated high-resolution grids of monthly climatic observations – the CRU TS3.10 Dataset, Int. J. Climatol., in press, doi:10.1002/joc.3711, 2013.

Hobbins, M. T.: Trends in pan evaporation and actual evapotranspiration across the conterminous U.S.: Paradoxical or complementary?, Geophys. Res. Lett., 31, L13503, doi:10.1029/2004GL019846, 2004.

Huntington, T. G.: Evidence for intensification of the global water cycle: Review and synthesis, J. Hydrol., 319, 83–95, doi:10.1016/j.jhydrol.2005.07.003, 2006.

IPCC: Appendix II – SRES Tables', in: Climate Change 2001: The Scientific Basis. Contribution of Working Group I to the Third Assessment Report of the Intergovernmental Panel on Climate Change, edited by: Houghton, J. T., Ding, Y., Griggs, D. J., Noguer, M., van der Linden, P. J., Dai, X., Maskell, K., and Johnson, C. A., Cambridge University Press, Cambridge, UK and New York, NY, USA, 881 pp., 2001.

Jung, M., Reichstein, M., Ciais, P., Seneviratne, S. I., Sheffield, J., Goulden, M. L., Bonan, G., Cescatti, A., Chen, J., de Jeu, R., Dolman, A. J., Eugster, W., Gerten, D., Gianelle, D., Gobron, N., Heinke, J., Kimball, J., Law, B. E., Montagnani, L., Mu, Q., Mueller, B., Oleson, K., Papale, D., Richardson, A. D., Roupsard, O., Running, S., Tomelleri, E., Viovy, N., Weber, U., Williams, C., Wood, E., Zaehle, S., and Zhang, K.: Recent decline in the global land evapotranspiration trend due to limited moisture supply, Nature, 467, 951–954, doi:10.1038/nature09396, 2010.

Kauffeldt, A., Halldin, S., Rodhe, A., Xu, C.-Y., and Westerberg, I. K.: Disinformative data in large-scale hydrological modelling, Hydrol. Earth Syst. Sci., 17, 2845–2857, doi:10.5194/hess-17-2845-2013, 2013.

Kelley, D. I., Colin Prentice, I., Harrison, S. P., Wang, H., Simard, M., Fisher, J. B., and Willis, K. O.: A comprehensive benchmarking system for evaluating global vegetation models, Biogeosciences Discuss., 9, 15723–15785, doi:10.5194/bgd-9-15723-2012, 2012.

Klein Goldewijk, K.: Estimating global land use change over the past 300 years: The HYDE database, Global Biochem. Cy., 15, 417–433, doi:10.1029/1999GB001232, 2001.

Klein Goldewijk, K. and Ramankutty, N.: Land cover change over the last three centuries due to human activities: The availability of new global data sets, GeoJournal, 61, 335–344, doi:10.1007/s10708-004-5050-z, 2004.

Krinner, G., Viovy, N., de Noblet-Ducoudré, N., Ogée, J., Polcher, J., Friedlingstein, P., Ciais, P., Sitch, S., and Prentice, I. C.: A dynamic global vegetation model for studies of the coupled atmosphere-biosphere system, Global Biochem. Cy., 19, GB1015, doi:10.1029/2003GB002199, 2005.

Kundzewicz, Z. W., Mata, L., Arnell, N. W., Döll, P., Jimenez, B., Miller, K., Oki, T., Sen, Z., and Shiklomanov, I.: The implications of projected climate change for freshwater resources and their management, Hydrolog. Sci. J., 53, 3–10, 2008.

Labat, D., Goddéris, Y., Probst, J. L., and Guyot, J. L.: Evidence for global runoff increase related to climate warming, Adv. Water Resour., 27, 631–642, doi:10.1016/j.advwatres.2004.02.020, 2004.

Legates, D. R., Lins, H. F., and McCabe, G. J.: Comments on "Evidence for global runoff increase related to climate warming" by Labat et al., Adv. Water Resour., 28, 1310–1315, doi:10.1016/j.advwatres.2005.04.006, 2005.

Legendre, P.: Studying beta diversity: ecological variance partitioning by multiple regression and canonical analysis. J. Plant Ecology, 1, 3-8, 2008.

Li, D., Pan, M., Cong, Z., Zhang, L., and Wood, E.: Vegetation control on water and energy balance within the Budyko framework, Water Resour. Res., 49, 969–976, doi:10.1002/wrcr.20107, 2013.

Li, Z. and Mölders, N.: Interaction of impacts of doubling CO_2 and changing regional land-cover on evaporation, precipitation, and runoff at global and regional scales, Int. J. Climatol., 28, 1653–1679, doi:10.1002/joc.1666, 2008.

Lo, M.-H. and Famiglietti, J. S.: Irrigation in California's Central Valley strengthens the southwestern U.S. water cycle, Geophys. Res. Lett., 40, 301–306, doi:10.1002/grl.50108, 2013.

McVicar, T. R., Roderick, M. L., Donohue, R. J., Li, L. T., Van Niel, T. G., Thomas, A., Grieser, J., Jhajharia, D., Himri, Y., Mahowald, N. M., Mescherskaya, A. V., Kruger, A. C., Rehman, S., and Dinpashoh, Y.: Global review and synthesis of trends in observed terrestrial near-surface wind speeds: Implications for evaporation, J. Hydrol., 416–417, 182–205, doi:10.1016/j.jhydrol.2011.10.024, 2012.

Milliman, J. D., Farnsworth, K. L., Jones, P. D., Xu, K. H., and Smith, L. C.: Climatic and anthropogenic factors affecting river discharge to the global ocean, 1951–2000, Global Planet. Change, 62, 187–194, doi:10.1016/j.gloplacha.2008.03.001, 2008.

Monteith, J. L.: Accommodation between transpiring vegetation and the convective boundary layer, J. Hydrol., 166, 251–263, 1995.

Mueller, B., Seneviratne, S. I., Jimenez, C., Corti, T., Hirschi, M., Balsamo, G., Ciais, P., Dirmeyer, P., Fisher, J. B., Guo, Z., Jung, M., Maignan, F., McCabe, M. F., Reichle, R., Reichstein, M., Rodell, M., Sheffield, J., Teuling, A. J., Wang, K., Wood, E. F., and Zhang, Y.: Evaluation of global observations-based evapotranspiration datasets and IPCC AR4 simulations, Geophys. Res. Lett., 38, L06402, doi:10.1029/2010gl046230, 2011.

Murray, S. J., Foster, P. N., and Prentice, I. C.: Evaluation of global continental hydrology as simulated by the Land-surface Processes and eXchanges Dynamic Global Vegetation Model, Hydrol. Earth Syst. Sci., 15, 91–105, doi:10.5194/hess-15-91-2011, 2011.

Murray, S. J., Watson, I. M., and Prentice, I.C.: The use of dynamic global vegetation models for simulating hydrology and the potential integration of satellite observations, Prog. Phys. Geog., 37, 63–97, doi:10.1177/0309133312460072, 2013.

Oki, T. and Kanae, S.: Global hydrological cycles and world water resources, Science, 313, 1068–1072, doi:10.1126/science.1128845, 2006.

Oliveira, P. J. C., Davin, E. L., Levis, S., and Seneviratne, S. I.: Vegetation-mediated impacts of trends in global radiation on land hydrology: a global sensitivity study, Global Change Biol., 17, 3453–3467, doi:10.1111/j.1365-2486.2011.02506.x, 2011.

Peel, M. C. and McMahon T. A.: Continental runoff: a quality-controlled global runoff data set, Nature, 444, E14, doi:10.1038/nature05480, 2006.

Peel, M. C., McMahon, T. A., and Finlayson, B. L.: Vegetation impact on mean annual evapotranspiration at a global catchment scale, Water Resour. Res., 46, W09508, doi:10.1029/2009WR008233, 2010.

Piao, S., Friedlingstein, P., Ciais, P., de Noblet-Ducoudre, N., Labat, D., and Zaehle, S.: Changes in climate and land use have a larger direct impact than rising CO_2 on global river runoff trends, Proc. Natl. Acad. Sci., 104, 15242–15247, doi:10.1073/pnas.0707213104, 2007.

Prentice, I. C. and Cowling, S. A.: Dynamic global vegetation models, in: Encyclopedia of Biodiversity, 2nd Edn., edited by: Levin, S. A., Academic Press, 607–689, 2013.

Prentice, I. C., Kelley, D. I., Foster, P. N., Friedlingstein, P., Harrison, S. P., and Bartlein, P. J.: Modeling fire and the terrestrial carbon balance, Global Biochem. Cy., 25, GB3005, doi:10.1029/2010gb003906, 2011.

Raupach, M. R.: Equilibrium evaporation and the convective boundary layer, Boundary-Layer Meteorol., 96, 107–141, 2000.

Raupach, M. R.: Combination theory and equilibrium evaporation, Quart. J. Roy. Meteorol. Soc., 127, 1149–1181, 2001.

Roderick, M. L. and Farquhar, G. D.: The cause of decreased pan evaporation over the past 50 years, Science, 298, 1410–1411, doi:10.1126/science.1075390, 2002.

Roderick, M. L. and Farquhar, G. D.: Changes in Australian pan evaporation from 1970 to 2002, Int. J. Climatol., 24, 1077–1090, doi:10.1002/joc.1061, 2004.

Rost, S., Gerten, D., Bondeau, A., Lucht, W., Rohwer, J., and Schaphoff, S.: Agricultural green and blue water consumption and its influence on the global water system, Water Resour. Res., 44, W09405, doi:10.1029/2007wr006331, 2008.

Rudolf, B., Hauschild, H., Rueth, W., and Schneider, U.: Terrestrial precipitation analysis: operational method and required density of point measurements, in: Global Precipitations and Climate Change, edited by: Desbois, M. and Desalmond, F., NATO ASI Series I, Vol. 20, Springer-Verlag, 173–186, 1994.

Schneider, U., Fuchs, T., Meyer-Christoffer, A., and Rudolf, B.: Global Precipitation Analysis Products of the GPCC, Global Precipitation Climatology Centre (GPCC), Deutscher Wetterdienst, Offenbach am Main, Germany, 2008.

Sellers, P. J., Bounoua, L., Collatz, G. J., Randall, D. A., Dazlich, D. A., Los, S. O., Berry, J. A., Fung, I., Tucker, C. J., Field, C. B., and Jensen, T. G.: Comparison of radiative and physiological effects of doubled atmospheric CO_2 on climate, Science, 271, 1402–1406, doi:10.1126/science.271.5254.1402, 1996.

Seneviratne, S. I., Corti, T., Davin, E. L., Hirschi, M., Jaeger, E. B., Lehner, I., Orlowsky, B., and Teuling, A. J.: Investigating soil moisture–climate interactions in a changing climate: A review, Earth-Sci. Rev., 99, 125–161, doi:10.1016/j.earscirev.2010.02.004, 2010.

Sheffield, J. and Wood, E. F.: Global trends and variability in soil moisture and drought characteristics, 1950–2000, from observation-driven simulations of the terrestrial hydrologic cycle, J. Climate, 21, 432–458, doi:10.1175/2007JCLI1822.1, 2008.

Sitch, S., Smith, B., Prentice, I. C., Arneth, A., Bondeau, A., Cramer, W., Kaplans, J. O., Levis, S., Lucht, W., Sykes, M. T., Thonicke, K., and Venevsky, S.: Evaluation of ecosystem dynamics, plant geography and terrestrial carbon cycling in the LPJ dynamic global vegetation model, Global Change Biol., 9, 161–185, 2003.

Teuling, A. J., Hirschi, M., Ohmura, A., Wild, M., Reichstein, M., Ciais, P., Buchmann, N., Ammann, C., Montagnani, L., Richardson, a. D., Wohlfahrt, G., and Seneviratne, S. I.: A regional perspective on trends in continental evaporation, Geophys. Res. Lett., 36, L02404, doi:10.1029/2008GL036584, 2009.

Ukkola, A. M. and Murray, S. J.: Hydrological evaluation of the LPX dynamic global vegetation model for small river catchments in the UK, Hydrol. Process., in press, 2013.

Uppala, S. M., Kållberg, P. W., Simmons, A. J., Andrae, U., Bechtold, V. D. C., Fiorino, M., Gibson, J. K., Haseler, J., Hernandez, A., Kelly, G. a., Li, X., Onogi, K., Saarinen, S., Sokka, N., Allan, R. P., Andersson, E., Arpe, K., Balmaseda, M. A., Beljaars, A. C. M., van de Berg, L., Bidlot, J., Bormann, N., Caires, S., Chevallier, F., Dethof, A., Dragosavac, M., Fisher, M., Fuentes, M., Hagemann, S., Holm, E., Hoskins, B. J., Isaksen, L., Jansses, P. A. E. M., Jenne, R., McNally, A. P., Mahfouf, J.-F., Morcrette, J.-J., Rayner, N. A., Saunders, R. W., Simon, P., Sterl, A., Trenberth, K. E., Untch. A., Vasiljevic, D., Viterbo, P., and Woollen, J.: The ERA-40 re-analysis, Q. J. Roy. Meteor. Soc., 131, 2961–3012, doi:10.1256/qj.04.176, 2005.

Wang, K. and Dickinson, R. E.: A review of global terrestrial evapotranspiration: observation, modeling, climatology and climatic variability, Rev. Geophys., 50, RG2005, doi:10.1029/2011RG000373, 2012.

Wang, K., Dickinson, R. E., Wild, M., and Liang, S.: Evidence for decadal variation in global terrestrial evapotranspiration between 1982 and 2002: 2. Results, J. Geophys. Res., 115, D20113, doi:10.1029/2010JD013847, 2010.

Weedon, G. P., Gomes, S., Viterbo, P., Shuttleworth, W. J., Blyth, E., Österle, H., Adam, J. C., Bellouin, N., Boucher, O., and Best, M.: Creation of the WATCH Forcing Data and its use to assess global and regional reference crop evaporation over land during the twentieth century, J. Hydrometeorol., 12, 823–848, doi:10.1175/2011JHM1369.1, 2011.

Wild, M., Grieser, J., and Schär, C.: Combined surface solar brightening and increasing greenhouse effect support recent intensification of the global land-based hydrological cycle, Geophys. Res. Lett., 35, L17706, doi:10.1029/2008gl034842, 2008.

Wohl, E., Barros, A., Brunsell, N., Chappell, N. A., Coe, M., Giambelluca, T., Goldsmith, S., Harmon, R., Hendrickx, J. M. H., Juvik, J., McDonnell, J., and Ogden, F.: The hydrology of the humid tropics, Nat. Clim. Change, 2, 655–662, doi:10.1038/nclimate1556, 2012.

Xu, C.-Y. and Singh, V. P.: Evaluation and generalization of radiation-based methods for calculating evaporation, Hydrol. Process., 14, 339–349, 2000.

Zeng, Z., Piao, S., Lin, X., Yin, G., Peng, S., Ciais, P., and Myneni, R. B.: Global evapotranspiration over the past three decades: estimation based on the water balance equation combined with empirical models, Environ. Res. Lett., 7, 014026, doi:10.1088/1748-9326/7/1/014026, 2012.

Zhang, L. K., Hickel, K., Dawes, W. R., Chiew, F. H. S., Western, A. W., and Briggs P. R.: A rational function approach for estimating mean annual evapotranspiration, Water Resour. Res., 40, W02502, doi:10.1029/2003WR002710, 2004.

Zhang, Y., Leuning, R., Chiew, F. H. S., Wang, E., Zhang, L., Liu, C., Sun, F., Peel, M. C., Shen, Y., and Jung, M.: Decadal trends in evaporation from global energy and water balances, J. Hydrometeorol., 13, 379–391, doi:10.1175/JHM-D-11-012.1, 2012.

Zobler, L.: A world soil file for global climate modelling, NASA Technical Memorandum 87802, NASA/GISS, New York, USA, 32 pp., 1986.

Chapter 3

Reduced streamflow in water-stressed climates consistent with CO_2 effects on vegetation

A.M. Ukkola[1,2], I.C. Prentice[1,3], T.F. Keenan[1], A.I.J.M. van Dijk[4], N.R. Viney[5], R.B. Myneni[6] and J. Bi[6]

[1]Department of Biological Sciences, Macquarie University, North Ryde, NSW 2109, Australia
[2] CSIRO Water for a Healthy Country Flagship, Black Mountain, ACT 2601, Australia
[3]AXA Chair of Biosphere and Climate Impacts, Department of Life Sciences and Grantham Institute for Climate Change, Imperial College, Silwood Park, Ascot SL5 7PY, United Kingdom
[4]Fenner School of Environment & Society, Australian National University, Canberra, ACT 0200, Australia
[5]CSIRO Land and Water, Canberra, ACT 2601, Australia
[6]Department of Earth and Environment, Boston University, Boston, MA 02215, United States

This chapter is presented as a journal article accepted for publication in *Nature Climate Change*:

Ukkola A.M., Prentice I.C., Keenan T.F., van Dijk A.I.J.M., Viney N.R., Myneni R.B. and Bi J., Reduced streamflow in water-stressed climates consistent with CO_2 effects on vegetation, *Nature Climate Change*, accepted.

3.1. Main

Global environmental change has implications for the spatial and temporal distribution of water resources, but quantifying its effects remains a challenge. The impact of vegetation responses to increasing atmospheric CO_2 concentration on the hydrological cycle is particularly poorly constrained[1–3]. Here we combine remotely sensed normalized difference vegetation index (NDVI) data and long-term water-balance evapotranspiration (ET) measurements from 190 unimpaired river basins across Australia to show (a) that the precipitation threshold for water limitation of vegetation cover has significantly declined during the past three decades, while (b) sub-humid and semi-arid basins are not only 'greening' in response to increased atmospheric CO_2 but also consuming more water, leading to significant (24–28%) reductions in streamflow. In contrast, wet and arid basins show small, non-significant changes in NDVI and reductions in ET. Our results suggest that projected future decreases in precipitation[4] will likely be compounded by increased vegetation water use, further reducing streamflow in water-stressed regions.

Experiments have shown that elevated atmospheric CO_2 affects vegetation productivity and water use[5]. CO_2 is the substrate for photosynthesis and concentrations above current ambient levels stimulate carbon assimilation by plants. This CO_2 fertilisation effect should in principle lead to increased biomass and green vegetation cover ('greening'). Simultaneously, increasing CO_2 lowers stomatal conductance, reducing water loss through leaves. Reduced stomatal conductance and/or stimulated photosynthesis lead to enhanced water use efficiency, the amount of water required to produce a unit of biomass. The effect of CO_2 on vegetation is commonly expected to manifest most strongly in water-limited environments[6,7], where moisture is the main limitation on plant growth. However, not all studies show a strong link between aridity and the strength of the CO_2 effect[8] and the magnitude of associated greening and water savings are generally not well constrained across species and ecosystems[9–11].

CO_2-induced structural and physiological changes in vegetation potentially have consequences for water resources. CO_2 fertilisation and associated greening tends to increase vegetation water consumption by increasing the amount of transpiring leaf area, whereas reduced stomatal conductance tends to decrease transpiration per unit leaf area – two effects with opposing consequences for streamflow[2]. Furthermore, increased vegetation cover can change the partitioning of rainfall into rainfall interception, infiltration and runoff, while shading by increased foliage cover may lead to reductions in soil evaporation by decreasing the amount of radiation reaching the ground surface[12]. It remains unresolved

whether these various processes in combination have led to a detectable imprint in ET or streamflow. At the global scale, both decreases and increases in ET due to CO_2 have been reported[1,2] and the results appear to be data- and model-dependent[3]. The direction and magnitude of the CO_2 effect on ET and streamflow thus remains poorly understood at catchment and regional scales. This situation is compounded by difficulties in estimating ET at large scales[13,14].

We investigated the correlates and potential causes of long-term changes in vegetation across Australia using remotely sensed NDVI. NDVI has been found to relate to primary productivity[15], foliage cover[16] and biomass[17] and has been widely employed to quantify vegetation trends[6,18,19] and processes[20]. We also examined long-term changes in ET and streamflow in unregulated, unimpaired Australian river basins in climates of varying aridity. ET was assessed by the water balance method, which relies directly on observations of precipitation and streamflow.

We first investigated the spatial distribution of long-term changes in NDVI across Australia. Large areas of Australia have undergone greening during 1982-2010 (Figure 3.1a); precipitation explained about 50% of these trends (calculated as the coefficient of determination from a linear regression of NDVI and precipitation trends). Strong greening was observed particularly in water-limited areas (marked by positive NDVI-precipitation correlation; Figure 3.1b), where 65% of significant ($P \leq 0.05$) NDVI trends were positive (excluding areas of significant precipitation increase).

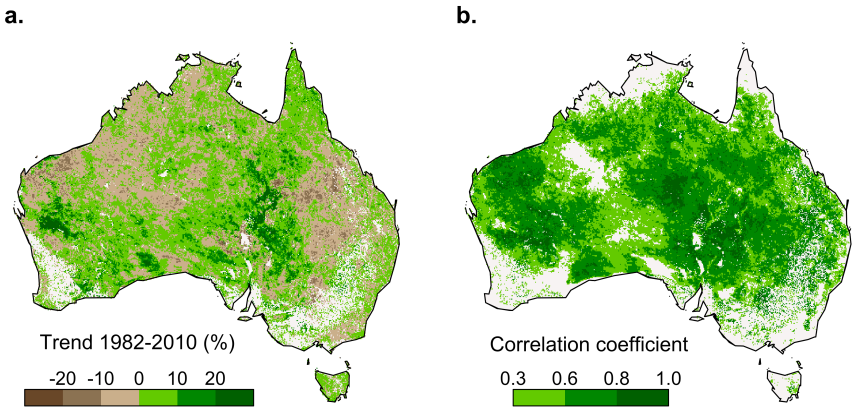

Figure 3.1 | Spatial patterns of vegetation greening. a, Pixel-by-pixel linear trends in annual NDVI. **b,** Areas of water-limited vegetation, determined as pixels with significant ($P \leq 0.10$) positive annual NDVI-precipitation correlations. Non-significant or negative correlations were masked out from panel b. Farmlands, irrigated areas and wetlands have been masked out from both panels.

We then quantified changes in the vegetation-precipitation relationship in areas of natural and semi-natural vegetation across Australia. By examining temporal changes in the upper 95th percentile bound for the spatial relationship between annual precipitation and NDVI (Figure 3.2, see Methods) we identified long-term changes in i) the maximum NDVI attainable for a given amount of precipitation, and ii) the extent of vegetation water limitation. We found that the maximum NDVI attainable for a given precipitation level has increased over time in water-limited areas (Figure 3.3a) (P = 0.059). This implies that a given amount of precipitation has sustained greater levels of plant production over time, which is consistent with CO_2 fertilisation. In addition, the breakpoint marking the precipitation limit where vegetation ceases to be water-limited decreased over time (P = 0.039) (Figure 3.3b). This trend indicates a relaxation of vegetation water limitation, consistent with the increased water use efficiency that is expected to accompany rising CO_2.

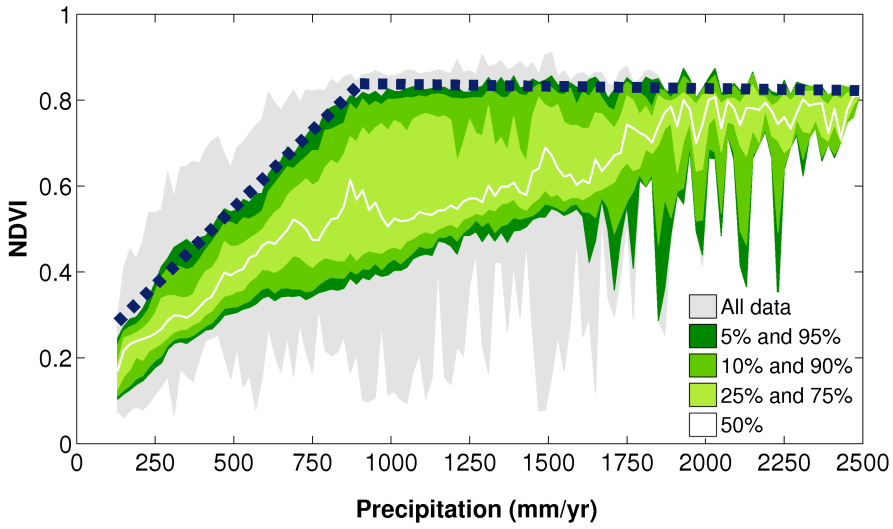

Figure 3.2 | Illustration of the breakpoint regression method. The first regression line represents the maximum NDVI attainable for a given amount of precipitation, under water-limited conditions. The breakpoint signifies the threshold where vegetation ceases to be water-limited. The data are the running mean 1983-1987. The coloured bands show the different percentiles.

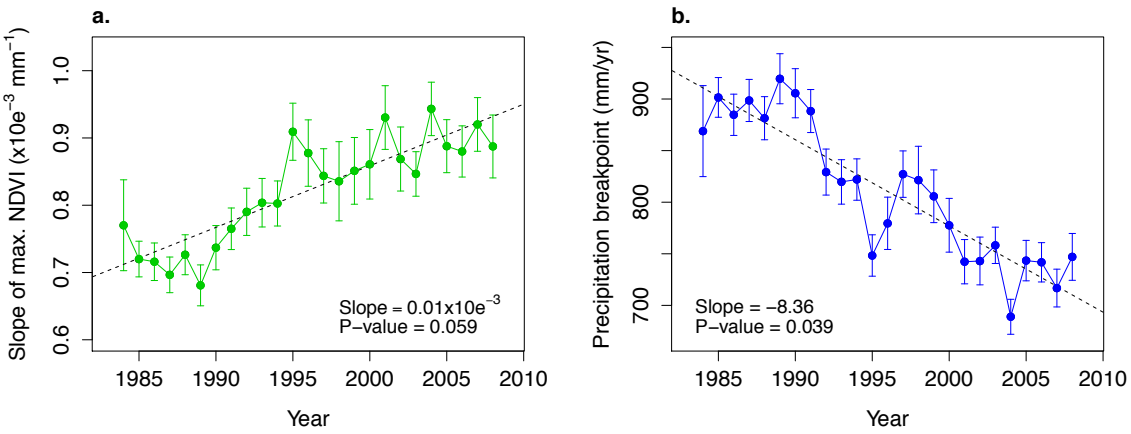

Figure 3.3 | Trends in water limitation threshold characteristics. a, the initial slope of maximum NDVI versus precipitation. **b,** the breakpoint (the precipitation level above which vegetation is no longer water-limited). Error bars are 95% confidence intervals. The black dashed lines show fitted linear trends.

To analyse long-term changes in vegetation and hydrology at the river basin scale, we calculated CO_2 sensitivity coefficients for NDVI and ET across basins grouped into four aridity categories (wet, sub-humid, semi-arid and arid), as theory would predict that a CO_2 effect should differ systematically between the categories. The sensitivity coefficients express the fractional change in ET and NDVI per unit fractional change in CO_2 concentration (after correcting ET and NDVI for precipitation and potential evapotranspiration (PET) variations, as detailed in Methods). A positive sensitivity coefficient of ET to CO_2 of comparable magnitude to that of NDVI would indicate that a CO_2 stimulation of vegetation cover dominates over a reduction in stomatal conductance with rising CO_2, due to an increased surface area of leaves for transpiration and rainfall interception. A negative sensitivity coefficient of ET to CO_2 (which can be of magnitude up to −1 at high CO_2 concentrations) indicates that the reduction in stomatal conductance with rising CO_2 dominates over the CO_2 stimulation of vegetation cover. We predict theoretical sensitivities around −0.6 in wet climates and −0.4 in arid climates due to the effect of a reduction in stomatal conductance with rising CO_2 on ET (see Methods).

In sub-humid and semi-arid basins, the data show a significant positive sensitivity coefficient of ET and NDVI to CO_2 (0.44 ± 0.14 and 0.18 ± 0.08 for ET, 0.10 ± 0.04 and 0.18 ± 0.11 for NDVI, respectively; Figure 4a). In sub-humid basins, the sensitivity coefficient of ET to CO_2 is similar to the sensitivity coefficient of ET to precipitation (0.64 ± 0.05, calculated from

uncorrected data; Supplementary Figure S3.2a and Supplementary Table S3.2). In semi-arid basins, the sensitivity coefficient of ET to CO_2 is about a fifth of its sensitivity coefficient to precipitation (0.86 ± 0.02). The CO_2 concentration increased by 48 ppm during the period 1982-2010. Based on the sensitivity coefficients the CO_2-induced ET increases during this time period amount to 43 mm in sub-humid and 14 mm in semi-arid basins, on average. These translate to a 6% and 2% increase, respectively, in mean annual ET (Figure 3.4b). The relative changes in mean annual ET due to CO_2 are similar to those due to precipitation (-6% and 1%, respectively; Supplementary Figure S3.2b and Supplementary Table S3.5) and significantly larger than those due to PET (-1% and 0%, respectively; Supplementary Figure S3.2b and Supplementary Table S3.6). Together with significant positive NDVI sensitivity coefficients to CO_2 (Figure 3.4a), this finding suggests an effect of rising CO_2 on both NDVI and ET, and that the fertilisation effect dominates over stomatal closure.

In wet basins, the sensitivity coefficient of ET to CO_2 was found to be negative (−0.42), consistent with theoretical predictions (see Methods), but this value was not statistically distinguishable from zero (Figure 3.4a). No greening was detected. In wet environments, vegetation cover is nearly complete and expected to be limited by light and nutrients rather than water. Thus limited greening should occur, and the principal effect of CO_2 on ET would be a decline due to reduced stomatal conductance.

We also found negative but non-significant CO_2 coefficients on ET (–0.33 ± 0.55) and NDVI (–0.11 ± 0.34) in arid basins (Figure 3.4a). This finding runs counter to the common expectation that CO_2 effects should be most pronounced in the most strongly water-limited environments. However, it is consistent with field experimental evidence showing no long-term change in biomass or water use efficiency under elevated CO_2 in a desert environment[8]. This lack of a detectable response has been attributed to a high frequency of years with very low precipitation, inhibiting any sustained increase in vegetation biomass[8]. Warm arid areas also tend to harbour a larger proportion of C_4 grasses, which we estimate to cover 43% of the area in arid basins on average (further discussed in Supplementary Section 3.4.1). C_4 plants show reduced stomatal conductance under elevated CO_2, consistent with the observed reduction in ET, but the stimulation of photosynthesis in C_4 plants is limited compared to C_3 plants that dominate in cooler and wetter regions[5,21] and only occurs under drought conditions[5]. The high proportion of C_4 vegetation may thus further contribute to the lack of a CO_2 fertilisation effect in arid basins.

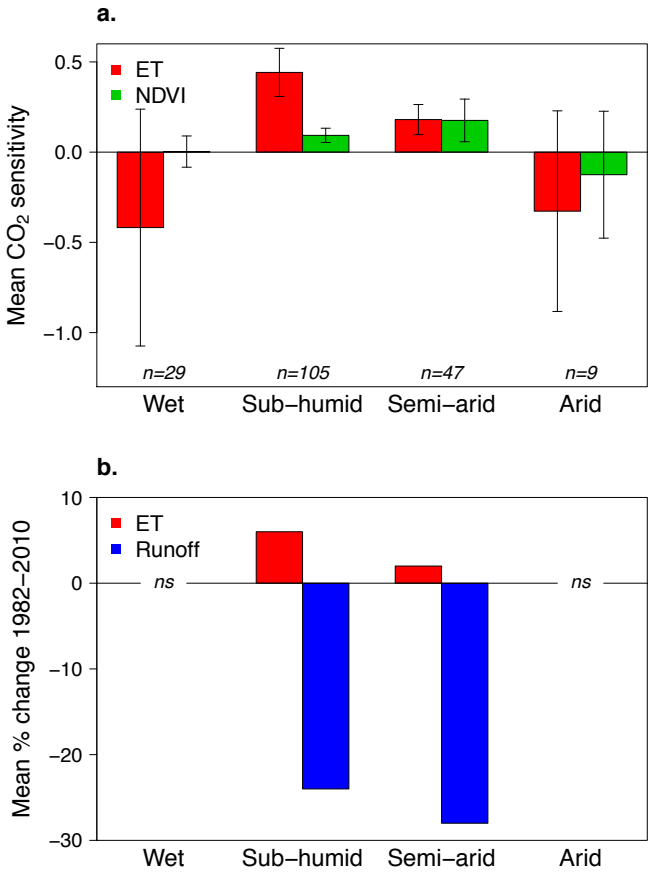

Figure 3.4 | CO_2 effects on ET, NDVI and runoff. a, Mean CO_2 sensitivity coefficients for each group of basins. The error bars are 95% confidence intervals. b, Relative change in ET and runoff due to CO_2 increase during 1982-2010. Non-significant (*ns*) changes in wet and arid basins were not shown.

We investigated the implications of the long-term ET changes for streamflow. Where ET exceeds streamflow, changes in ET are magnified in streamflow. This was apparent in sub-humid and semi-arid basins, where a small (2-6%) increase in ET led to substantial percentage reductions in streamflow. Calculated streamflow (factoring out precipitation effects) declined during 1982-2010 by 24% in sub-humid basins and by 28% in semi-arid basins (Figure 3.4b), which, considering the CO_2 sensitivities for these regions, is consistent with a response to CO_2. Given the actual observed declining trend in precipitation in the sub-humid basins (−3 mm/yr^2, $P < 0.001$; Supplementary Figure S3.4), increasing CO_2 is likely to have aggravated the pressure on water resources in these basins. In arid basins, a 4% decrease in ET would have led to a 132% increase in streamflow and in wet basins a 5% ET decrease would have led to a 5% increase in streamflow. However, neither effect is

statistically significant, so we cannot detect a CO_2 effect on streamflow in either the wettest or the driest regions on the basis of these measurements.

Our results provide evidence that rising atmospheric CO_2 has led to observable changes in terrestrial ecosystems and hydrology across a large part of Australia, with implications for carbon and water cycling at regional to global scales. Terrestrial ecosystems worldwide currently withdraw about a quarter of all anthropogenically emitted CO_2 when averaged over a decade[22]. A recent study[23] showed that semi-arid areas, particularly in Australia, play a major regional and even global role in modulating interannual variations in the rate of terrestrial carbon uptake. Increased carbon sequestration rates due to CO_2-induced greening in these semi-arid regions may lead to enhanced uptake of CO_2 from the atmosphere in the future. Furthermore, the response to rising CO_2 has the potential to either magnify or counteract future changes in precipitation. Precipitation is projected to decline in semi-arid and arid Australia during the 21st century[4] and increasing CO_2 is thus likely to put further pressure on water resources in already water-stressed regions. Our results may have similar implications for other water-limited subtropical regions in the Mediterranean, southern Africa and the Americas where precipitation is also projected to decline with increasing global temperature[4]. We conclude that increasing atmospheric CO_2 has likely left a detectable imprint on Australian ecosystems and hydrology, and such responses should be taken into account in future projections of water resources.

3.2. Methods

3.2.1. Core datasets

Normalised Difference Vegetation Index. We obtained a time series of third-generation NDVI (NDVI3g) from the Global Inventory Modelling and Mapping Studies (GIMMS)[24]. This dataset is gridded at 0.083° spatial resolution and was averaged from biweekly to annual time steps. The annual average for a given grid cell was determined only if >80% of biweekly values were available and was set to missing otherwise. Similarly, pixel trends were only calculated for pixels with annual time series >80% complete. Basin-specific NDVI values were obtained by averaging gridded data over basin areas.

Climatic variables. Monthly climatic fields (precipitation, minimum and maximum air temperature and shortwave radiation) were obtained from the ANUCLIM archive[25]. The Australia-wide data are gridded at 0.05° spatial resolution and were produced by the

ANUSPLIN software package[25,26] from meteorological station data using a thin-plate smoothing spline.

Annual time series of atmospheric CO_2 concentrations was obtained from National Oceanic & Atmospheric Administration Earth System Research Laboratory (NOAA ESRL; www.esrl.noaa.gov/gmd/ccgg/trends/). The data report the mean annual CO_2 concentration measured at Mauna Loa observatory in parts per million. We ignored latitudinal differences in CO_2 concentration as these are small compared to the signal of interest.

Potential evapotranspiration (PET) was calculated using the Priestley-Taylor method as in Gallego-Sala *et al.* (2010)[27], using inputs of shortwave radiation and the mean of minimum and maximum air temperature from the ANUCLIM archive. The Priestley-Taylor method has been shown to be appropriate for estimating large-scale PET[28,29] and has been adopted in other basin-scale studies[14,30,31].

Water-balance evapotranspiration. Water-balance evapotranspiration was calculated as the difference of observed annual precipitation and streamflow integrated over the river basin area. The water-balance method remains the most firmly observationally-based estimator of ET, but assumes negligible changes in soil water storage at annual to decadal time scales (see Supplementary Section 3.4.1 for further discussion). Streamflow time series were acquired from the Zhang *et al.* (2013)[32] streamflow collation for unregulated catchments across Australia. Gaps in the water-balance ET time series (accounting for <5% of monthly records) were filled using simulations from the Australian Water Availability Project[33], further detailed in Supplementary Section 3.4.1.

Study basins. The 190 study basins were chosen based on the completeness of streamflow records (> 95%) and the extent of irrigated and farmed land (< 5% of basin area). The basins were classified into wet, sub-humid, semi-arid and arid using the climatological aridity index A ($A = PET/P$, where PET = annual mean potential ET and P = annual mean precipitation) (see Supplementary Figure S3.1 for basin locations and aridity classification). River basins with mean annual aridity index <1 were classified as wet, 1-2 as sub-humid, 2-5 as semi-arid and >5 as arid (adapted from UNEP (1997)[34]). See Supplementary Section 3.4.1 for further details on basin selection and classification criteria.

3.2.2. Breakpoint regression

Five-year running mean NDVI values were binned according to their corresponding precipitation values. Following Donohue et al. (2013)[6], the 95th percentile value was determined for each 20 mm wide precipitation bin separately for each running mean. Breakpoint regression was applied to the 95th percentile values to calculate the first regression slope marking the maximum NDVI attainable for a given precipitation and the breakpoint where the vegetation-precipitation relationship plateaus and vegetation ceases to be water-limited. We then constructed time series of the slopes and breakpoints (Figure 3) and determined linear trends for both variables. As running means were used to construct the time series, degrees of freedom were adjusted when determining the significance of trends. Farmlands, irrigated areas and wetlands were excluded from this analysis using the Dynamic Land Cover Dataset of Australia[35] (see Supplementary Section 3.4.1).

3.2.3. CO_2 sensitivity coefficients

Estimation of observed CO2 coefficients. Dimensionless CO_2 sensitivity coefficients were calculated from NDVI and ET corrected for precipitation and PET (a function of temperature and shortwave radiation). Precipitation and PET present the main climatic constraints on plant growth[36] and are the two first-order controls on ET[37]. The effects of precipitation and PET were removed using linear regression: separately for each basin, annual ET (E) and NDVI were regressed against precipitation and PET and the annual corrected values were calculated as the sum of regression residual and the 1982-2010 mean of the variable. The corrected annual variables were then log-transformed and regressed against log-transformed annual CO_2 concentrations (C_a) to derive the CO_2 sensitivity coefficients $\sigma_{ET} = \partial \ln E / \partial \ln C_a$ and $\sigma_{NDVI} = \partial \ln NDVI / \partial \ln C_a$. The sensitivity coefficients represent the fractional change in the relevant variable per unit fractional change in CO_2, so that a change in ET (mm) due to CO_2 is well approximated by $\Delta E/E \approx \sigma_E . \Delta C_a / C_a$ for $\Delta E << E$ and $\Delta C_a << C_a$ (as in this study). ET and NDVI sensitivities to precipitation were calculated from uncorrected data using the same principles (further detailed in Supplementary Section 3.4.2).

Prediction of theoretical ET sensitivity to CO_2. Theoretical sensitivity of ET (E) to CO_2 concentration (C_a) for C_3 photosynthesis on a unit leaf area basis can be calculated by writing the CO_2 assimilation rate (A) and E in the form of diffusion equations:

$$A = g_s C_a (1 - \chi) \quad (1)$$

and

$$E = 1.6\, g_s\, D \quad (2)$$

where g_s is the stomatal conductance to CO_2, χ is the ratio of internal CO_2 concentration (C_i) to C_a, and D is the vapour pressure deficit. χ is a function of D and leaf temperature[38,39] and typically takes values from 0.4-0.5 in arid climates to 0.8-0.9 in wet climates. Substitution of g_s from equation (1) into equation (2) yields

$$E = 1.6\, (D/C_a)\, A/(1 - \chi) \quad (3)$$

Differentiating with respect to C_a, holding D and χ constant, gives:

$$\sigma_{ET} = (C_a/E)\, \partial E/\partial C_a = \sigma_A - 1 \quad (4)$$

where σ_A is the sensitivity of A to C_a:

$$\sigma_A = (C_a/A)\, \partial A/\partial C_a \quad (5)$$

Equation (4) implies that the sensitivity of E to C_a approaches –1 as the CO_2 fertilization effect on A saturates. However, so long as A is increasing with C_a, the sensitivity is smaller in magnitude than –1. The sensitivity of A to C_a can be calculated conservatively by invoking the co-ordination hypothesis (approximate equality of the carboxylation- and electron transport-limited rates of photosynthesis under field conditions: see e.g. Maire *et al.* (2012)[40]). With the further assumption that limitation by the maximum rate of electron transport (J_{max}) is not relevant in the field (because Rubisco limitation takes over at the highest light levels), we can express the assimilation rate as

$$A = \varphi_0\, I_{abs}\, (C_i - \Gamma^*/C_a)/(C_i + 2\Gamma^*/C_a) \quad (6)$$

where φ_0 is the intrinsic quantum efficiency of C_3 photosynthesis, I_{abs} is the absorbed photosynthetic photon flux density and Γ^* is the photorespiratory compensation point. Differentiating A with respect to C_a, holding χ constant, gives:

$$\sigma_A = \Gamma^*/C_a\, [1/(\chi - \Gamma^*/C_a) + 2/(\chi + 2\Gamma^*/C_a)] \quad (7)$$

Evaluating equations (7) and then (4) at 25˚C, C_a = 370 ppm for illustration gives σ_E = –0.61 for χ = 0.8 and –0.38 for χ = 0.5.

Acknowledgements

The authors are very grateful to Prof. Michael Hutchinson (Australian National University) and colleagues for providing the climate data used in this study. We would also like to thank Dr. Randall Donohue (CSIRO Land and Water) for useful discussions. A.U. has been supported by an international Macquarie University Research Excellence scholarship and a CSIRO Water for a Healthy Country Flagship top-up scholarship. T.F.K. acknowledges support from a Macquarie University Research Fellowship. This paper is a contribution to the AXA Chair Programme in Biosphere and Climate Impacts, and the Imperial College initiative on Grand Challenges in Ecosystems and the Environment.

3.3. References

1. Gedney, N. *et al.* Detection of a direct carbon dioxide effect in continental river runoff records. *Nature* **439,** 835–838 (2006).

2. Piao, S. *et al.* Changes in climate and land use have a larger direct impact than rising CO_2 on global river runoff trends. *Proc. Natl. Acad. Sci.* **104,** 15242–15247 (2007).

3. Alkama, R., Decharme, B., Douville, H. & Ribes, A. Trends in global and basin-scale runoff over the late twentieth century: methodological issues and sources of uncertainty. *J. Clim.* **24,** 3000–3014 (2011).

4. Collins, M. *et al.* in *Climate Change 2013: The Physical Science Basis. Contribution of Working Group I to the Fifth Assessment Report of the Intergovernmental Panel on Climate Change* (eds. Stocker, T. F. et al.) 1029–1136 (Cambridge University Press, 2013).

5. Leakey, A. D. B. *et al.* Elevated CO_2 effects on plant carbon, nitrogen, and water relations: six important lessons from FACE. *J. Exp. Bot.* **60,** 2859–2876 (2009).

6. Donohue, R. J., Roderick, M. L., McVicar, T. R. & Farquhar, G. D. Impact of CO_2 fertilization on maximum foliage cover across the globe's warm, arid environments. *Geophys. Res. Lett.* **40,** 1–5 (2013).

7. Hovenden, M. J., Newton, P. C. D. & Wills, K. E. Seasonal not annual rainfall determines grassland biomass response to carbon dioxide. *Nature* **511,** 583–586 (2014).

8. Newingham, B. A. *et al.* No cumulative effect of 10 years of elevated [CO_2] on perennial plant biomass components in the Mojave Desert. *Glob. Chang. Biol.* **19,** 2168–81 (2013).

9. Bradley, K. L. & Pregitzer, K. S. Ecosystem assembly and terrestrial carbon balance under elevated CO_2. *Trends Ecol. Evol.* **22,** 538–547 (2007).

10. Nowak, R. S., Ellsworth, D. S. & Smith, S. D. Functional responses of plants to elevated atmospheric CO_2 -do photosynthetic and productivity data from FACE experiments support early predictions? *New Phytol.* **162,** 253–280 (2004).

11. Morgan, J. A. *et al.* Water relations in grassland and desert ecosystems exposed to elevated atmospheric CO_2. *Oecologia* **140,** 11–25 (2004).

12. Raz-Yaseef, N., Rotenberg, E. & Yakir, D. Effects of spatial variations in soil evaporation caused by tree shading on water flux partitioning in a semi-arid pine forest. *Agric. For. Meteorol.* **150,** 454–462 (2010).

13. Douville, H., Ribes, A., Decharme, B., Alkama, R. & Sheffield, J. Anthropogenic influence on multidecadal changes in reconstructed global evapotranspiration. *Nat. Clim. Chang.* **3,** 59–62 (2013).

14. Ukkola, A. M. & Prentice, I. C. A worldwide analysis of trends in water-balance evapotranspiration. *Hydrol. Earth Syst. Sci.* **17,** 4177–4187 (2013).

15. Myneni, R. B. & Williams, D. L. On the Relationship between FAPAR and NDVI. *Remote Sens. Environ.* **49,** 200–211 (1994).

16. Lu, H., Raupach, M. R., McVicar, T. R. & Barrett, D. J. Decomposition of vegetation cover into woody and herbaceous components using AVHRR NDVI time series. *Remote Sens. Environ.* **86,** 1–18 (2003).

17. Hunt, E. R. Relationship between woody biomass and PAR conversion efficiency for estimating net primary production from NDVI. *Int. J. Remote Sens.* **15,** 1725–1729 (1994).

18. De Jong, R., de Bruin, S., de Wit, A., Schaepman, M. E. & Dent, D. L. Analysis of monotonic greening and browning trends from global NDVI time-series. *Remote Sens. Environ.* **115,** 692–702 (2011).

19. Beck, H. E. *et al.* Global evaluation of four AVHRR–NDVI data sets: Intercomparison and assessment against Landsat imagery. *Remote Sens. Environ.* **115,** 2547–2563 (2011).

20. Glenn, E. P., Huete, A. R., Nagler, P. L. & Nelson, S. G. Relationship between remotely-sensed vegetation indices, canopy attributes, and plant physiological processes: what vegetation indices can and cannot tell us about the landscape. *Sensors* **8,** 2136–2160 (2008).

21. Ehleringer, J. R., Cerling, T. E. & Helliker, B. R. C_4 photosynthesis, atmospheric CO_2, and climate. *Oecologia* **112,** 285–299 (1997).

22. Le Quéré, C. *et al.* Trends in the sources and sinks of carbon dioxide. *Nat. Geosci.* **2,** 831–836 (2009).

23. Poulter, B. *et al.* Contribution of semi-arid ecosystems to interannual variability of the global carbon cycle. *Nature* **509,** 600–603 (2014).

24. Pinzon, J. E. & Tucker, C. J. A non-stationary 1981-2012 AVHRR NDVI3g time series. *Remote Sens.* **6,** 6929–6960 (2014).

25. Xu, T. & Hutchinson, M. F. New developments and applications in the ANUCLIM spatial climatic and bioclimatic modelling package. *Environ. Model. Softw.* **40,** 267–279 (2013).

26. Kesteven, J. L. & Landsberg, J. J. *Developing a national forest productivity model. Technical report no.23, National Carbon Accounting System*. 1–102 (2004).

27. Gallego-Sala, A. *et al.* Bioclimatic envelope model of climate change impacts on blanket peatland distribution in Great Britain. *Clim. Res.* **45,** 151–162 (2010).

28. Raupach, M. R. Equilibrium evaporation and the convective boundary layer. *Boundary-Layer Meteorol.* **96,** 107–141 (2000).

29. Raupach, M. R. Combination theory and equilibrium evaporation. *Q. J. R. Meteorol. Soc.* **127,** 1149–1181 (2001).

30. Guerschman, J. P. *et al.* Scaling of potential evapotranspiration with MODIS data reproduces flux observations and catchment water balance observations across Australia. *J. Hydrol.* **369,** 107–119 (2009).

31. Zhang, L. *et al.* A rational function approach for estimating mean annual evapotranspiration. *Water Resour. Res.* **40,** W02502 (2004).

32. Zhang, Y. *et al. Collation of Australian modeller's streamflow dataset for 780 unregulated Australian catchments*. 1–115 (CSIRO Water for a Healthy Country Flagship Report, 2013).

33. Raupach, M. R. *et al. Australian Water Availability Project (AWAP): CSIRO Marine and Atmospheric Research Component: Final Report for Phase 3*. (2009).

34. UNEP (United Nations Environment Programme). *World Atlas of Desertification*. 182 (1997).

35. Lymburner, L. *et al. The National Dynamic Land Cover Dataset*. 1–95 (2011).

36. Nemani, R. R. *et al.* Climate-driven increases in global terrestrial net primary production from 1982 to 1999. *Science.* **300,** 1560–1563 (2003).

37. Zhang, Y. *et al.* Decadal Trends in Evaporation from Global Energy and Water Balances. *J. Hydrometeorol.* **13,** 379–391 (2012).

38. Medlyn, B. E. *et al.* Reconciling the optimal and empirical approaches to modelling stomatal conductance. *Glob. Chang. Biol.* **17,** 2134–2144 (2011).

39. Prentice, I. C., Dong, N., Gleason, S. M., Maire, V. & Wright, I. J. Balancing the costs of carbon gain and water transport: testing a new theoretical framework for plant functional ecology. *Ecol. Lett.* **17,** 82–91 (2014).

40. Maire, V. *et al.* The coordination of leaf photosynthesis links C and N fluxes in C_3 plant species. *PLoS One* **7,** e38345 (2012).

3.4. Supplementary Information

This Supplementary Information provides further details on the datasets and data processing (Section 3.4.1.) and the calculation of CO_2 sensitivity coefficients (Section 3.4.2.).

3.4.1. Description of datasets

3.4.1.1. Study basins

The 190 study basins were selected from the Zhang *et al.* (2013)[1] streamflow collection based on the completeness of streamflow records and land use within the basins. Basins meeting the following criteria were included in the analysis:

- Intensive land use or irrigated land constituted less than 5% of the basin area
- Daily streamflow time series during 1982-2010 was >95% complete
- Fewer than 12 consecutive months had missing daily values present

Nested basins were only included if the larger host basins were excluded from the analysis. Basin boundaries and the extent of irrigated and intensive land use were obtained from Zhang *et al.* (2013)[1]. Land use classification was based on the basin-scale land use dataset of the Bureau of Rural Sciences (BRS, 2010)[2], which was drawn from multiple sources including fine-scale satellite imagery and various land registers and has a variable resolution up to 12.5 m. The original streamflow dataset only includes unregulated basins where irrigated or intensive land use accounts for ≤10% of land area, which we have further restricted to ≤5%.

The selected basins were classified into wet, sub-humid, semi-arid and arid by adapting the classification of the United Nations Environment Program (UNEP)[3] (Supplementary Figure 1). The climatic aridity index *A* was used to achieve this, defined as PET/P (where PET is annual mean potential evapotranspiration and P is annual mean precipitation). The threshold between wet and sub-humid classes was set to $A = 1$ where P and PET converge, the UNEP classification was followed otherwise. There are 29 basins in the wet category, 105 in sub-humid, 47 in semi-arid and 9 in the arid category.

Wet and sub-humid basins are dominated by closed and open woody vegetation, covering on average 92% and 88% of basin area, respectively. Semi-arid basins have a combination of herbaceous (25%) and mainly scarce or scattered woody vegetation (55%). Arid basins are covered by herbaceous vegetation (43%) and sparse or scattered shrubland (53%).

Using an empirical method[4,5], we estimate that nearly all herbaceous vegetation in the semi-arid and arid basins consists of C_4 species that dominate in warm, arid environments with high light availability[4,6,7]. Basin vegetation cover information was derived from the Dynamic Land Cover Dataset of Australia, further described in section 3.4.1.3.

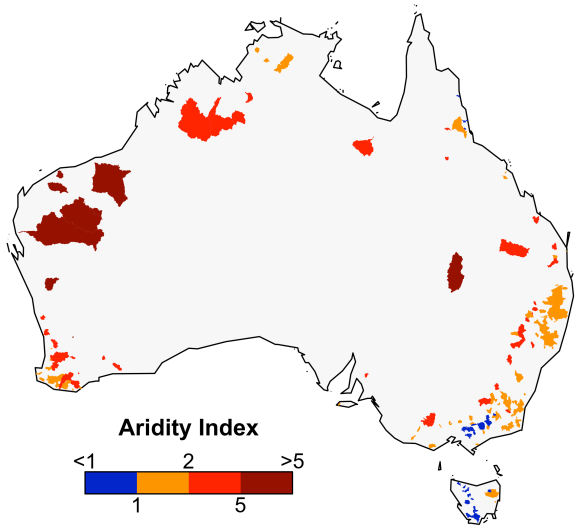

Supplementary Figure S3.1 | Study basins and classification according to aridity index.

3.4.1.2. Water-balance evapotranspiration

Annual water-balance evapotranspiration was calculated as the difference of observed annual precipitation and runoff integrated over the basin area. Basin precipitation estimates were acquired by averaging gridded ANUCLIM annual precipitation over the basin areas.

The water-balance method remains the most firmly observationally based estimator of ET but assumes negligible changes in soil water storage. We tested for lags in annual runoff relative to annual precipitation. The Pearson linear correlation coefficient for non-lagged runoff and precipitation was 0.81 across all basins. When runoff was lagged by one year relative to precipitation, the correlation decreases to 0.15. As the correlation analysis points to no significant lags and other studies have found soil moisture is mainly driven by precipitation[8] (explicitly included in the water-balance method), we assumed water storage changes to be negligible at annual to decadal time scales.

Gaps in the water balance ET time series were filled using simulations from the Australian Water Availability Project (AWAP)[9]. We used AWAP streamflow estimates to calculate simulated "water-balance" ET (AWAP ET), estimated at monthly time scales as the difference between observed ANUCLIM precipitation and simulated streamflow. We evaluated the agreement between observed and AWAP ET in four basins with contrasting rainfall regimes (wet, dry, summer-dominant and winter-dominant) during the whole study period and separately for the driest and wettest years. The pattern of interannual variability was found to agree well in each case but the magnitude of simulated ET was found to be systematically higher than observations (evaluated from normalised mean squared errors[10] which varied between 0.07 – 1.12 when comparing annual totals and 0.07 – 0.42 for annual deviations from the mean). To remove the bias prior to gap filling, simulated ET was re-scaled so that the mean ET in each basin equalled that of observations. The re-scaled monthly ET data were then used to fill missing months in observed ET time series.

3.4.1.3. Dynamic Land Cover Dataset

The Dynamic Land Cover Dataset of Australia[11] offers gridded land cover observations across Australia at 250m resolution and was used to mask out areas of non-natural vegetation. The data were re-gridded to the GIMMS NDVI3g resolution using nearest neighbour resampling and farm- and wetlands, irrigated and non-vegetated bare or built areas were identified using the dataset, corresponding to classes 1-11 in the original dataset. Grid cells belonging to the above land use classes were then removed from the breakpoint analysis and Figure 3.3.

3.4.1.4. Trend analysis

All trends in the study were calculated using ordinary least-squares linear regression. The linear trends were compared with trends calculated using the non-parametric Mann-Kendall Tau-b test with Sen's slope estimates. The two estimates were found to be in good agreement and the results were not found to depend on the trend test chosen. Where 5-year running means were used, the degrees of freedom were adjusted before determining the significance of trends by dividing the number of observations by 5.

3.4.2. CO_2 sensitivity coefficients

We calculated CO_2 sensitivity coefficients separately for each basin and averaged them for each basin class to derive mean sensitivity coefficients (Supplementary Table 1). Student's t-tests were used to determine whether the mean coefficients were distinguishable from zero and to derive 95% confidence intervals. Using the mean sensitivity coefficients we could calculate the absolute change in ET due to CO_2 increase (ΔE_{CO2}) from

$$\Delta E_{CO2}/E \approx \sigma_{ET} \Delta C_a/C_a \quad (8)$$

where E and C_a are the reference values defined as the mean of the variables during 1982-1986; and similarly for NDVI (Supplementary Table 4). ΔC_a is the change in CO_2 concentration calculated as the difference between reference C_a and the 2010 concentration. Runoff changes were calculated as $\Delta R_{CO2} = [P - (E + \Delta E_{CO2})] - (P - E)$, where P is the reference precipitation.

We also calculated precipitation and PET sensitivity coefficients for comparison using the same principle: $\sigma_E(P) = \partial \ln E/\partial \ln P$ and $\sigma_{NDVI}(P) = \partial \ln(NDVI)/\partial \ln P$; and similarly for PET. Precipitation sensitivity coefficients are detailed in Supplementary Table 2 and were calculated from uncorrected annual ET and NDVI data. PET sensitivity coefficients are shown in Supplementary Table 3 and were calculated from annual data corrected for precipitation (the effect of precipitation was removed using regression residuals as in the calculation of CO_2 sensitivity coefficients, detailed in the main Methods). By substituting C_a with P (PET), equation (8) could be used to estimate the absolute change in ET due to precipitation (PET) change (ΔE_P) (and similarly for NDVI). Absolute changes in runoff were calculated as $\Delta R_P = [(P + \Delta P) - (E + \Delta E_P)] - (P - E)$, where ΔP is the precipitation change during 1982-2010 (Supplementary Table 5); and similarly for PET (Supplementary Table 6). Precipitation and PET do not change smoothly like CO_2 and interannual variations particularly in precipitation can be large. ΔP (ΔPET) was therefore estimated by linear regression of annual precipitation (PET) against time, then calculating the difference between reference P (PET) and the fitted value for 2010.

Supplementary Table S3.1 | Mean CO_2 sensitivity coefficients and 95% confidence intervals.

Basin class	ET	NDVI
Wet	−0.42 ± 0.65	0.03 ± 0.08
Sub-humid	0.44 ± 0.14	0.10 ± 0.04
Semi-arid	0.18 ± 0.08	0.18 ± 0.11
Arid	−0.33 ± 0.55	−0.11 ± 0.34

Supplementary Table S3.2 | Mean precipitation sensitivity coefficients and 95% confidence intervals.

Basin class	ET	NDVI
Wet	0.54 ± 0.09	−0.02 ± 0.01
Sub-humid	0.64 ± 0.05	0.05 ± 0.02
Semi-arid	0.86 ± 0.03	0.12 ± 0.02
Arid	0.93 ± 0.04	0.15 ± 0.03

Supplementary Table S3.3 | Mean PET sensitivity coefficients and 95% confidence intervals.

Basin class	ET	NDVI
Wet	0.20 ± 0.54	-0.06 ± 0.05
Sub-humid	-0.42 ± 0.13	-0.07 ± 0.04
Semi-arid	-0.43 ± 0.14	-0.12 ± 0.07
Arid	-0.06 ± 0.12	-0.12 ± 0.14

Supplementary Table S3.4 | Mean absolute and relative changes in ET, runoff and NDVI due to CO_2 increase during 1982-2010.

Basin class	ET (mm)	ET (%)	Runoff (mm)	Runoff (%)	NDVI (unitless)	NDVI (%)
Wet	−41	−5.5	41	5.2	0.003	0.4
Sub-humid	43	5.8	−43	−24.2	0.010	1.3
Semi-arid	14	2.4	−14	−28.5	0.013	2.4
Arid	−12	−4.3	12	132.4	−0.004	−1.4

Supplementary Table S3.5 | Mean absolute and relative changes in ET, runoff and NDVI due to precipitation change during 1982-2010.

Basin class	ET (mm)	ET (%)	Runoff (mm)	Runoff (%)	NDVI (unitless)	NDVI (%)
Wet	−27	−3.7	−76	−9.7	0.001	0.1
Sub-humid	−40	−5.4	−37	−21.1	−0.003	−0.4
Semi-arid	7	1.1	2	3.5	0.001	0.2
Arid	39	14.0	4	47.3	0.006	2.3

Supplementary Table S3.6 | Mean absolute and relative changes in ET, runoff and NDVI due to PET change during 1982-2010.

Basin class	ET (mm)	ET (%)	Runoff (mm)	Runoff (%)	NDVI (unitless)	NDVI (%)
Wet	5	0.7	-5	-0.7	-0.002	-0.2
Sub-humid	-7	-0.9	7	7.0	-0.001	-0.2
Semi-arid	-1	-0.1	1	1.6	0.000	0.0
Arid	0	0.0	0	-0.6	0.000	0.0

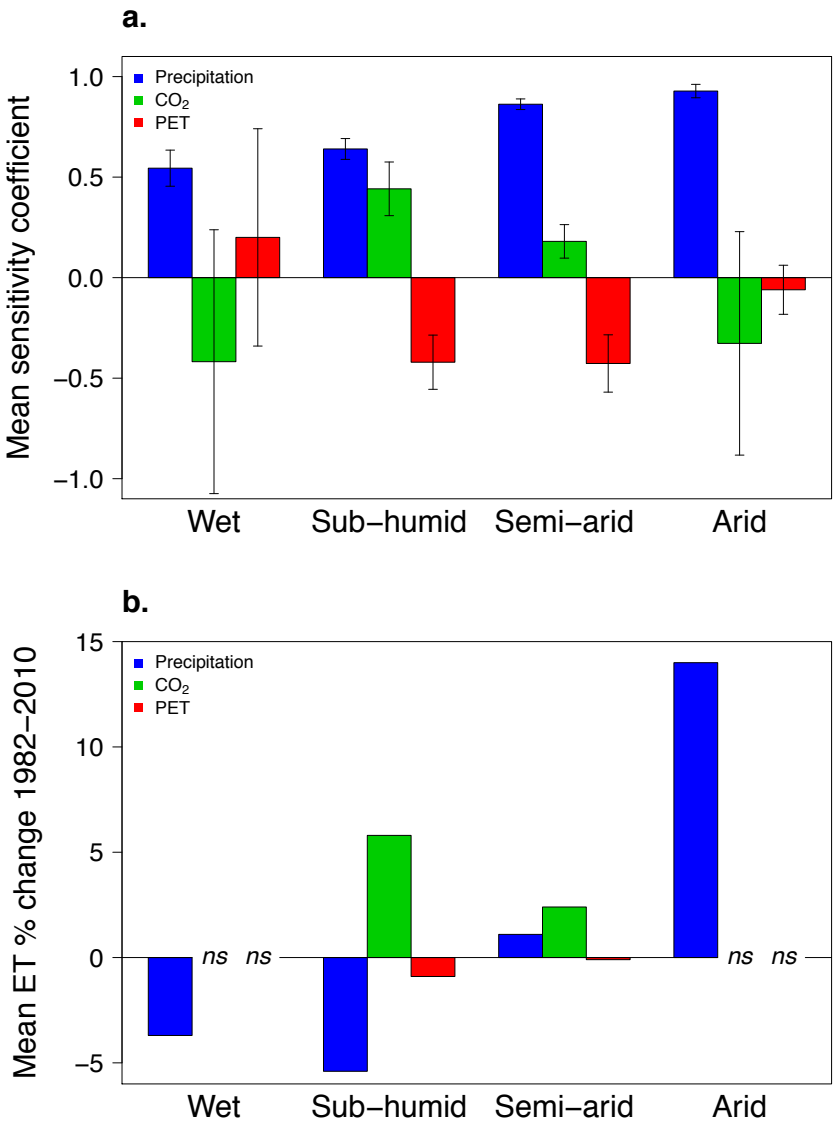

Supplementary Figure S3.2 | Contributions from precipitation, CO_2 and PET to ET change during 1982-2010. a, Mean ET sensitivity coefficients to precipitation, CO_2 and PET for each group of basins. The error bars are 95% confidence intervals. **b,** Relative change in ET due precipitation, CO_2 and PET during 1982-2010. Non-significant (*ns*) changes were not shown.

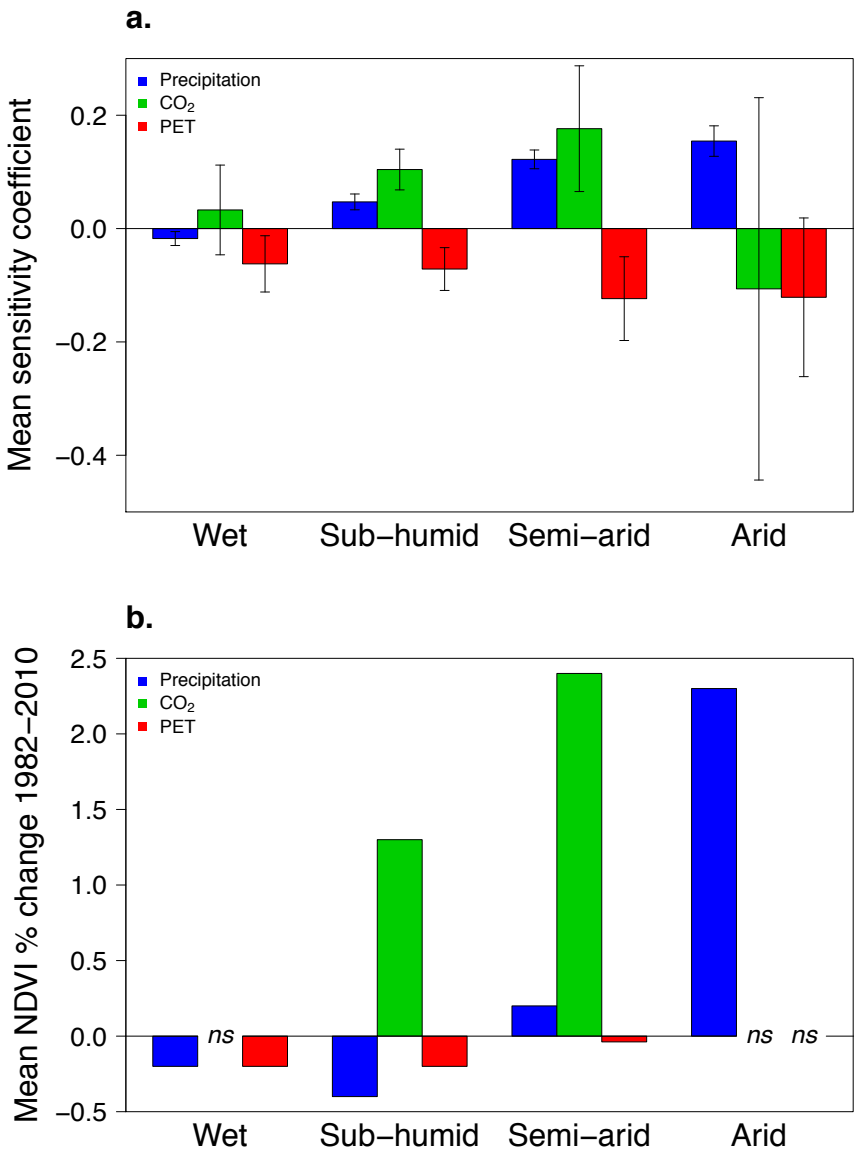

Supplementary Figure S3.3 | Contributions from precipitation, CO_2 and PET to NDVI change during 1982-2010. a, Mean NDVI sensitivity coefficients to precipitation, CO_2 and PET for each group of basins. The error bars are 95% confidence intervals. **b,** Relative change in NDVI due precipitation, CO_2 and PET during 1982-2010. Non-significant (*ns*) changes were not shown.

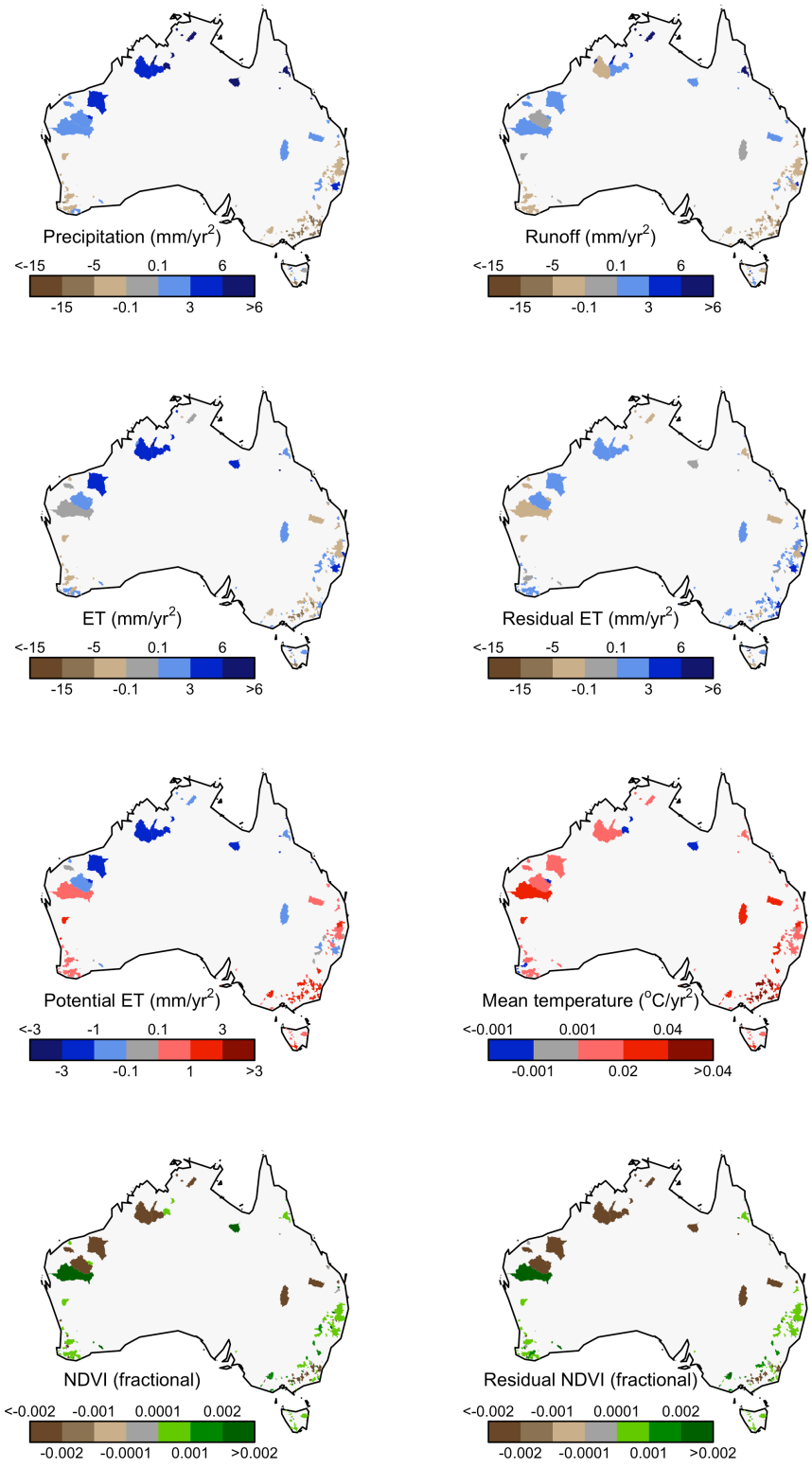

Supplementary Figure S3.4 | Basin-scale trends in hydrological, climatological and vegetation variables.

3.4.3. References

1. Zhang, Y. *et al. Collation of Australian modeller's streamflow dataset for 780 unregulated Australian catchments*. 1–115 (CSIRO Water for a Healthy Country Flagship Report, 2013).

2. BRS. *Catchment scale land use mapping for Australia update March 2010 (CLUM update 3/10) dataset*. (2010).

3. UNEP (United Nations Environment Programme). *World Atlas of Desertification*. 182 (1997).

4. Hattersley, P. W. The distribution of C_3 and C_4 grasses in Australia in relation to climate. *Oecologia* **57,** 113–128 (1983).

5. Donohue, R. J. *et al.* Evaluation of the remote-sensing-based DIFFUSE model for estimating photosynthesis of vegetation. *Remote Sens. Environ.* **155,** 349–365 (2014).

6. Still, C. J., Berry, J. a., Collatz, G. J. & DeFries, R. S. Global distribution of C_3 and C_4 vegetation: Carbon cycle implications. *Global Biogeochem. Cycles* **17,** 1006 (2003).

7. Lopes dos Santos, R. a. *et al.* Abrupt vegetation change after the Late Quaternary megafaunal extinction in southeastern Australia. *Nat. Geosci.* **6,** 627–631 (2013).

8. Sheffield, J. & Wood, E. F. Global Trends and Variability in Soil Moisture and Drought Characteristics, 1950–2000, from Observation-Driven Simulations of the Terrestrial Hydrologic Cycle. *J. Clim.* **21,** 432–458 (2008).

9. Raupach, M. R. *et al. Australian Water Availability Project (AWAP): CSIRO Marine and Atmospheric Research Component: Final Report for Phase 3*. (2009).

10. Kelley, D. I. *et al.* A comprehensive benchmarking system for evaluating global vegetation models. *Biogeosciences* **10,** 3313–3340 (2013).

11. Lymburner, L. *et al. The National Dynamic Land Cover Dataset*. 1–95 (2011).

Chapter 4

Vegetation buffers the water-resource impacts of environmental change

A.M. Ukkola[1], T.F. Keenan[1], D.I. Kelley[1] and I.C. Prentice[1,2]

[1]Department of Biological Sciences, Macquarie University,
North Ryde, NSW 2109, Australia
[2]AXA Chair of Biosphere and Climate Impacts, Department of
Life Sciences and Grantham Institute for Climate Change,
Imperial College, Silwood Park, Ascot SL5 7PY, United Kingdom

This chapter is presented as a journal article in preparation for *Proceedings of the National Academy of Sciences*:

Ukkola A.M., Keenan T.F., Kelley D.I. and Prentice I.C., Vegetation buffers the water-resource impacts of environmental change, *Proceedings of the National Academy of Sciences*, in prep.

4.1. Main

Future environmental change is expected to modify the global hydrological cycle, with consequences for the regional distribution of freshwater supplies. Regional precipitation projections, however, differ largely between models, making future water resource projections highly uncertain. Using two representative concentration pathways (RCP) (1) and nine climate models, we estimate 21st century water resources across Australia, employing both a process-based dynamic vegetation model (2) and a simple hydrological framework commonly used in water resource studies (3). We show surprisingly robust, pathway-independent regional patterns of change in water resources despite large uncertainties in precipitation projections. Increasing plant water use efficiency (due to the changing atmospheric CO_2) and reduced green vegetation cover (due to the changing climate) relieves pressure on water resources for the highly populated, humid coastal regions of Australia. In semi-arid regions, by contrast, runoff declines are amplified by CO_2-induced greening, which leads to increased vegetation water use. Overall, vegetation acts as a buffer in regions with robust declines in precipitation, but negatively affects water resources where precipitation increases or remains uncertain. These findings highlight the importance of including vegetation dynamics in future water resource projections, and suggest that future water resource declines may be smaller than previously expected.

General circulation models (GCMs) from the newest generation of the Coupled Model Intercomparison Project (4) (CMIP5) suggest consistent 21st century temperature increases and, on average, increasing precipitation globally (5). But changes in regional precipitation patterns remain stubbornly uncertain, despite advances in modelling capability (5, 6). High uncertainty has hindered robust projections of water resources, especially in regions with naturally hypervariable climates. Australia is a continent with exceptionally high interannual and inter-decadal climate variability, with runoff variability about twice that typical in the Northern Hemisphere (7). Due to the general aridity of the continent its water resources are vulnerable to future precipitation changes, and it has been identified as a likely hotspot for future water scarcity (8).

Water resources are also dependent on vegetation state and function, both of which are affected by environmental change. Elevated CO_2 is known to increase the efficiency with which plants use water, and precipitation changes can also influence vegetation cover and water use. Studies of historical and future runoff (9, 10) often point to increased runoff due to CO_2-induced increases in water use efficiency (in particular, stomatal closure allowing water to be conserved), which can be observed both at the leaf (11) and ecosystem (12) scales.

However, a recent analysis (13) showed these water savings do not necessarily lead to increased runoff, due to changes in vegetation state and function. This is particularly true in drier climates, where the net effect of elevated CO_2 is a reduction in runoff, due to the effect of CO_2-induced vegetation greening (increase in foliage cover) (14). In intermediate climates, the magnitude of CO_2 effects was found to be comparable to precipitation-driven changes in runoff. These multi-factor interactions suggest that climate induced changes in vegetation state and function may play a large, yet to date poorly constrained role in mediating future water resources.

Here we examine potential future changes in water resources in Australia and evaluate the role of long-term responses of vegetation state and function to environmental change. To do so, we use two contrasting approaches, in combination with climate projections from nine general circulation models. The first approach is the Fu-Zhang formulation of the simple Budyko hydrological framework (3), a well-established empirical model widely employed in studies of water resources (3, 15). It accounts for the joint effects of precipitation and potential evapotranspiration (PET) on actual evapotranspiration (AET) and runoff. The second is the process-oriented Land surface Processes and eXchanges Dynamic Global Vegetation Model (LPX DGVM), a complex coupled water-carbon-vegetation model, which successfully reproduces observed vegetation CO_2 effects on hydrology in Australia (16) (see Methods for detailed model descriptions and evaluation). By contrasting results from the two models, we separate the effects of vegetation processes from direct climate effects on future runoff projections. We show that, despite widespread disagreement regarding precipitation projections between GCMs and scenarios, vegetation acts to buffer the impacts of changes in precipitation, serving to both protect Australia's future water resources, and reduce uncertainty in future water resource projections.

In agreement with previous studies (reviewed in ref. (5)), the nine GCMs included in this study show large uncertainties in projected future precipitation patterns in large parts of Australia, including key economic and agricultural areas in eastern Australia, where the majority of the Australian population resides. The climate models project a robust decrease in precipitation in south-western Australia, irrespective of the RCP (Figure 4.1) and are in modest agreement on decreased precipitation along south-east and north-east coastal regions and increased precipitation in parts of arid central Australia.

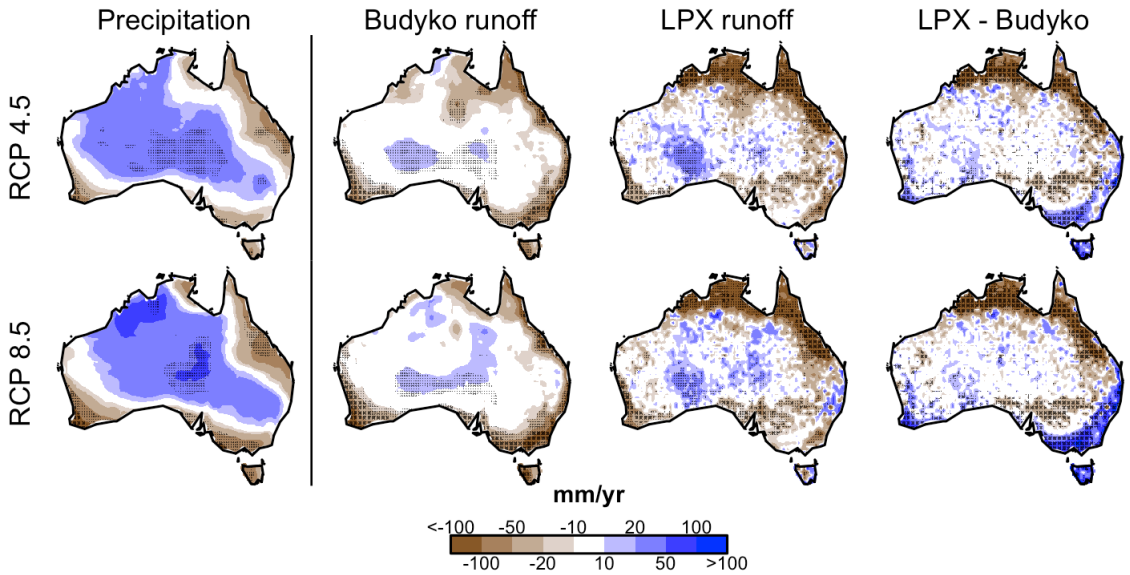

Figure 4.1 | Projected future anomalies in precipitation and Budyko- and LPX-simulated runoff under two projected climate scenarios. LPX-Budyko shows the difference between Budyko- and LPX-simulated future ensemble runoff anomaly. Here stippling indicates where Budyko and LPX simulations differ significantly, as determined from a two-tailed Student's t-test (large stippling shows where t-test *p*-value ≤ 0.5 and small stippling where 0.5 < *p*-value ≤ 1.0); elsewhere stippling indicates the robustness of signal as measured by the standard deviation (sd) of the model results divided by the ensemble mean (large stippling shows where sd ≤ 0.5 and small stippling where 0.5 < sd ≤ 1.0). The anomalies were calculated as the difference between the 2070-2099 future ensemble mean and the 1960-1990 historical mean of the variable.

Despite uncertainties in future precipitation, we project robust regional reductions in runoff along much of coastal and inland eastern Australia (Figure 4.1). Some of these reductions are precipitation-driven, particularly in south-western Australia, and exacerbated by increasing PET (Supplementary Figure S4.1). However, a comparison of Budyko and LPX projections shows the reductions in runoff in areas of declining precipitation are much larger when excluding vegetation dynamics. A CO_2-induced increase in water use efficiency, and modest decreases in green vegetation cover, alleviate the runoff declines predicted (by the Budyko approach) from direct climate effects. In contrast, in northern Australia where the actual precipitation changes are highly uncertain, strong CO_2-induced greening leads to increased actual evapotranspiration (ET) (Figure 4.2) and reduced runoff. These strong reductions are not, or hardly, present under constant CO_2 (particularly under RCP8.5; Supplementary Figures 4.2 and 4.3) with the LPX model or in the Budyko model projections. The CO_2 effect is accompanied by increased dry season fuel moisture and a decrease in

wind speed, which reduces fire risk and enables continued expansion of tree cover (woody thickening) in savanna ecosystems (17), further increasing vegetation water use in the north.

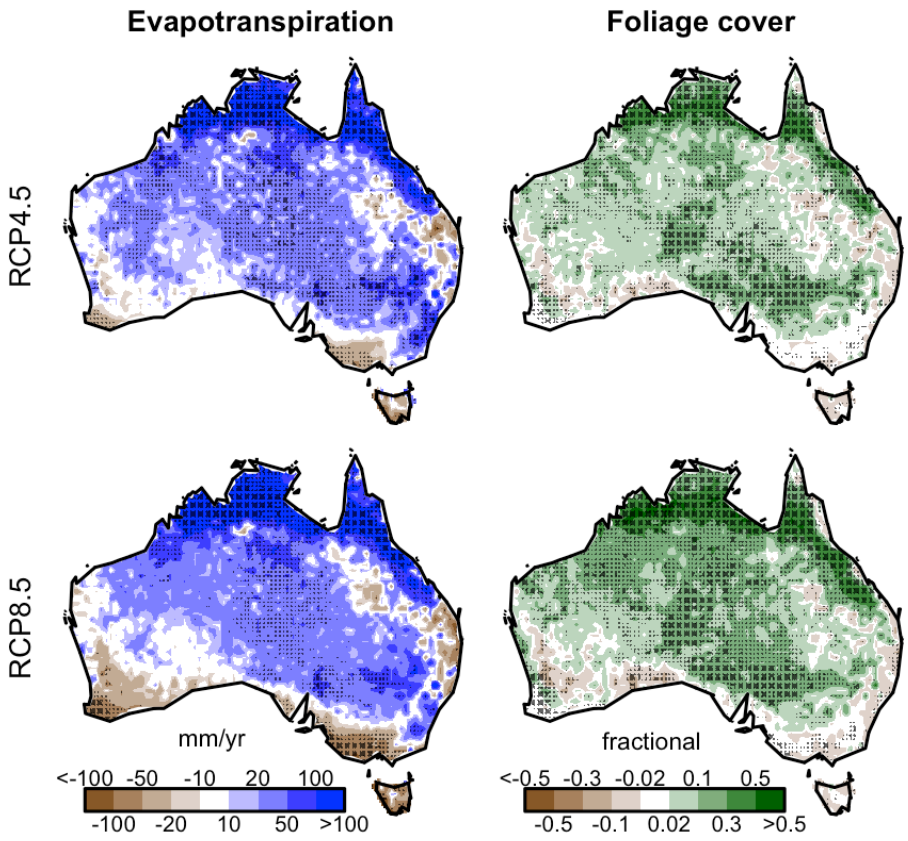

Figure 4.2 | Future anomalies in LPX-simulated ET and foliage cover under RCP4.5 and RCP8.5. The anomalies were calculated as the difference between the 2070-2099 future ensemble mean and the 1960-1990 historical mean of the variable. Stippling indicates the robustness of signal as measured by the standard deviation (sd) of the model results divided by the ensemble mean (large stippling shows where sd ≤ 0.5 and small stippling where 0.5 < sd ≤ 1.0).

The largest deviations in hydrology and vegetation cover from historical levels are projected to take place relatively soon, during the first half of the 21st century (Figure 4.3). Declines in precipitation and runoff are projected from the LPX ensemble mean in wet and sub-humid regions. These declines are accompanied by increasing AET and foliage cover (consistent with a CO_2 fertilisation effect) in sub-humid climates, even though these regions are also projected to become progressively more arid (as measured by the aridity index; Supplementary Figure S4.4). Although large inter-model variations persist, the projected

changes are largely independent of the RCP, despite strong divergence in projected temperatures and PET under the two RCPs (Supplementary Figure S4.4). The global greenhouse emissions trajectory therefore does not appear to be the most important uncertainty for the prediction of future water resources.

Larger uncertainties are associated with the use of different climate models, and natural variability as represented by the models. Interannual variability in runoff and precipitation is expected, and projected, to remain large (Figure 4.3). The El Niño Southern Oscillation (ENSO) is a major driver of climate in Australia, and brings extreme conditions including droughts and floods particularly to the eastern parts of the continent (18). Although future changes to the mean ENSO state remain uncertain (19), extreme El Niño events are projected to become more frequent (20). The Indian Ocean Dipole (IOD) is also prominent in its effects on precipitation in central, southern and northern Australia, and its extreme phases too are projected to increase in frequency in a warming world (21). The continuing high interannual variability in Australia, together with more frequent extreme states of the two principal variability modes, will inevitably pose challenges for water management.

Our results demonstrate the importance of including vegetation dynamics in projections of water resources and the need to consider coupled water, carbon and vegetation effects on AET and runoff. Despite large uncertainties in future precipitation projections, our analysis suggests significant and coherent changes in runoff across large parts of the continent. In northern Australia as well as parts of the Murray-Darling basin, the largest river system on the continent and a key agricultural area accounting for 40% of the value of Australia's agricultural production (22), CO_2-induced vegetation responses are projected to reduce water resources but are accompanied by enhanced natural vegetation productivity. Despite vegetation water savings due to reduced stomatal conductance under elevated CO_2, parts of highly populated coastal regions, along with agricultural areas in southwestern Australia, are projected to suffer reductions in water resources. Independent of the assumed greenhouse emissions scenario, large reductions in Australian water resources are projected to occur within a few decades. The reductions are not as extreme, however, as they would be without the influence of dynamic vegetation.

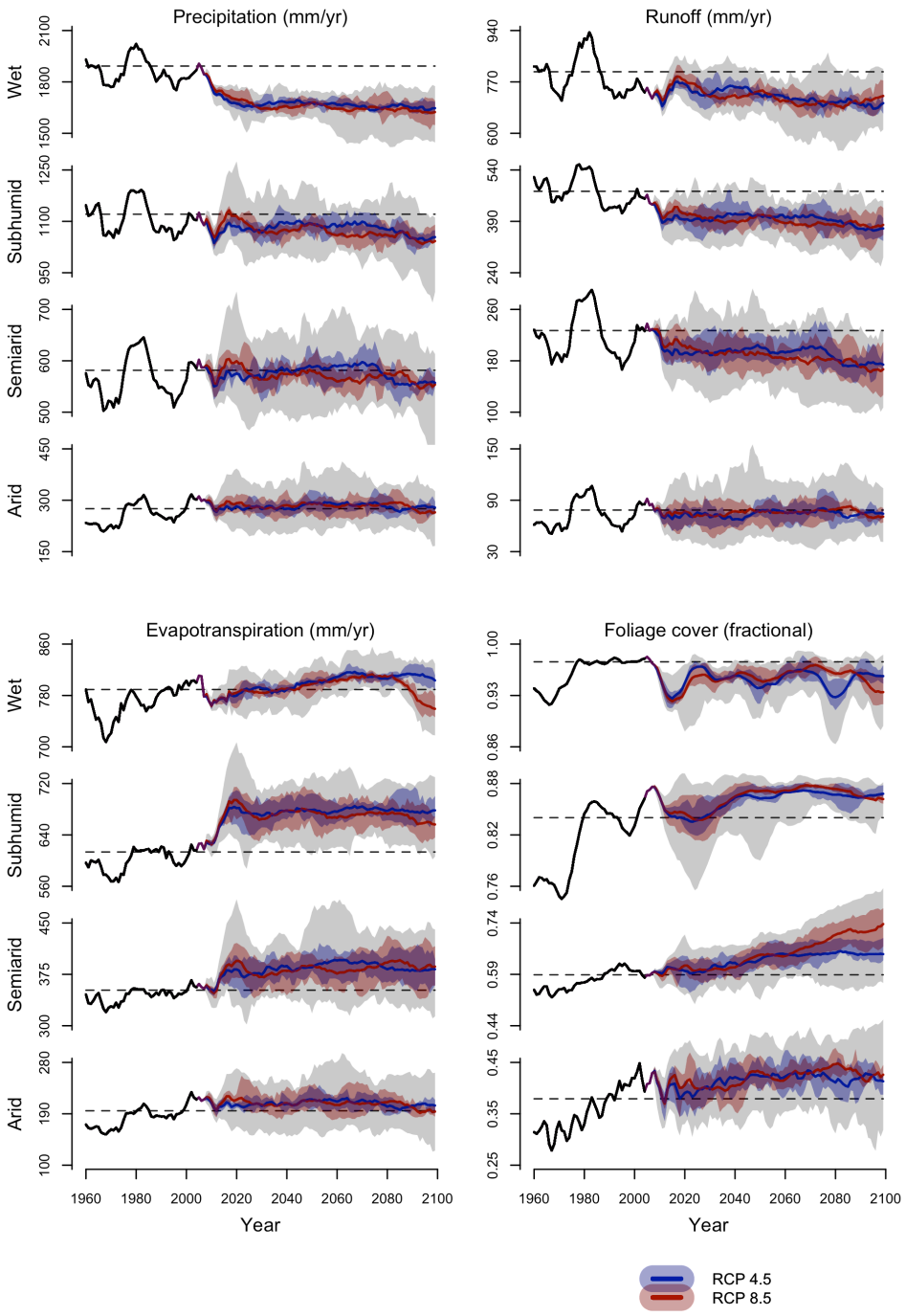

Figure 4.3 | Historical and future time series of precipitation and LPX-simulated runoff, ET and foliage cover in different aridity regimes. The solid black line shows the historical period (1960-2005) and the dotted line the historical mean of the variable during 1960-1990. The coloured lines show the future ensemble means and the coloured shading indicates model interquartile ranges for each RCP. The grey shading shows the combined full model range of both RCPs. Aridity categories were constructed as described in Supplementary Figure S4.5. The time series were subsequently smoothed using 10-year running means.

4.2. Methods

LPX Dynamic Global Vegetation Model. The Land surface Processes and eXchanges Dynamic Global Vegetation Model (LPX DGVM) is a process-based model that simulates interactions between terrestrial vegetation dynamics, and land-atmosphere carbon and water cycles. The model explicitly simulates dynamic ecosystem structure and function, including foliage cover, primary production and carbon allocation, evapotranspiration, competition and disturbances, but in common with most other vegetation models does not include nutrient constraints on CO_2 assimilation. LPX is based on a coupled photosynthesis-water balance scheme that explicitly couples CO_2 assimilation with transpiration. The model has been extensively evaluated for hydrology (16, 23–25) and ecosystem dynamics (25–27). We use the latest model version (LPX-Mv1) with improved fire-vegetation dynamics, benchmarked specifically for Australia (2). Key model processes are further detailed in Supplementary Section 4.4.1. LPX simulates AET directly but for consistency with historical observations, we have defined AET as the difference between precipitation and runoff in this study.

We evaluated the model's ability to capture observed water-balance AET and vegetation sensitivities to precipitation and CO_2 across 190 Australian river basins (13) grouped by aridity (see Supplementary section 4.4.1). This was achieved using sensitivity coefficients ($\sigma_{Ca} = \partial \ln E / \partial \ln C_a$ and $\sigma_P = \partial \ln E / \partial \ln P$, where C_a is ambient CO_2 concentration, E actual ET and P precipitation), which represent the fractional change in E per unit fractional change in C_a or P (and similarly for foliage cover). σ_{Ca} has a clear theoretical expectation in terms of underlying processes (28) whereby a negative coefficient implies the CO_2 response is dominated by stomatal closure reducing ET and a positive coefficient indicates CO_2 fertilisation dominates over stomatal closure increasing ET (13). The effects of precipitation (and PET in the case of AET) were removed from observed and simulated AET and foliage cover prior to calculating CO_2 sensitivities, as detailed in Supplementary Section 4.4.1. Despite spatial variability in the CO_2 response in both the model and observations, LPX captures mean AET sensitivity to CO_2 and precipitation successfully across aridity gradients, with the exception of slightly underestimating precipitation sensitivity in dry climates (Figure 4.4). Model evaluation for foliage cover is presented in Supplementary Figure S4.6.

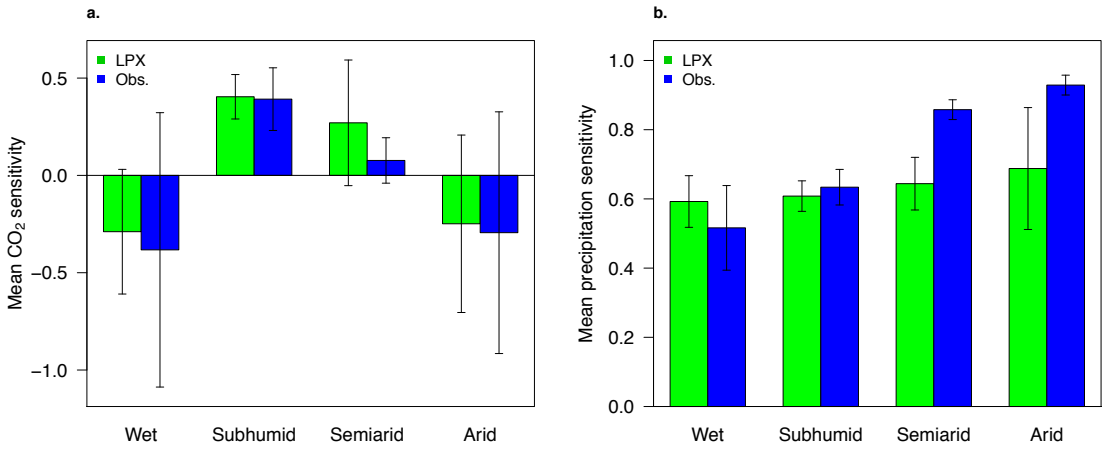

Figure 4.4 | Evaluation of the LPX DGVM for observed ET sensitivity to CO_2 and precipitation. Comparison of LPX-predicted and observed **a,** CO_2 and **b,** precipitation sensitivity for river basins grouped by aridity. The error bars show 95% confidence intervals.

Budyko framework. The Budyko framework is a widely employed empirical hydrological model based on the premise of water and energy availability as the controls on evapotranspiration and runoff. The model simulates AET (E_a) from precipitation (P) and PET (E_p), assuming no net change in soil water storage (3):

$$E_a = E_p [1 + MI – (1 + MI^{\omega})^{1/\omega}] \quad (1)$$

where MI is the moisture index, P/E_p. The model parameter ω represents catchment properties, including vegetation, soil and topography, and accounts for errors in precipitation and PET (29). Although several studies have suggested that the model's single parameter ω is in part a function of vegetation properties, there is no generally accepted way to account for vegetation effects on ω (29). The model was thus employed to represent the effects of climate alone and the parameter was set to a constant value of 3.09. This value was derived by non-linear optimisation against historical E_a from 190 Australian river basins (13) and is close to values used in previous studies (3, 15). Budyko-simulated runoff was calculated as the difference between precipitation and simulated E_a.

Historical simulations. LPX was forced using monthly fields of climate (maximum, minimum and mean air temperature, precipitation, cloud cover, number of wet days and wind speed), monthly lightning climatology and annual CO_2 concentrations. The Budyko model was driven

with monthly precipitation and Priestley-Taylor PET calculated from cloud cover and mean air temperature. Full model and spin-up protocols and input data sources are detailed in Supplementary Section 4.4.2.

Future projections. Both models were forced from 2006 to 2099 with bias-corrected climate projections at 0.5° spatial resolution from nine global climate models from the CMIP5 archive (4) (see Supplementary Section 4.4.3) under two Representative Concentration Pathways (1) (RCP4.5 and RCP8.5), leading to 18 projections for each model. RCP4.5 is an intermediate scenario where radiative forcing (RF) stabilises at 4.5 W m^{-2} by 2100 and atmospheric CO_2 concentration reaches 576 ppm (ensemble average) by 2080 after which it stabilises. RCP8.5 is an extreme trajectory where RF reaches 8.5 W m^{-2} and atmospheric CO_2 concentration 1231 ppm by 2100. The GCMs, bias correction and modelling protocols are further discussed in Supplementary Section 4.4.3.

Acknowledgements

We thank the CMIP5 project for making future climate simulations publicly available. Patrick Bartlein and Kenji Izumi (University of Oregon) assisted with the production of the future model inputs. A.U. is supported by an iMQRES scholarship from Macquarie University. T.F.K acknowledges support from a Macquarie University Research Fellowship. This work is a contribution to AXA Chair Programme in Biosphere and Climate Impacts and the Grand Challenges in Ecosystems and the Environment initiative at Imperial College London.

4.3. References

1. Van Vuuren DP, et al. (2011) The representative concentration pathways: an overview. *Clim Change* 109:5–31.

2. Kelley DI, Harrison SP, Prentice IC (2014) Improved simulation of fire–vegetation interactions in the Land surface Processes and eXchanges dynamic global vegetation model (LPX-Mv1). *Geosci Model Dev* 7:2411–2433.

3. Zhang L, et al. (2004) A rational function approach for estimating mean annual evapotranspiration. *Water Resour Res* 40:W02502.

4. Taylor KE, Stouffer RJ, Meehl G a. (2012) An Overview of CMIP5 and the Experiment Design. *Bull Am Meteorol Soc* 93:485–498.

5. Collins M, et al. (2013) Long-term Climate Change: Projections, Commitments and Irreversibility. *Climate Change 2013: The Physical Science Basis. Contribution of Working Group I to the Fifth Assessment Report of the Intergovernmental Panel on Climate Change*, eds Stocker TF, et al. (Cambridge University Press, Cambridge, United Kingdom and New York, NY, USA), pp 1029–1136.

6. Knutti R, Sedláček J (2012) Robustness and uncertainties in the new CMIP5 climate model projections. *Nat Clim Chang* 3:369–373.

7. Chiew FHS, McMahon TA (1993) Detection of trend or change in annual flow of Australian rivers. *Int J Climatol* 13:643–653.

8. Prudhomme C, et al. (2014) Hydrological droughts in the 21st century, hotspots and uncertainties from a global multimodel ensemble experiment. *Proc Natl Acad Sci U S A* 111:3262–7.

9. Gedney N, et al. (2006) Detection of a direct carbon dioxide effect in continental river runoff records. *Nature* 439:835–838.

10. Davie JCS, et al. (2013) Comparing projections of future changes in runoff from hydrological and biome models in ISI-MIP. *Earth Syst Dyn* 4:359–374.

11. Field CB, Jackson RB, Mooney HA (1995) Stomatal response to increased CO_2: Implication from the leaf to the global scale. *Plant Cell Environ* 18:1214–1225.

12. Keenan TF, et al. (2013) Increase in forest water-use efficiency as atmospheric carbon dioxide concentrations rise. *Nature* 499:324–327.

13. Ukkola AM, et al. Reduced streamflow in water-stressed climates consistent with CO_2 effects on vegetation. *Nat Clim Chang* accepted.

14. Betts RA, Cox PM, Lee SE, Woodward FI (1997) Contrasting physiological and structural vegetation feedbacks in climate change simulations. *Nature* 387:796–799.

15. Yang D, et al. (2007) Analyzing spatial and temporal variability of annual water-energy balance in nonhumid regions of China using the Budyko hypothesis. *Water Resour Res* 43:W04426.

16. Murray SJ, Foster PN, Prentice IC (2011) Evaluation of global continental hydrology as simulated by the Land-surface Processes and eXchanges Dynamic Global Vegetation Model. *Hydrol Earth Syst Sci* 15:91–105.

17. Kelley DI, Harrison SP (2014) Enhanced Australian carbon sink despite increased wildfire during the 21st century. *Environ Res Lett* 9:104015.

18. King AD, Donat MG, Alexander L V., Karoly DJ (2014) The ENSO-Australian rainfall teleconnection in reanalysis and CMIP5. *Clim Dyn* 44:2623-2635.

19. Collins M, et al. (2010) The impact of global warming on the tropical Pacific Ocean and El Niño. *Nat Geosci* 3:391–397.

20. Cai W, et al. (2014) Increasing frequency of extreme El Niño events due to greenhouse warming. *Nat Clim Chang* 4:111–116.

21. Cai W, et al. (2014) Increased frequency of extreme Indian Ocean Dipole events due to greenhouse warming. *Nature* 510:254–8.

22. Potter NJ, Chiew FHS, Frost AJ (2010) An assessment of the severity of recent reductions in rainfall and runoff in the Murray–Darling Basin. *J Hydrol* 381:52–64.

23. Gerten D, Schaphoff S, Haberlandt U, Lucht W, Sitch S (2004) Terrestrial vegetation and water balance —hydrological evaluation of a dynamic global vegetation model. *J Hydrol* 286:249–270.

24. Ukkola AM, Murray SJ (2014) Hydrological evaluation of the LPX dynamic global vegetation model for small river catchments in the UK. *Hydrol Process* 28:1939–1950.

25. Kelley DI, et al. (2013) A comprehensive benchmarking system for evaluating global vegetation models. *Biogeosciences* 10:3313–3340.

26. Sitch S, et al. (2003) Evaluation of ecosystem dynamics, plant geography and terrestrial carbon cycling in the LPJ dynamic global vegetation model. *Glob Chang Biol* 9:161–185.

27. Prentice IC, et al. (2011) Modeling fire and the terrestrial carbon balance. *Global Biogeochem Cycles* 25:GB3005.

28. Prentice IC, Dong N, Gleason SM, Maire V, Wright IJ (2014) Balancing the costs of carbon gain and water transport: testing a new theoretical framework for plant functional ecology. *Ecol Lett* 17:82–91.

29. Roderick ML, Farquhar GD (2011) A simple framework for relating variations in runoff to variations in climatic conditions and catchment properties. *Water Resour Res* 47:W00G07.

4.4. Supplementary Information

This Supplementary Information further describes the LPX model (Section 4.4.1), and historical (Section 4.4.2) and future modelling protocols, including the Global Climate Models and bias correction methods (Section 4.4.3).

4.4.1. Description of the LPX DGVM

4.4.1.1. Overview

The Land surface Processes and eXchanges Dynamic Global Vegetation Model (LPX-DGVM) (1, 2) is a process-based model that represents dynamic coupled vegetation-water-carbon interactions. The LPX-DGVM is a development of the Lund-Potsdam-Jena (LPJ) model (3, 4) with improved fire dynamics. The model simulates ecosystem processes based on plant functional types (PFT), distinguished by life form, leaf type, phenology as well as climatic range for trees and photosynthetic pathway for grasses (1). The model simulates temporal variations in ecosystem structure (such as leaf area index, height and foliage projective cover), composition (PFTs), and function (including productivity, ET and runoff) in a modular framework at 0.5° spatial resolution. The model has been evaluated against global and local hydrological data (4, 5) as well as vegetational, atmospheric and hydrological benchmarks (1, 2, 6). The model and its predecessors have been widely employed in global and regional studies of vegetation processes, carbon and water cycling, as well as fire dynamics (2, 7–9). A detailed discussion of vegetation dynamics is provided in Sitch et al. (2003) (3), hydrology in Gerten et al. (2004) (4) and fire dynamics in Kelley et al. (2014) (1) and Prentice et al. (2011) (2). LPX CO_2 effects and fire dynamics are briefly detailed below.

4.4.1.2. CO_2 effects

LPX simulates CO_2 effects on vegetation and hydrology based on a coupled photosynthesis-water balance scheme, which explicitly couples CO_2 assimilation with transpiration. Atmospheric CO_2 regulates stomatal conductance (*gc*) rates required to sustain a given photosynthetic rate. When water is not limiting, the potential maximum rate of stomatal conductance (gc_{max}) is calculated from a PFT-specific minimum canopy conductance (g_{min}), day-time net photosynthesis (A_d), ambient CO_2 concentration (C_a) and the ratio of intercellular to ambient CO_2 concentration (λ) (4):

$$gc_{\max} = gc_{\min} + 1.6A_d / [C_a(1-\lambda)] \quad (1)$$

λ is set to 0.4 for C_4 plants and 0.8 for C_3 plants. Transpiration (D) under well-watered conditions is calculated from gc_{max}, equilibrium evapotranspiration (E_q; evaporation from a well-watered surface in the absence of advection(10, 11)) and the fraction of day-time when the canopy is wet (w) following Monteith (1995) (4, 12):

$$D = (1-w)E_q\alpha_m / (1 + gc_m / gc_{\max}) \quad (2)$$

where α_m is a maximum Priestley-Taylor coefficient (1.391) and gc_m is the scaling conductance (3.26 mm s^{-1}). If D is greater than available water supply (S; a function of soil water content and soil properties), it is reduced in such a way to be consistent with an empirical relationship between S and gc formulated by Monteith (1995) (4, 12). When D is not limited by S and the plant experiences no water stress, plants respire and photosynthesise at their maximum rate. When C_a increases, gc_{max} is decreased for a given A_d and the threshold where D becomes supply-limited is increased. Thus, under elevated CO_2 maximum photosynthesis rates can occur at lower moisture availability, and higher photosynthetic rates in moisture-stress conditions, leading to a CO_2 fertilisation effect allowing increased productivity in drier conditions. The assimilated carbon (after accounting for respiration and reproductive costs) is allocated to leaf, sapwood and root production using fixed fractions. Therefore, increased photosynthesis leads to increases in foliage cover in the model.

Secondary effects of CO_2-induced vegetation structural changes also include possible changes to rainfall partitioning into interception, infiltration and surface runoff and the efficiency of water uptake from deeper soil layers. In addition, increased foliage cover may reduce the amount of radiation reaching the ground surface, thus reducing soil evaporation. These processes are also explicitly simulated in the model.

FPC for each PFT is determined annually as a function of total crown area (CA), plant population density (PD) and the average individual FPC (FPC_{ind}) (3):

$$FPC = CA \cdot PD \cdot FPC_{ind} \quad (3)$$

Total FPC, the measure used in this study, varies between 0 (bare ground) and 1. Runoff is calculated daily as the residual of precipitation minus interception (I), transpiration from the upper (0.5 m) and lower (1.0m) fixed-depth soil layers and surface evaporation from the top

soil layer (E_s) (8). Surface and subsurface runoff are diagnosed separately from water in surplus to field capacity for each soil layer. Water percolating through the lower soil layer is assumed to contribute to subsurface rate and is calculated as a function of soil texture, moisture and depth (4, 8). Runoff used in this study is the sum of percolation, surface and subsurface runoff. *I* is a function of precipitation, leaf area index, daily phenology and biome. E_s is determined as the multiple of E_q, a Priestley-Taylor coefficient (set to 1.32 following Hobbins et al. (2001) (13)), relative soil moisture of the top 0.2 m soil layer and the fraction of grid cell not covered by vegetation (4). The model does not include a river routing scheme or simulate lateral distribution of water between grid cells.

4.4.1.3. Fire dynamics

Fire is a major ecosystem process in Australia (7, 14), and is a major control on vegetation and hydrology (15–17). We use the latest version of LPX (LPX-Mv1) with an improved process-based fire model specifically designed to simulate Australian fire regimes and fire-adapted vegetation (1). LPX-Mv1 implements changes to processes regulating fuel ignition, decomposition and moisture content to improve the simulation of fire occurrence and spread. LPX-Mv1 also includes adaptive bark thickness to better simulate fire resilience and new resprouting tropical and temperate broadleaf tree PFTs to better simulate post-fire recovery. The model was benchmarked specifically for Australia and was shown to better simulate Australian fire regimes, vegetation composition and vegetation post-fire recovery compared to previous model versions (1).

4.4.1.4. Evaluation of historical simulations

We evaluated LPX-DGVM for simulation of observed historical ET and vegetation sensitivity to CO_2 and precipitation across 190 Australian river basins during 1982-2006. Observed vegetation sensitivities were determined from GIMMS3g Normalised Difference Vegetation Index data (18) at 0.083° spatial resolution and ET from water-balance evapotranspiration calculated from observed runoff (19) and gridded precipitation at 0.05° spatial resolution from the ANUCLIM archive (20). These were compared to LXP-simulated values of ET and foliage projective cover (FPC). All basin-specific values were extracted from gridded data using areal weighting and the basins grouped by their 1982-2010 mean aridity index (A = PET/P) as in Ukkola et al. (accepted) (21). River basins with A < 1 were classified as wet, 1-2 as subhumid, 2-5 as semiarid and >5 as arid. The effects of precipitation (and PET for AET)

were removed from observed and LPX-simulated AET and vegetation cover prior to determining CO_2 sensitivities. This was achieved using linear regression: separately for each basin, annual AET and FPC were regressed against precipitation (and PET in the case of AET) and the annual corrected values were calculated as the sum of the regression residual and the 1982-2006 mean of the variable. All variables were then log-transformed for calculation of precipitation and CO_2 sensitivities.

Comparison of ET sensitivities is presented in the main paper. Simulated and observed FPC sensitivities are shown in Supplementary Figure S4.6. The model captures observed mean sensitivities successfully in subhumid and semiarid basins. However, in wet regions the model fails to capture the positive CO_2 sensitivity and negative precipitation sensitivity. The model also overestimated FPC sensitivity to precipitation in arid regions, whilst CO_2 sensitivity in these regions is highly spatially variable. Whilst FPC changes in the wet and arid areas should be interpreted cautiously, they do not undermine the findings from a water resources perspective. The wet regions occupy only a small area (Supplementary Figure S4.5) and mainly include the sparsely populated northeast Australia and western Tasmania. Arid regions occupy much of central Australia but are largely uninhabited and have minimal surface water resources.

4.4.2. Historical simulations

4.4.2.1. Budyko framework

The Budyko model was run on a monthly time step from 1901 to 2005 using observed monthly climate from the CRU TS 3.1 archive. The model inputs include precipitation and potential evapotranspiration, calculated from cloud cover and mean air temperature using the Priestley-Taylor method as in Gallego-Sala et al. (2010) (22). The model parameter ω was set to 3.09, derived from non-linearly optimising the model for historical annual water-balance evapotranspiration measurements from 190 Australian river basins for the period 1982-2010 (21).

4.4.2.2. LPX DGVM

The model was run at daily time step at 0.5° spatial resolution for Australia using monthly inputs of climate (mean, maximum and minimum temperature, precipitation, cloud cover and

number of wet days) from the CRU TS3.1 archive (23), monthly wind speed from the National Center for Environmental Prediction (NCEP) reanalysis dataset (24), monthly lightning climatology (http://gcmd.nasa.gov/ records/GCMD_lohrmc.html) and annual CO_2 concentrations (a combination of ice core and atmospheric measurements from Mauna Loa and South Pole (25) supplemented by data from NOAA-CDML (http://www.esrl.noaa.gov/ gmd/) global averaged concentrations for the period 1980-2006). The NCEP wind speed data were interpolated to 0.5° from the original resolution of 1.82° using bilinear interpolation. Soil properties were described using nine fixed soil texture classes (26). The monthly inputs were stochastically disaggregated to daily values.

The model was initialised using detrended historical climate and constant CO_2 at 286 ppm until the slow carbon pools were in equilibrium. The model was subsequently run for the period 1850-2005 using transient CO_2. Detrended climate was used until 1901 (and until 1947 for wind speed) and transient climate thereafter. Full details of input datasets and LPX modelling protocols are provided in Kelley and Harrison (2014) (7).

4.4.3. Future simulations

4.4.3.1. Global Climate Models

We used projected future climate realisations from nine Global Climate Models (GCMs) from the latest Coupled Model Intercomparison Project (CMIP5) (27) forced by two alternative Representative Concentration Pathway (RCP) scenarios (28): RCP4.5 and RCP8.5. RCP4.5 is an intermediate radiative forcing (RF) scenario that stabilizes at 4.5 W m^{-2} by 2100. RCP8.5 is an extreme RF scenario where RF reaches 8.5 W m^{-2} by 2100. Four of the GCMs are coupled ocean-atmosphere models, the further five models also include a marine and terrestrial carbon cycle. The models, their type and horizontal resolution are listed in Supplementary Table S4.1.

4.4.3.2. Bias correction of GCM outputs

GCMs are known to include systematic biases in their representation of key variables, such as precipitation, when compared to historical observations (29). To correct for these biases and to allow for a smooth transition between historical and future model climate inputs, we bias-corrected future GCM outputs using an anomaly-based method, which preserves the interannual variability of each GCM. The bias-correction method is fully described in Kelley et

al. (2014) (7), but will be briefly described here. We first calculated month-by-month anomalies between the simulated RCP-driven future climate and the simulated historical climate for the 1961-1990 baseline. As the GCM resolutions differ, the anomalies were subsequently regridded to a common resolution of 0.5° for consistency with historical model inputs using bilinear interpolation. The regridded monthly anomalies were then added to the observed historical climate for the 1961-1990 baseline.

Supplementary Table S4.1 | GCMs used in this study. OA indicates a coupled ocean-atmosphere model, OAC models also include a representation of marine and terrestrial carbon cycle. Model resolutions have been rounded to one decimal point.

Model name	Research centre	Type	Resolution (latitude, longitude)
CNRM-CM5	Centre National de Recherches Meterologique	OA	1.4°, 1.4°
GISS-CM5	NASA Goddard Institute for Space Studies	OA	2.0°, 2.5°
HadGEM2-CC	Hadley Centre, UK Meteorological Centre	OA	1.2°, 1.9°
MRI-CGCM3	Meteorological Research Institute	OA	1.2°, 1.2°
BCC-CSM1-1	Beijing Climate Center	OAC	2.8°, 2.8°
HadGEM2-ES	Hadley Centre, UK Meteorological Office	OAC	1.2°, 1.9°
IPSL-CM5a-LR	Institut Pierre-Simon Laplace	OAC	1.9°, 3.8°
MIROC-ESM	Japan Agency for Marine-Earth Science and Technology	OAC	2.8°, 2.8°
MPI-ESM-LR	Max Planck Institute for Meteorology	OAC	1.9°, 1.9°

4.4.3.3. Budyko and LPX simulation protocols

Both models were run from 2006 to 2099 using the same monthly climate input variables as for historical simulations (and annual CO_2 concentrations for LPX). The models were run separately for the nine GCM realisations under each alternative RCP, resulting in 18 projections for each model.

We also performed an additional set of simulations with LPX holding CO2 concentration at 2006 levels (380.8 ppm) in order to separate the effects of future CO2 fertilisation from the effects of climate.

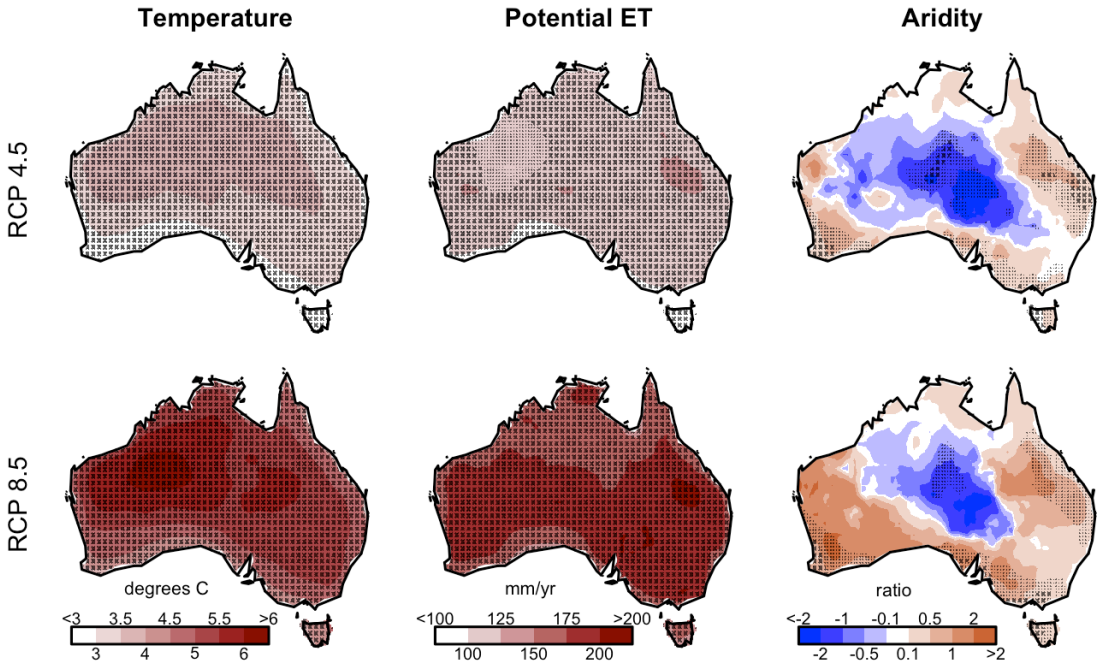

Supplementary Figure S4.1 | Projected future anomalies in mean temperature, potential ET and aridity. The anomalies were calculated as the difference between the 2070-2099 future ensemble mean and the 1960-1990 historical mean of the variable. Stippling indicates the robustness of signal as measured by the standard deviation (sd) of the model results divided by the ensemble mean (large stippling shows where sd ≤ 0.5 and small stippling where 0.5 < sd ≤ 1.0).

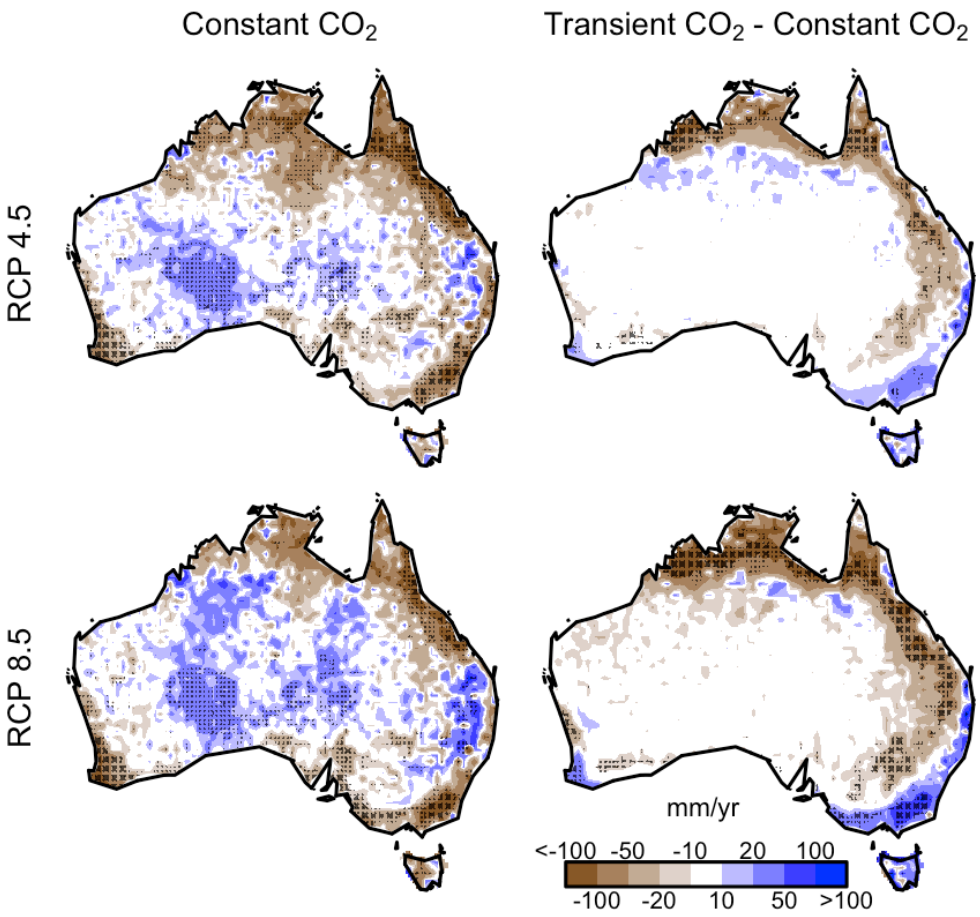

Supplementary Figure S4.2 | Projected future anomalies in runoff under constant CO_2 and comparison to transient CO_2 projections. **a,** LPX-simulated future runoff anomaly with constant CO_2 at 380.8 ppm (2006 level) under RCP4.5 and RCP8.5. The anomalies were calculated as the difference between the 2070-2099 future ensemble mean and the 1960-1990 historical mean of the variable. Stippling indicates the robustness of signal as measured by the standard deviation (sd) of the model results divided by the ensemble mean (large stippling shows where sd ≤ 0.5 and small stippling where 0.5 < sd ≤ 1.0). **b,** difference between simulated future runoff anomaly under transient (presented Figure 1) and constant CO_2. Here stippling indicates where the two simulations differ significantly, as determined from a two-tailed Student's t-test (large stippling shows where t-test *p*-value ≤ 0.5 and small stippling where 0.5 < *p*-value ≤ 1.0).

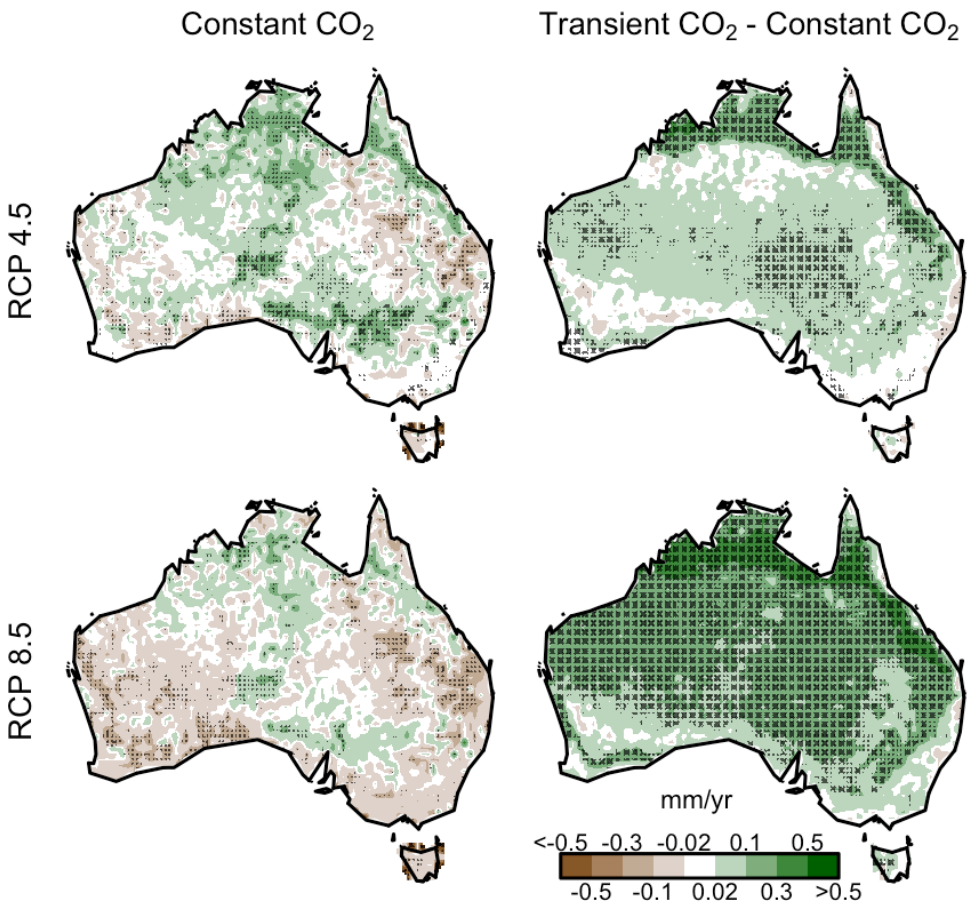

Supplementary Figure S4.3 | Projected future anomalies in foliage cover under constant CO_2 and comparison to transient CO_2 projections. **a,** LPX-simulated future foliage cover anomaly with constant CO_2 at 380.8 ppm (2006 level) under RCP4.5 and RCP8.5. The anomalies were calculated as the difference between the 2070-2099 future ensemble mean and the 1960-1990 historical mean of the variable. Stippling indicates the robustness of signal as measured by the standard deviation (sd) of the model results divided by the ensemble mean (large stippling shows where sd ≤ 0.5 and small stippling where 0.5 < sd ≤ 1.0). **b,** difference between simulated future foliage cover anomaly under transient (presented Figure 3) and constant CO_2. Here stippling indicates where the two simulations differ significantly, as determined from a two-tailed Student's t-test (large stippling shows where t-test *p*-value ≤ 0.5 and small stippling where 0.5 < *p*-value ≤ 1.0).

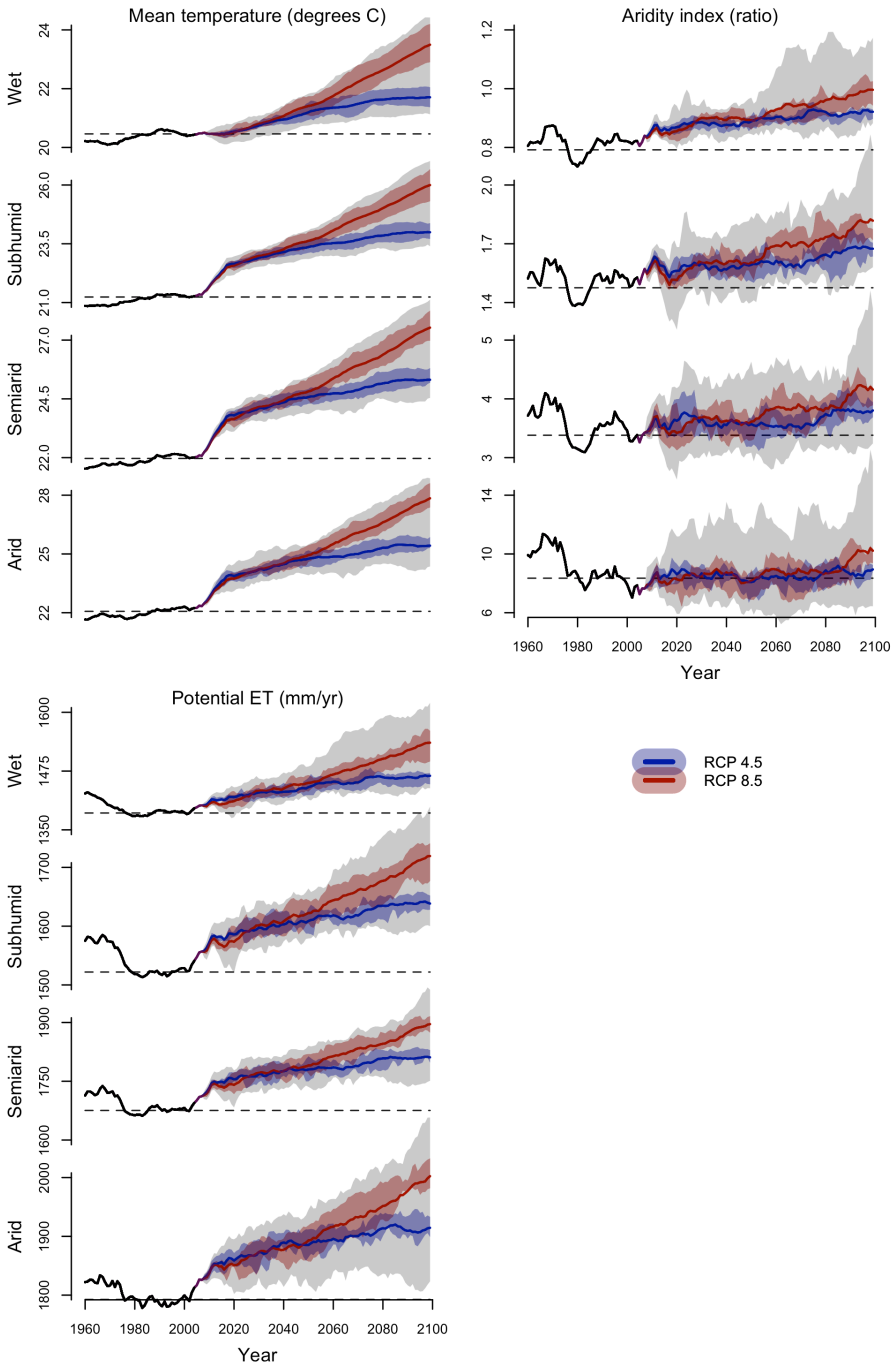

Supplementary Figure S4.4 | Historical and future time series of mean temperature, potential ET and aridity index in different aridity regimes. The solid black line shows the historical period (1960-2005) and the dotted line the historical mean of the variable during 1960-1990. The coloured lines show the future ensemble means and the coloured shading indicates model interquartile ranges for each RCP. The grey shading shows the combined full model range of both RCPs. To construct the time series, grid cells were grouped by their historical mean aridity into four categories (wet, subhumid, semiarid and arid) and the mean of the variable was calculated annually across all grid cells within each category (see Supplementary Figure 1 for spatial distribution of aridity categories). The time series were subsequently smoothed using 10-year running means.

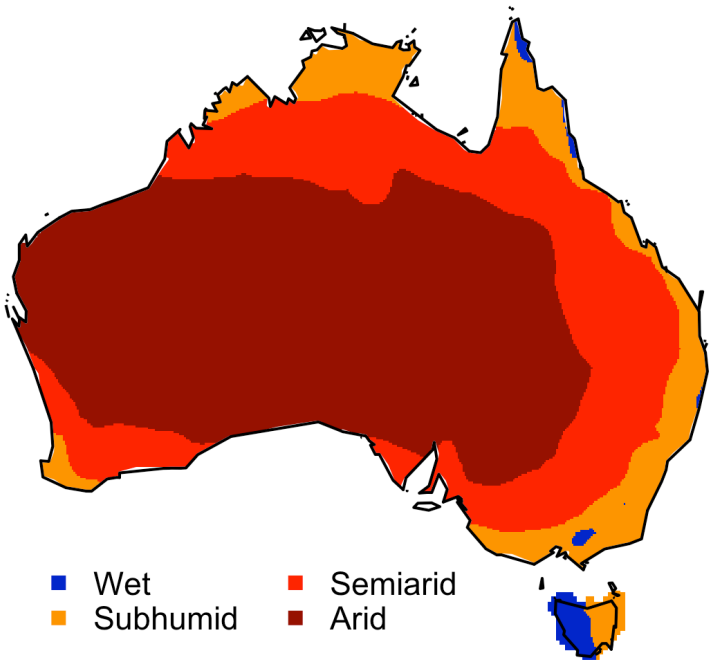

Supplementary Figure S4.5 | Historical aridity. Grid cells were categorised according to their 1960-1990 mean aridity index using the thresholds detailed in Section 1.

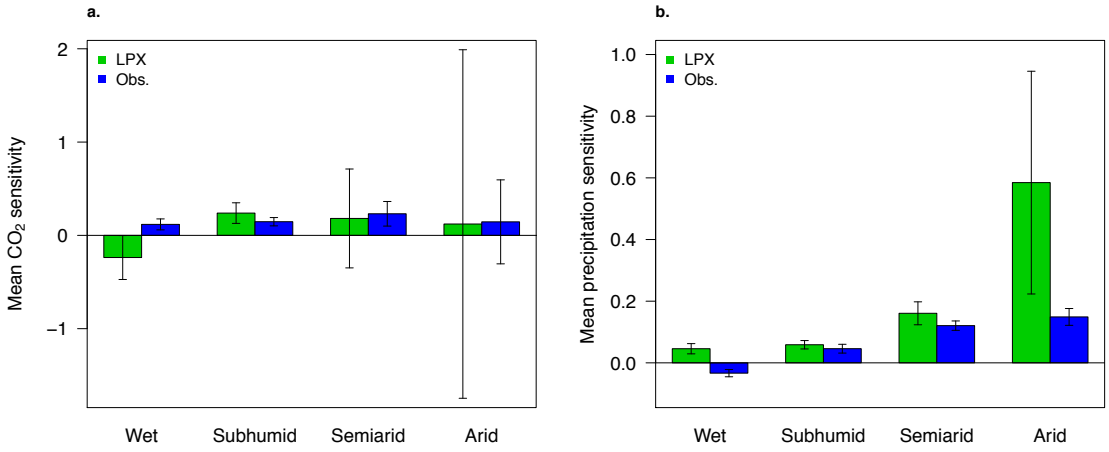

Supplementary Figure S4.6 | Evaluation of the LPX-DGVM for observed FPC sensitivity to CO_2 and precipitation. Comparison of LPX-predicted and observed sensitivity to **a,** CO_2 and **b,** precipitation for river basins grouped by aridity. The error bars show 95% confidence intervals.

4.4.4. References

1. Kelley DI, Harrison SP, Prentice IC (2014) Improved simulation of fire–vegetation interactions in the Land surface Processes and eXchanges dynamic global vegetation model (LPX-Mv1). *Geosci Model Dev* 7:2411–2433.

2. Prentice IC, et al. (2011) Modeling fire and the terrestrial carbon balance. *Global Biogeochem Cycles* 25:GB3005.

3. Sitch S, et al. (2003) Evaluation of ecosystem dynamics, plant geography and terrestrial carbon cycling in the LPJ dynamic global vegetation model. *Glob Chang Biol* 9:161–185.

4. Gerten D, Schaphoff S, Haberlandt U, Lucht W, Sitch S (2004) Terrestrial vegetation and water balance—hydrological evaluation of a dynamic global vegetation model. *J Hydrol* 286:249–270.

5. Ukkola AM, Murray SJ (2014) Hydrological evaluation of the LPX dynamic global vegetation model for small river catchments in the UK. *Hydrol Process* 28:1939–1950.

6. Kelley DI, et al. (2013) A comprehensive benchmarking system for evaluating global vegetation models. *Biogeosciences* 10:3313–3340.

7. Kelley DI, Harrison SP (2014) Enhanced Australian carbon sink despite increased wildfire during the 21st century. *Environ Res Lett* 9:104015.

8. Murray SJ, Foster PN, Prentice IC (2011) Evaluation of global continental hydrology as simulated by the Land-surface Processes and eXchanges Dynamic Global Vegetation Model. *Hydrol Earth Syst Sci* 15:91–105.

9. Martin Calvo M, Prentice IC, Harrison SP (2014) Climate versus carbon dioxide controls on biomass burning: a model analysis of the glacial-interglacial contrast. *Biogeosciences* 11:6017–6027.

10. Eichinger WE, Parlange MB, Stricker H (1996) On the concept of equilibrium evaporation and the value of the Priestley-Taylor coefficient. *Water Resour Res* 32:161–164.

11. Fisher JB, Whittaker RJ, Malhi Y (2011) ET come home: potential evapotranspiration in geographical ecology. *Glob Ecol Biogeogr* 20:1–18.

12. Monteith JL (1995) Accommodation between transpiring vegetation and the convective boundary layer. *J Hydrol* 166:251–263.

13. Hobbins MT, Ramirez JA, Brown TC (2001) The complementary relationship in estimation of regional evapotranspiration: an enhanced advection-aridity model. *Water Resour Res* 37:1389–1403.

14. Kelley D (2014) Modelling Australian fire regimes. Dissertation (Macquarie University).

15. Murphy BP, et al. (2013) Fire regimes of Australia: a pyrogeographic model system. *J Biogeogr* 40(6):1048–1058.

16. Murphy BP, Lehmann CER, Russell-Smith J, Lawes MJ (2014) Fire regimes and woody biomass dynamics in Australian savannas. *J Biogeogr* 41:133–144.

17. Johansen MP, Hakonson TE, Breshears DD (2001) Post-fire runoff and erosion from rainfall simulation: contrasting forests with shrublands and grasslands. *Hydrol Process* 15:2953–2965.

18. Pinzon JE, Tucker CJ (2014) A non-stationary 1981-2012 AVHRR NDVI3g time series. *Remote Sens* 6:6929–6960.

19. Zhang Y, et al. (2013) *Collation of Australian modeller's streamflow dataset for 780 unregulated Australian catchments* (CSIRO Water for a Healthy Country Flagship Report).

20. Xu T, Hutchinson MF (2013) New developments and applications in the ANUCLIM spatial climatic and bioclimatic modelling package. *Environ Model Softw* 40:267–279.

21. Ukkola AM, et al. CO_2-induced greening reduces streamflow in water-stressed climates. *Nat Clim Chang* accepted.

22. Gallego-Sala A, et al. (2010) Bioclimatic envelope model of climate change impacts on blanket peatland distribution in Great Britain. *Clim Res* 45:151–162.

23. Harris I, Jones PD, Osborn TJ, Lister DH (2014) Updated high-resolution grids of monthly climatic observations - the CRU TS3.10 Dataset. *Int J Climatol* 34:623–642.

24. Kalnay E, et al. (1996) The NCEP/NCAR 40-year reanalysis project. *Bull Am Meteorol Soc* 77:437–471.

25. Rayner NA, Brohan P, Parker DE, Folland CF (2006) Improved analyses of changes and Uncertainties in Sea Surface Temperature Measured In Situ since the Mid-Nineteenth Century: The HadSST2 Dataset. *J Clim* 19:446–469.

26. FAO (1991) The digitized soil map of the world (release 1.0). *World Soil Resources Report 67/1*, ed Food and Agriculture Organisation of the United Nations (Rome, Italy).

27. Taylor KE, Stouffer RJ, Meehl G a. (2012) An Overview of CMIP5 and the Experiment Design. *Bull Am Meteorol Soc* 93:485–498.

28. Van Vuuren DP, et al. (2011) The representative concentration pathways: an overview. *Clim Change* 109:5–31.

29. Hempel S, Frieler K, Warszawski L, Schewe J, Piontek F (2013) A trend-preserving bias correction – the ISI-MIP approach. *Earth Syst Dyn* 4:219–236.

Chapter 5

Conclusions

5.1. Conclusions

This thesis has investigated historical evapotranspiration (ET) trends in Australia and globally, and produced future projections of water resources in Australia based on alternative models and climate scenarios. Trends in water-balance ET were first investigated across river basins globally. Many studies have concentrated on detecting global runoff trends but ET has received much less attention, in part due to the difficulty in measuring ET at large scales. ET is a key ecosystem variable accounting for 60% of global land precipitation and understanding historical ET changes is important for evaluating climate change impacts on water, carbon and energy cycling (Douville et al., 2013).

Despite remaining the most observationally based method for determining basin-scale ET, water-balance ET estimates have not been widely used to detect historical trends. But they provide a very useful source of information on ET in basins where streamflow records are available. Furthermore, previous studies have generally attributed ET trends based on a limited set of drivers, focusing on specific attributes such as land use or CO_2 effects in combination with climate (e.g. Gedney et al., 2006; Gordon et al., 2005). This study considered all proposed drivers, relying on observations to the greatest extent possible. Significant ET trends were identified only in a small minority of catchments, despite widespread changes in precipitation and other drivers. Global terrestrial ET (and precipitation) is expected to increase due to global warming resulting in intensification of the hydrological cycle. Previous studies relying on water balance, pan evaporation and other indirect evidence (reviewed in Huntington, 2006) have pointed to increased ET over different continents, but the present study did not provide evidence of widespread increases in terrestrial ET during the late 20th century.

The results confirmed the dominant role of precipitation in controlling ET. In dry environments precipitation accounts for virtually all variability in ET and for as much as 50% even in wet basins. Foliage cover was found to exert a secondary but significant control in both dry and wet environments. However, based on LPX modelling, no CO_2 effects were detected in this global analysis. The attribution of ET trends in wet basins remained difficult but was improved compared to a previous study (Zhang et al., 2012), which could only account for 9% of ET trends based on precipitation. Wet environments show more complex interactions between water, energy and vegetation processes and more widespread land use change than dry regions; but these remain difficult to quantify from available data (Wohl et al., 2012). This problem is compounded by data uncertainties in humid regions, particularly in the tropics where both precipitation and streamflow data remain uncertain (Fekete et al., 2004). Further work is thus required to better understand ET variations in wet environments.

The water-balance method has limitations that were not quantified in the current study. In the absence of suitable soil moisture observations, the study assumed negligible changes in soil water storage at annual time scales. Remotely sensing techniques, such as the Gravity Recovery and Climate Experiment (GRACE) and microwave products, now exist for the recent satellite era and have been increasingly used to estimate soil water changes at monthly time scales (Seneviratne et al., 2010; Seoane et al., 2013; Zeng et al., 2012). As the present study analysed ET observations for the pre-satellite era, the use of such datasets was not possible and soil water storage changes were thus ignored, although it was demonstrated statistically that this was unlikely to compromise the results. For the same reason, the water-balance method cannot be reliably applied to seasonal scales. In seasonal or highly variable climates, runoff generation can be highly concentrated to specific seasons or individual rainfall events; these dynamics may not be reflected in annual totals.

In common with previous studies, the global study relied on models to quantify CO_2 effects on ET and runoff, resulting in large uncertainties in the magnitude and direction of CO_2 effects. CO_2 effects on vegetation and hydrology across river basins in Australia during 1982-2010 were next investigated, relying solely on high quality streamflow and climate observations available for the Australian continent. The method used sensitivity coefficients whose theoretically expected values could be derived from a novel ecophysiological framework (Prentice et al., 2014). Contrary to a common expectation, the study reported significant *increases* in plant water use, leading to runoff declines of 24-28% in sub-humid and semi-arid climates, attributable to CO_2-induced greening during the last three decades. After accounting for concurrent decreases in precipitation, observed runoff has overall declined by 30% in sub-humid Australian basins since 1982. Sub-humid zones in Australia support substantial human populations and agriculture; the added pressure on water resources due to climatic and CO_2 effects have important implications for the management of water resources in these regions.

No CO_2 fertilisation effect on vegetation was detected in wet basins. Here increasing CO_2 was shown to reduce ET on average, but the effect was not statistically significant. The nature of CO_2 effects in arid environments also remained unclear, due to the limited number of arid basins with available data (nine). Conceptual models predict that arid ecosystems should be the most responsive to increased CO_2, and a significant fertilisation effect has been reported across the world's warm, arid regions based on remotely sensed vegetation data (Donohue et al., 2013). However, experimental evidence suggest increased plant productivity cannot be sustained in the most arid environments due to the high frequency of low precipitation years in which productivity is extremely limited (Newingham et al., 2013).

The proportion of C_4 vegetation is also important for determining ecosystem responses to elevated CO_2. C_4 plants are favoured in warm, arid ecosystems due to their greater water use efficiency and higher photosynthetic capacity in light-saturated conditions compared to C_3 plants. C_4 plants respond to elevated CO_2 very differently to C_3 plants, only benefiting from atmospheric CO_2 concentrations beyond current ambient levels under drought conditions through relieved water stress (Leakey et al., 2009). C_4 vegetation strongly dominates in central and northern Australia (Still et al., 2003) and may thus contribute to the lack of a CO_2 effect in arid basins. Arid ecosystems cover ca. 20% of the world's land surface (Smith et al., 2000) and present a large potential carbon sink under increased water availability (Evans et al., 2014); further research is thus warranted to better understand the impacts of elevated CO_2 in arid environments.

The study quantified the hydrological effects of elevated CO_2. CO_2-induced vegetation changes also have important consequences for carbon storage and climate feedbacks. Currently marine and terrestrial ecosystems take up around half of global greenhouse emissions, curbing the growth of atmospheric CO_2 concentrations and consequently radiative forcing (Ballantyne et al., 2012). This fraction has remained unchanged despite accelerating emissions, pointing to increased uptake of carbon by ecosystems (Poulter et al., 2014; Le Quéré et al., 2013). These reductions in radiative forcing may be offset by decreased surface albedo and consequent warming due to increased absorption of incoming shortwave radiation resulting from vegetation greening (Betts, 2000). This can counteract positive effects of CO_2 fertilisation in water-limited regions where warming can aggravate water stress, whereas it may further promote plant productivity in temperature-limited regions. These are important qualifications for future climate change and ecosystem function but are not yet well constrained in the future projections available today (Friend et al., 2014; Notaro et al., 2007).

The future evolution of regional water resources and their interactions with vegetation and climatic processes also remain highly uncertain. Projections of future water resources in Australia were produced using alternative model-based climate scenarios driven by two of the Representative Concentration Pathways (RCP) used by climate modelling groups for the Intergovernmental Panel on Climate Change (IPCC). The process-based LPX model with full vegetation dynamics was contrasted with the simple Budyko framework, which accounts for climatic effects but not vegetation processes. By comparing the two models, direct climate effects could be separated from the effects of vegetation processes on water resources. LPX has been successfully benchmarked against hydrological and vegetational data sets. The model version used incorporates a fire module specifically designed for Australian fire

regimes (Kelley et al., 2013, 2014). This model was shown here to successfully reproduce observed historical ET and vegetation sensitivities to CO_2 and precipitation, and thus offers a suitable model for estimating future hydrological changes in Australia.

Precipitation forecasts remain a major source of uncertainty in future projections of water resources. The nine climate models employed in this study simulated robust decreases in precipitation in southwestern Australia but generally disagreed elsewhere. Despite large uncertainties in projected precipitation, robust changes in runoff were shown. The projections were largely independent of the choice of RCP, despite temperature and potential ET diverging strongly. The study showed that future declines in runoff in the populated eastern and southwestern regions of Australia are likely to be significantly overestimated unless vegetation responses to changing climate and CO_2 concentrations are considered. In northern Australia, vegetation greening (due to CO_2 fertilisation and decreased fire occurrence) were projected to increase plant water use and consequently water stress, but were accompanied by increased natural vegetation productivity.

LPX was shown to compare well against observations but does not account for some potentially important soil and climate feedbacks. In common with most other vegetation models, LPX does not currently consider potential nutrient constraints on CO_2 assimilation. Nitrogen (N) and phosphorus (P) are the main nutrients limiting plant productivity and carbon storage. Nitrogen 'limitation' is commonly considered to constrain warming- or CO_2-induced increases in plant productivity (Hungate et al., 2003), although experiments and theory suggest that tropical forests and savanna, accounting for about half of global terrestrial biomass and productivity, are largely phosphorus limited (Wang et al., 2010). The extent to which the carbon costs of N and/or P acquisition constrain the CO_2 fertilization effect remains controversial and in need of clarification, particularly as 'carbon-water' models such as LPX do not overestimate terrestrial carbon uptake (Xu-Ri and Prentice, in revision). LPX projects a strong fertilisation effect in arid regions, particularly under the high-end ('business as usual') emissions scenario (RCP8.5); but this has a negligible effect on runoff, which is mostly simulated to increase or to remain unchanged (though these changes were not robust between different climate forcings). There are still many uncertain assumptions about water-carbon interactions, which are represented differently among the available process-based vegetation models and contribute significantly to uncertainties in simulated CO_2 effects (De Kauwe et al., 2013). Furthermore, off-line simulations cannot account for climate-vegetation feedbacks, such as changes in surface albedo and radiative forcing, which can only be achieved through dynamic coupling of climate and vegetation models.

The Budyko model, has been widely shown to capture climatic effects on ET but the physical meaning of the model's single parameter is poorly understood (Roderick and Farquhar, 2011). The parameter represents "catchment properties" including soil, topography and vegetation but despite attempts to determine the parameter from soil and vegetation variables (Donohue et al., 2012; Yang et al., 2007), a formulation relying on easily observable attributes is lacking. Studies have argued the parameter should mainly relate to vegetation as other catchment properties, such as topography, soil and geology remain unchanged at decadal to centurial time scales (Donohue et al., 2010; Roderick and Farquhar, 2011). An improved formulation of the parameter could, in principle, account for CO_2 effects as well as hydrological impacts of vegetation responses to other environmental conditions such as climate and fire to provide a simple empirical approach for quantifying vegetation and climate impacts on hydrology as a simple and transparent alternative to process-based models. Here, however, the model's principal use has been to indicate a default outcome of climate changes, without taking vegetation effects into account.

This thesis has presented a comprehensive analysis of historical ET trends and related them to specific climatic and vegetation processes, exploiting extensive observational datasets. CO_2 effects on hydrology have remained particularly controversial in the literature due to conflicting reports on the magnitude and direction of effects. Here, unambiguous results were shown based on observations of water and vegetation in Australia. This analysis can be extended to other continents and ecosystems, making use of widely available runoff observations and global remotely sensed vegetation datasets. Finally, the potential role of vegetation as a buffer for negative effects of climate change on water resources was illustrated and the need to consider coupled vegetation and hydrological processes in investigations of historical and future ET and runoff.

5.2. References

Ballantyne, A. P., Alden, C. B., Miller, J. B., Tans, P. P. and White, J. W. C.: Increase in observed net carbon dioxide uptake by land and oceans during the past 50 years, Nature, 488, 70–72, doi:10.1038/nature11299, 2012.

Betts, R. A.: Offset of the potential carbon sink from boreal forestation by decreases in surface albedo, Nature, 408, 187–190, 2000.

Donohue, R. J., Roderick, M. L. and McVicar, T. R.: Can dynamic vegetation information improve the accuracy of Budyko's hydrological model?, J. Hydrol., 390, 23–34, doi:10.1016/j.jhydrol.2010.06.025, 2010.

Donohue, R. J., Roderick, M. L. and McVicar, T. R.: Roots, storms and soil pores: Incorporating key ecohydrological processes into Budyko's hydrological model, J. Hydrol., 436-437, 35–50, doi:10.1016/j.jhydrol.2012.02.033, 2012.

Donohue, R. J., Roderick, M. L., McVicar, T. R. and Farquhar, G. D.: Impact of CO_2 fertilization on maximum foliage cover across the globe's warm, arid environments, Geophys. Res. Lett., 40, 1–5, doi:10.1002/grl.50563, 2013.

Douville, H., Ribes, A., Decharme, B., Alkama, R. and Sheffield, J.: Anthropogenic influence on multidecadal changes in reconstructed global evapotranspiration, Nat. Clim. Chang., 3, 59–62, doi:10.1038/nclimate1632, 2013.

Evans, R. D., Koyama, A., Sonderegger, D. L., Charlet, T. N., Newingham, B. A., Fenstermaker, L. F., Harlow, B., Jin, V. L., Ogle, K., Smith, S. D. and Nowak, R. S.: Greater ecosystem carbon in the Mojave Desert after ten years exposure to elevated CO_2, Nat. Clim. Chang., 4, 394–397, doi:10.1038/NCLIMATE2184, 2014.

Fekete, B. M., Vörösmarty, C. J., Roads, J. O. and Willmott, C. J.: Uncertainties in precipitation and their impacts on runoff estimates, J. Clim., 17, 294–304, 2004.

Friend, A. D., Lucht, W., Rademacher, T. T., Keribin, R., Betts, R., Cadule, P., Ciais, P., Clark, D. B., Dankers, R., Falloon, P. D., Ito, A., Kahana, R., Kleidon, A., Lomas, M. R., Nishina, K., Ostberg, S., Pavlick, R., Peylin, P., Schaphoff, S., Vuichard, N., Warszawski, L., Wiltshire, A. and Woodward, F. I.: Carbon residence time dominates uncertainty in terrestrial vegetation responses to future climate and atmospheric CO_2, Proc. Natl. Acad. Sci. U. S. A., 111, 3280–3285, doi:10.1073/pnas.1222477110, 2014.

Gedney, N., Cox, P. M., Betts, R. A., Boucher, O., Huntingford, C. and Stott, P. A.: Detection of a direct carbon dioxide effect in continental river runoff records, Nature, 439, 835–838, doi:10.1038/nature04504, 2006.

Gordon, L. J., Steffen, W., Jönsson, B. F., Folke, C., Falkenmark, M. and Johannessen, Å.: Human modification of global water vapor flows from the land surface, Proc. Natl. Acad. Sci., 102, 7612–7617, doi:10.1073/pnas.0500208102, 2005.

Hungate, B. A., Dukes, J. S., Shaw, M. R., Luo, Y. and Field, C. B.: Nitrogen and climate change, Science, 302, 1512–1514, 2003.

Huntington, T. G.: Evidence for intensification of the global water cycle: Review and synthesis, J. Hydrol., 319, 83–95, doi:10.1016/j.jhydrol.2005.07.003, 2006.

De Kauwe, M. G., Medlyn, B. E., Zaehle, S., Walker, A. P., Dietze, M. C., Hickler, T., Jain, A. K., Luo, Y., Parton, W. J., Prentice, I. C., Smith, B., Thornton, P. E., Wang, S., Wang, Y.-P., Wårlind, D.,

Weng, E., Crous, K. Y., Ellsworth, D. S., Hanson, P. J., Seok Kim, H.-, Warren, J. M., Oren, R. and Norby, R. J.: Forest water use and water use efficiency at elevated CO_2: a model-data intercomparison at two contrasting temperate forest FACE sites, Glob. Chang. Biol., 19, 1759–1779, doi:10.1111/gcb.12164, 2013.

Kelley, D. I., Harrison, S. P. and Prentice, I. C.: Improved simulation of fire–vegetation interactions in the Land surface Processes and eXchanges dynamic global vegetation model (LPX-Mv1), Geosci. Model Dev., 7, 2411–2433, doi:10.5194/gmd-7-2411-2014, 2014.

Kelley, D. I., Prentice, I. C., Harrison, S. P., Wang, H., Simard, M., Fisher, J. B. and Willis, K. O.: A comprehensive benchmarking system for evaluating global vegetation models, Biogeosciences, 10, 3313–3340, doi:10.5194/bg-10-3313-2013, 2013.

Leakey, A. D. B., Ainsworth, E. a, Bernacchi, C. J., Rogers, A., Long, S. P. and Ort, D. R.: Elevated CO_2 effects on plant carbon, nitrogen, and water relations: six important lessons from FACE, J. Exp. Bot., 60, 2859–76, doi:10.1093/jxb/erp096, 2009.

Newingham, B. A., Vanier, C. H., Charlet, T. N., Ogle, K., Smith, S. D. and Nowak, R. S.: No cumulative effect of 10 years of elevated [CO_2] on perennial plant biomass components in the Mojave Desert., Glob. Chang. Biol., 19, 2168–81, doi:10.1111/gcb.12177, 2013.

Notaro, M., Vavrus, S. and Liu, Z.: Global vegetation and climate change due to future increases in CO_2 as projected by a fully coupled model with dynamic vegetation, J. Clim., 20, 70–90, doi:10.1175/JCLI3989.1, 2007.

Poulter, B., Frank, D., Ciais, P., Myneni, R. B., Andela, N., Bi, J., Broquet, G., Canadell, J. G., Chevallier, F., Liu, Y. Y., Running, S. W., Sitch, S. and van der Werf, G. R.: Contribution of semi-arid ecosystems to interannual variability of the global carbon cycle., Nature, 509, 600–603, doi:10.1038/nature13376, 2014.

Prentice, I. C., Dong, N., Gleason, S. M., Maire, V. and Wright, I. J.: Balancing the costs of carbon gain and water transport: testing a new theoretical framework for plant functional ecology., Ecol. Lett., 17, 82–91, doi:10.1111/ele.12211, 2014.

Le Quéré, C., Andres, R. J., Boden, T., Conway, T., Houghton, R. a., House, J. I., Marland, G., Peters, G. P., van der Werf, G. R., Ahlström, A., Andrew, R. M., Bopp, L., Canadell, J. G., Ciais, P., Doney, S. C., Enright, C., Friedlingstein, P., Huntingford, C., Jain, a. K., Jourdain, C., Kato, E., Keeling, R. F., Klein Goldewijk, K., Levis, S., Levy, P., Lomas, M., Poulter, B., Raupach, M. R., Schwinger, J., Sitch, S., Stocker, B. D., Viovy, N., Zaehle, S. and Zeng, N.: The global carbon budget 1959–2011, Earth Syst. Sci. Data, 5, 165–185, doi:10.5194/essd-5-165-2013, 2013.

Roderick, M. L. and Farquhar, G. D.: A simple framework for relating variations in runoff to variations in climatic conditions and catchment properties, Water Resour. Res., 47, W00G07, doi:10.1029/2010WR009826, 2011.

Seneviratne, S. I., Corti, T., Davin, E. L., Hirschi, M., Jaeger, E. B., Lehner, I., Orlowsky, B. and Teuling, A. J.: Investigating soil moisture–climate interactions in a changing climate: A review, Earth-Science Rev., 99, 125–161, doi:10.1016/j.earscirev.2010.02.004, 2010.

Seoane, L., Ramillien, G., Frappart, F. and Leblanc, M.: Regional GRACE-based estimates of water mass variations over Australia: validation and interpretation, Hydrol. Earth Syst. Sci., 17, 4925–4939, doi:10.5194/hess-17-4925-2013, 2013.

Smith, S. D., Huxman, T. E., Zitzer, S. F., Charlet, T. N., Housman, D. C., Coleman, J. S., Fenstermaker, L. K., Seemann, J. R. and Nowak, R. S.: Elevated CO_2 increases productivity and invasive species success in an arid ecosystem, Nature, 408, 79–82, doi:10.1038/35040544, 2000.

Still, C. J., Berry, J. a., Collatz, G. J. and DeFries, R. S.: Global distribution of C_3 and C_4 vegetation: Carbon cycle implications, Global Biogeochem. Cycles, 17, 1006, doi:10.1029/2001GB001807, 2003.

Wang, Y. P., Law, R. M. and Pak, B.: A global model of carbon, nitrogen and phosphorus cycles for the terrestrial biosphere, Biogeosciences, 7, 2261–2282, doi:10.5194/bg-7-2261-2010, 2010.

Wohl, E., Barros, A., Brunsell, N., Chappell, N. A., Coe, M., Giambelluca, T., Goldsmith, S., Harmon, R., Hendrickx, J. M. H., Juvik, J., McDonnell, J. and Ogden, F.: The hydrology of the humid tropics, Nat. Clim. Chang., 2, 655–662, doi:10.1038/nclimate1556, 2012.

Xu-Ri and Prentice, I. C.: Quantifying terrestrial demand for newly fixed nitrogen: is there a missing source?, in revision.

Yang, D., Sun, F., Liu, Z., Cong, Z., Ni, G. and Lei, Z.: Analyzing spatial and temporal variability of annual water-energy balance in nonhumid regions of China using the Budyko hypothesis, Water Resour. Res., 43, W04426, doi:10.1029/2006WR005224, 2007.

Zeng, Z., Piao, S., Lin, X., Yin, G., Peng, S., Ciais, P. and Myneni, R. B.: Global evapotranspiration over the past three decades: estimation based on the water balance equation combined with empirical models, Environ. Res. Lett., 7, 014026, doi:10.1088/1748-9326/7/1/014026, 2012.

Zhang, Y., Leuning, R., Chiew, F. H. S., Wang, E., Zhang, L., Liu, C., Sun, F., Peel, M. C., Shen, Y. and Jung, M.: Decadal Trends in Evaporation from Global Energy and Water Balances, J. Hydrometeorol., 13, 379–391, doi:10.1175/JHM-D-11-012.1, 2012.